Molecular Evaluation of Enzalutamide Resistance in Prostate Cancer

A thesis submitted to the University of Dublin, Trinity College for the degree of

Doctor in Medicine, Clinical Medicine (M.D.)

by

John Aird

Supervisor:

Prof. Stephen Finn

Department of Histopathology

University of Dublin

Trinity College

May 2020

Declaration

I declare that this thesis has not been submitted as an exercise for a degree at this or any other university and it is entirely my own work.

I agree to deposit this thesis in the University's open access institutional repository or allow the Library to do so on my behalf, subject to Irish Copyright Legislation and Trinity College Library conditions of use and acknowledgement.

I consent to the examiner retaining a copy of the thesis beyond the examining period, should they so wish (EU GDPR May 2018).

_____

John Aird

Summary

Prostate cancer is a leading cause of cancer related death in men. As prostate cancer cells are dependent on androgen receptor (AR) signalling for continued growth, anti-androgen therapy is initially effective in treating most patients with locally advanced or metastatic PCa. However, resistance to anti-androgen therapies inevitably develops in all patients leading to castration resistant prostate cancer (CRPC), which is currently incurable. In most cases of drug resistance, AR signalling is maintained despite castration levels of androgens. The molecular underpinnings for how this occurs and how it can be overcome have yet to be fully elucidated.

Non-coding RNAs, initially thought to be redundant parts of the genome, are now known to be involved in the regulation of key cellular processes in human tumourigenesis and in the development of drug resistance. Long non-coding RNAs (lncRNAs) are non-coding RNAs > 200 nucleotides in length and over 100,000 have been identified in the human genome. Whether all these lncRNAs play a functional role in cellular biology and what that role may be, is still largely unknown.

The objective of this study was to evaluate the molecular mechanisms underlying resistance to the anti-androgen enzalutamide in PCa. An isogenic cell line model with clones of varying resistance to enzalutamide was used. Microarray analysis was performed and differentially expressed lncRNAs and mRNAs identified. Six lncRNAs were validated by qPCR as being significantly overexpressed in enzalutamide resistant PCa cells - *SPRY4-IT1, DPP10-AS1, FLJ26850, SARCC, RP11-222K16.2* and *RP11-1C8.7*. These lncRNAs were not previously known to be associated with PCa. One of these lncRNAs, *SARCC*, was previously reported to bind to the AR in renal cell carcinoma. Using a cloning strategy, SARCC was stably overexpressed in enzalutamide sensitive cells resulting in increased resistance to enzalutamide, thus suggesting a functional role for *SARCC* in enzalutamide resistance.

Five mRNAs were also validated by qPCR as being significantly overexpressed in enzalutamide resistant PCa cells - *CTAG1B, PEG10, SPINK1, PITX2* and *PCDH7*. The reported functions of the proteins encoded by these 5 mRNAs offer possible mechanisms for how resistance to enzalutamide could develop, such as modulating AR signalling and

affecting neuroendocrine differentiation. This is the first time that an association with enzalutamide resistance has been reported for these mRNAs.

In conclusion, this study contributed significantly to the understanding of the development of resistance in PCa by identifying a number of previously unknown lncRNAs and mRNAs associated with enzalutamide resistance. This information could provide the basis for further investigative work into potential treatment targets. It could also form the basis for a biomarker test predicting the development of resistance to enzalutamide or helping to stratify patients based on their likelihood to respond to therapy.

Acknowledgements

I would like to thank Professor Stephen Finn and Professor Steven Gray for their support, help and guidance throughout this project. I was very lucky to work in a supportive environment in St. James's Hospital and would not have completed this project without that support. A special thanks to SG for his patience as I went through my learning curve of learning to pipette, run gels etc.!

A special thank you to Dr. Anne-Marie Baird for all her help, advice and troubleshooting throughout this project. She was always extremely generous with her time and energy despite juggling numerous other responsibilities herself and I really appreciate all the help she gave me.

I would also like to thank Dr. Lauren Brady, Dr. Marvin Lim and Mark Wright for their help with my experiments and providing advice and feedback when I ran into difficulties.

Thank you to Prof. Elaine Kay who encouraged me to undertake this M.D. and for making numerous introductions and providing much appreciated career advice to me.

This project was partly funded by a grant from the Pathological Society of Great Britain and Ireland for which I am very grateful for having received.

Lastly, I want to thank my wife Grace without whom this project would never have been attempted or completed. She was a constant support and sacrificed a huge amount of her time and energy while I worked late nights, early mornings and weekends - I'm forever grateful.

Table of Contents

List of Tables

List of Figures

Abbreviations

ADT:	Androgen deprivation therapy
AFAP1-AS1:	AFAP1 antisense RNA 1
ANOVA:	Analysis of variance
AR:	Androgen receptor
ARE:	Androgen response element
AR-V7:	AR splice variant-7
BCL-2:	B-cell lymphoma 2
BPE:	Bovine pituitary extract
BPH:	Benign prostatic hyperplasia
BTG1:	BTG anti-proliferation factor 1
CHD1:	Chromodomain helicase DNA binding protein 1
CRPC:	Castration resistant prostate cancer
CTAG1B:	Cancer/testis antigen 1B
CTBP1	C-terminal binding protein 1
CTBP1-AS	C-terminal binding protein 1 antisense
CYP17:	Cytochrome P450 family 17
DGCR5:	DiGeorge syndrome critical region gene 5
DGUOK-AS1:	DGUOK antisense RNA 1
DHT:	Dihydrotestosterone
DMSO:	Dimethyl sulfoxide
DPP10:	Dipeptidyl peptidase like 10
DPP10-AS1:	DPP10 antisense RNA 1
DRAIC:	Downregulated RNA in androgen independent cells
EDTA:	Ethylene-diamine tetra-acetic acid
EGF:	Epidermal growth factor
EMT:	Epithelial to mesenchymal transition
ERG:	ETS-related gene
EtOH:	Ethanol
ETS:	E26 transformation-specific
ETV1:	ETS Variant 1
ETV4:	ETS Variant 4
ETV5:	ETS Variant 5

FBS:	Foetal bovine serum
FEZF1-AS1:	FEZF1 Antisense RNA 1
FKBP1A:	FKBP prolyl isomerase 1A
GAS-5:	Growth arrest specific 5
GO:	Gene Ontology
GWAS:	Genome wide association study
HERPUD1:	Homocysteine Inducible ER Protein with Ubiquitin-like domain 1
HOTAIR:	HOX Transcript Antisense RNA
HOTTIP:	HOXA distal transcript antisense RNA
HOXB13:	Homeobox B13
HPV-18:	Human papilloma virus 18
IMS:	Industrial methylated spirits
KISS1:	KiSS-1 metastasis suppressor
KLK2:	Kallikrein related peptidase 2
KLK3:	Kallikrein related peptidase 3
LAF:	Laminar air flow unit
LEF1:	Lymphoid enhancer binding factor 1
LEF1-AS1:	LEF1 antisense RNA 1
LH:	Luteinising hormone
LHRH:	Luteinising hormone-releasing hormone
LncRNA:	Long non-coding RNA
LUCAT1:	Lung cancer-associated transcript 1
MEG3:	Maternally expressed 3
NDRG1:	N-Myc Downstream Regulated 1
NKX3.1:	NK3 Homeobox 1
NY-ESO-1:	New York esophageal squamous cell carcinoma
P/S:	Penicillin/streptomycin
PART-1:	Prostate androgen-regulated transcript 1
PAP:	Prostatic acid phosphatase
PBS:	Phosphate buffered saline
PCa:	Prostate cancer
PCAT14:	Prostate cancer associated transcript 14
PCAT18:	Prostate cancer associated transcript 18

PCAT29: Prostate cancer associated transcript 29

PCDH7: Protocadherin 7

PCGEM1: Prostate cancer gene expression marker 1

PCR: Polymerase chain reaction

PEG10: Paternally expressed 10

PIN: Prostatic intraepithelial neoplasia

PITX2: Paired like homeodomain 2

PSA: Prostate-specific antigen

PTEN: Phosphatase and tensin homolog

RBM5: RNA binding motif protein 5

SLC45A3: Solute carrier family 45 member 3

SARCC: Suppressing Androgen Receptor in Renal Cell Carcinoma

SNHG7: Small nucleolar RNA host gene 7

SNHG12: Small nucleolar RNA host gene 12

SNHG15: Small nucleolar RNA host gene 15

SNP: Single nucleotide polymorphism

SOCS2-AS1: Suppressor of cytokine signalling 2 antisense (*SOCS-AS1*)

SPINK1: Serine protease inhibitor Kazal-type 1

SPOP: Speckle type POZ protein

SPRY4: Sprouty RTK signaling antagonist 4

SPRY4-IT1: SPRY4 intronic transcript 1

TCGA: The Cancer Genome Atlas Program

TMPRSS2: Transmembrane serine protease 2

WNT2B: Wnt family member 2B

Units

bp:	base pairs
°C:	degrees Celsius
g:	grams
h:	hour(s)
µg:	microgram
µL:	microlitre
µM:	micromolar
kB:	kilobases
kg:	kilograms
L:	litre(s)
M:	molar
mg:	milligram
min:	minutes
mL:	millilitre
mM:	millimolar
mm:	millimetre
n:	number (sample size)
pg:	picogram
rpm:	revolutions per minute
s:	second(s)
U:	unit(s)
v/v:	volume per volume

Publications and Presentations

RNAs as candidate diagnostic and prognostic markers of prostate cancer – from cell line models to liquid biopsies.
Lim MCJ, Baird AM, **Aird JJ,** Greene J, Kapoor D, Gray SG, McDermott R, Finn SP. Diagnostics. 2018 Aug 30;8(3).

Carcinogenesis in prostate cancer: The role of long non-coding RNAs.
Aird JJ, Baird AM, Lim MCJ, McDermott R, Finn SP, Gray SG. Noncoding RNA Res. 2018 Feb 1;3(1):29-38.

Identification and validation of novel long non-coding RNA signatures of enzalutamide resistance in prostate cancer (Abstract).
Aird JJ, Gray SG, Baird AM, Lim MCJ, McDermott R, Finn SP. Modern Pathology 2018 Mar. Vol 31, 323–403.

Oral Presentation
Long non-coding RNAs associated with enzalutamide resistance in prostate cancer. National Academic Trainee Network Meeting, Dublin, September 2017.

Poster Presentations
Identification and validation of novel long non-coding RNA signatures of enzalutamide resistance in prostate cancer. United States and Canadian Academy of Pathology (USCAP) Annual Meeting, Vancouver, Canada, March 2018.

Awards and Grants

British Division of the International Association of Pathology Travel Grant to attend USCAP Annual Meeting, Vancouver, 2018.

Highly commended award for oral presentation at the National Academic Trainee Network Meeting, Dublin, Ireland, 2017.

Recipient of a research grant for £10,000 from the Pathological Society of Great Britain and Ireland.

Chapter 1 Introduction

1.1 Introduction

The human prostate is a secondary sex organ, the function of which is to produce fluids that form part of semen and to help propel this fluid into the urethra during ejaculation. Unlike other male secondary sex tissues, such as the seminal vesicles, the prostate gland is highly susceptible to oncogenic transformation making this small gland of outsized importance in male morbidity and mortality. The androgen receptor (AR) signalling pathway is central to the development and progression of prostate cancer (PCa). Treatments directed at blocking this pathway are usually effective at treating PCa initially but, unfortunately, resistance to these therapies develops in nearly all patients. This resistant form of PCa, termed castration resistant prostate cancer (CRPC), is currently incurable. Understanding the mechanisms through which treatment resistance develops is a key challenge in PCa research. With the use of molecular pathology techniques, our understanding of how resistance develops has improved over recent years, but this has yet to lead to a significant reduction in PCa mortality which remains one of the main causes of cancer related death in men.

1.2 The Prostate Gland

Anatomy and Physiology

The prostate gland is located just below the bladder and surrounds part of the urethra (Figure 1.1). It contains three glandular zones: the central, transition and peripheral zones, and a fourth non-glandular zone called the anterior fibromuscular stroma (Figure 1.2). The peripheral zone accounts for 70% of the prostate volume and is the most common site for malignancy [1]. The transition zone surrounds the urethra as it enters the prostate gland and accounts for 10% of the prostate volume. It is also the site of benign prostatic hyperplasia (BPH) [1]. The central zone surrounds the ejaculatory ducts and accounts for 20% of the prostate volume [1].

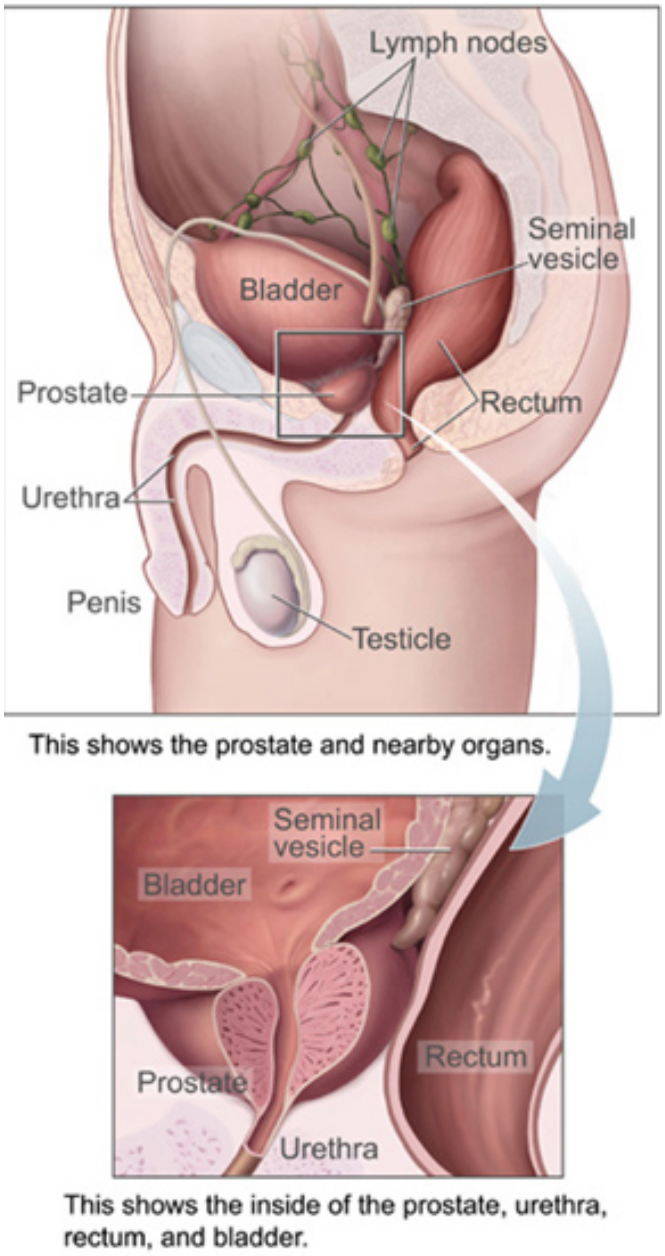

Figure 1.1: Prostate gland in relation to other organs.

(Source: National Cancer Institute, What you need to know about Prostate Cancer)

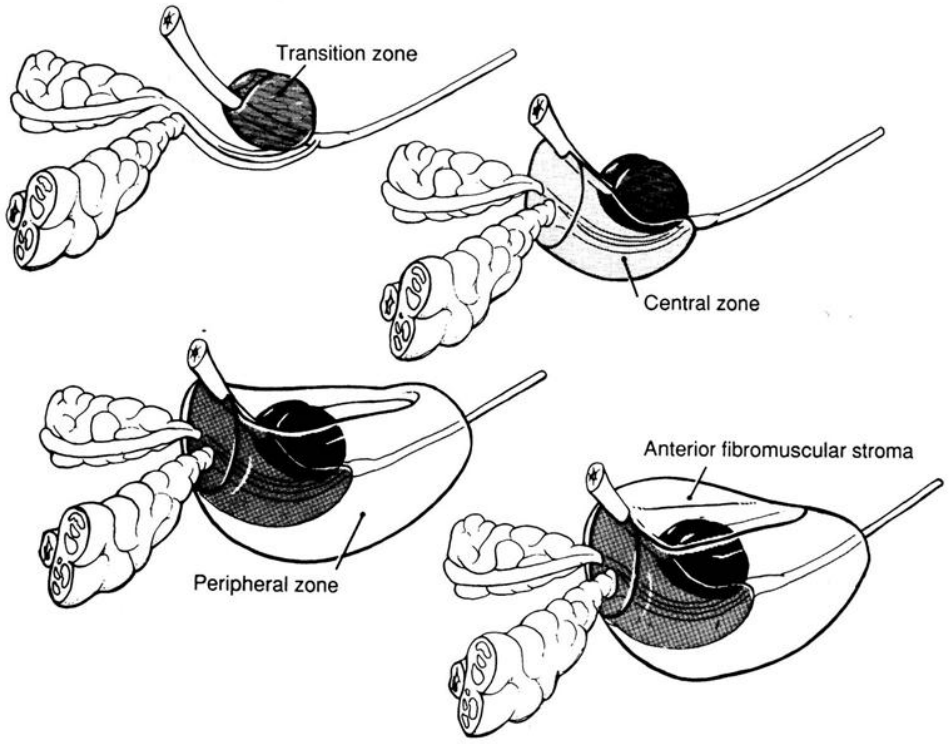

Figure 1.2: Zonal anatomy of the prostate gland.

(Source: The zonal anatomy of the prostate, McNeal JE, Prostate, 1981;2(1):35-49)

The prostate gland contains a system of branching ducts surrounded by a fibromuscular stroma. The glandular epithelium is made up of an outer layer of luminal cells and an inner layer of non-secretory basal cells (Figure 1.3). The luminal cells produce prostate-specific antigen (PSA) and prostatic acid phosphatase (PAP), which alter semen to improve sperm motility. Luminal cells express cytokeratins 8 and 18 whereas basal cells express cytokeratins 5 and 14, and p63 [2, 3]. Each cell population can be identified by immunohistochemical (IHC) testing for these cytokeratins, which is useful as malignant glands do not contain basal cells whereas benign glands do. Within the basal layer are occasional intermediate cells that co-express luminal and basal markers [3]. It remains unclear whether intermediate cells represent a functionally distinct cell type. Rare neuroendocrine cells are also present and express secreted neuropeptides and other hormones [4]. A layer of smooth muscle lines the epithelium and contracts to aid expulsion of prostatic fluid during ejaculation [5]. The stroma also contains a large population of mature fibroblasts, blood vessels, lymphatics, nerves and immune cells.

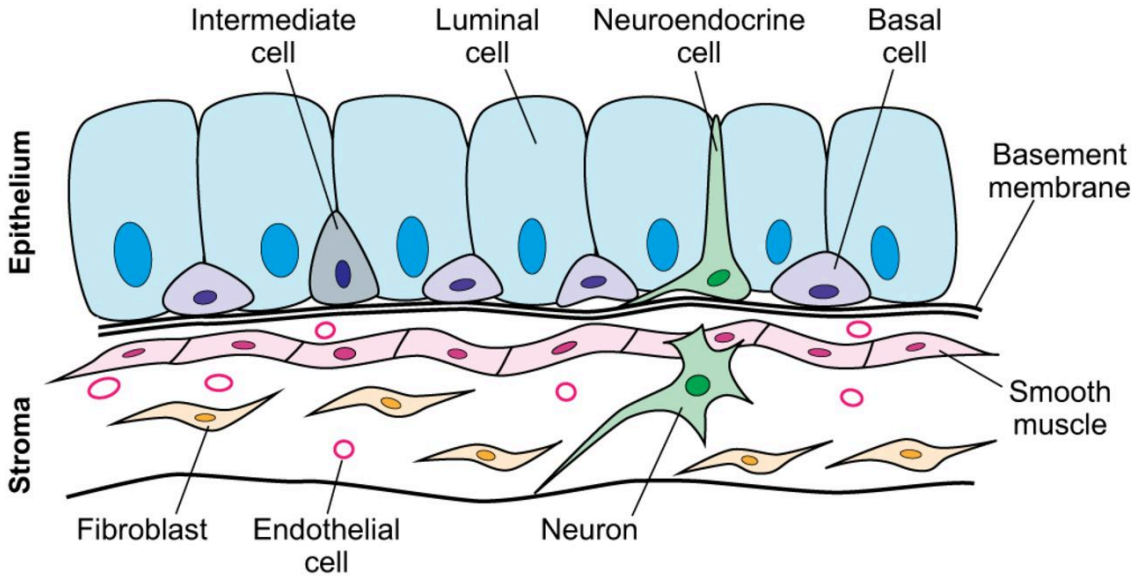

Figure 1.3: Diagram of different cells in the prostate gland.

(Source: Toivanen R et. al, Prostate organogenesis: tissue induction, hormonal regulation and cell type specification. Development 2017 144:1382-1398)

Embryology

The prostate gland arises from the endoderm, in contrast to other tissues of the male reproductive system, which arise from the mesoderm [5]. This may explain the comparatively high rate of tumorigenesis in the prostate gland as it is essentially an extension of the hindgut and shares an embryological origin with other important sites of tumorigenesis such as the colon, rectum, pancreas and liver.

Epithelial budding from the urogenital sinus forms the primitive prostate at about 10 weeks gestation [6]. This is prompted by androgens produced by Leydig cells. Prostate organogenesis then continues under the influence of circulating androgens which cause tissue outgrowth and branching to form a system of ducts composed of solid epithelial cords [5]. The solid epithelial cords undergo canalization to form the ductal lumina and then differentiate into the various epithelial cell types.

1.3 Prostate Cancer

Epidemiology

Prostate cancer is the second most commonly diagnosed non-skin cancer in men with an estimated 1.3 million new cases worldwide in 2018 [7]. There were an estimated 359,000 deaths associated with PCa in 2018 worldwide, making it the fifth leading cause of cancer death in men [7]. In Ireland, prostate cancer is the most frequently diagnosed non-skin cancer, with an estimated 3,500 new cases per year [8]. There are an estimated 520 deaths per year making it the 3rd most common cause of cancer death in men after lung and colorectal cancer [8].

For such a common cancer, there is little known about the aetiology of PCa. Incidence rates are highest among Sub-Saharan African men and men of African descent in the United States and the Caribbean, reflecting ethnic and genetic predisposition [9]. There is also strong evidence that family history influences the risk of PCa, as men with a father or brother diagnosed with PCa are at a two to threefold higher risk compared to men with no family history [10]. Germline mutations in certain genes such as Homeobox B13 (*HOXB13*), *BRCA2* and Lynch syndrome are associated with an increased risk of PCa [11]. More than 20 genome wide association studies (GWAS) have been published identifying 77 single nucleotide polymorphisms (SNPs) associated with an increased risk of PCa [12]. Most of these SNPs are located in chromosome 8q24, in a non-coding region in the vicinity of the *C-MYC* gene [13].

There is some evidence that dietary carcinogens, oestrogens, taller height and smoking are positively associated with PCa [14-20], whereas increased physical activity and diets rich in tomatoes and fish are negatively associated with PCa development and recurrence [21-23]. Obesity is associated with an increased risk of PCa mortality and recurrence [24]. An overview of prostate carcinogenesis is summarised in Figure 1.4.

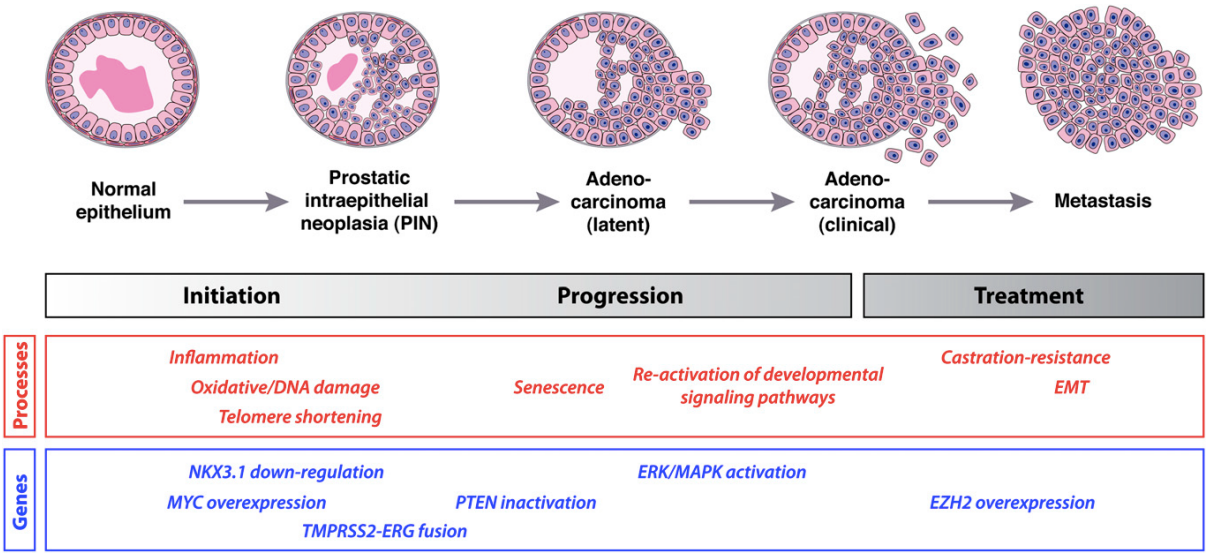

Figure 1.4: Overview of prostate carcinogenesis.

(Source: Shen et. al, Molecular genetics of prostate cancer: new prospects for old challenges; Genes Dev. 2010 Sep 15;24(18):1967-2000)

Androgen signalling

Androgen signalling plays a central role in PCa development, progression and recurrence after treatment [25]. The AR is an intracellular, ligand-activated transcription factor that mediates the biological actions of androgens [26]. It is a member of the steroid receptor subfamily of nuclear receptors sharing structural and functional features with the glucocorticoid, mineralocorticoid, progesterone and oestrogen receptors [25]. Testosterone is the main circulating androgen, secreted primarily by the testes after stimulation by luteinising hormone (LH) (Figure 1.5). It circulates in the blood where it is bound to albumin and sex-hormone-binding globulin. When free testosterone enters prostate epithelial cells, 90% is converted into dihydrotestosterone (DHT) by 5alpha-reductase (Figure 1.6). DHT is the more active hormone, having a 5-fold higher affinity for the AR than testosterone. In the absence of androgen binding, the AR is bound to heat shock protein complexes, thus preventing it from binding with DNA [25]. Upon binding with DHT, the AR dissociates from the heat shock proteins and translocates from the cytoplasm into the nucleus. The AR then binds to androgen response elements (AREs) in the DNA leading to the transcription of target genes such as Kallikrein related peptidase 2 (*KLK2*), *KLK3* and NK3 Homeobox 1 (*NKX3.1)* [27]. This leads to biological responses such as the promotion of differentiation of luminal cells and the production of PSA. In PCa, the

functions of the AR are less clear but involve the expression of genes associated with cell cycle regulation, survival and growth [25].

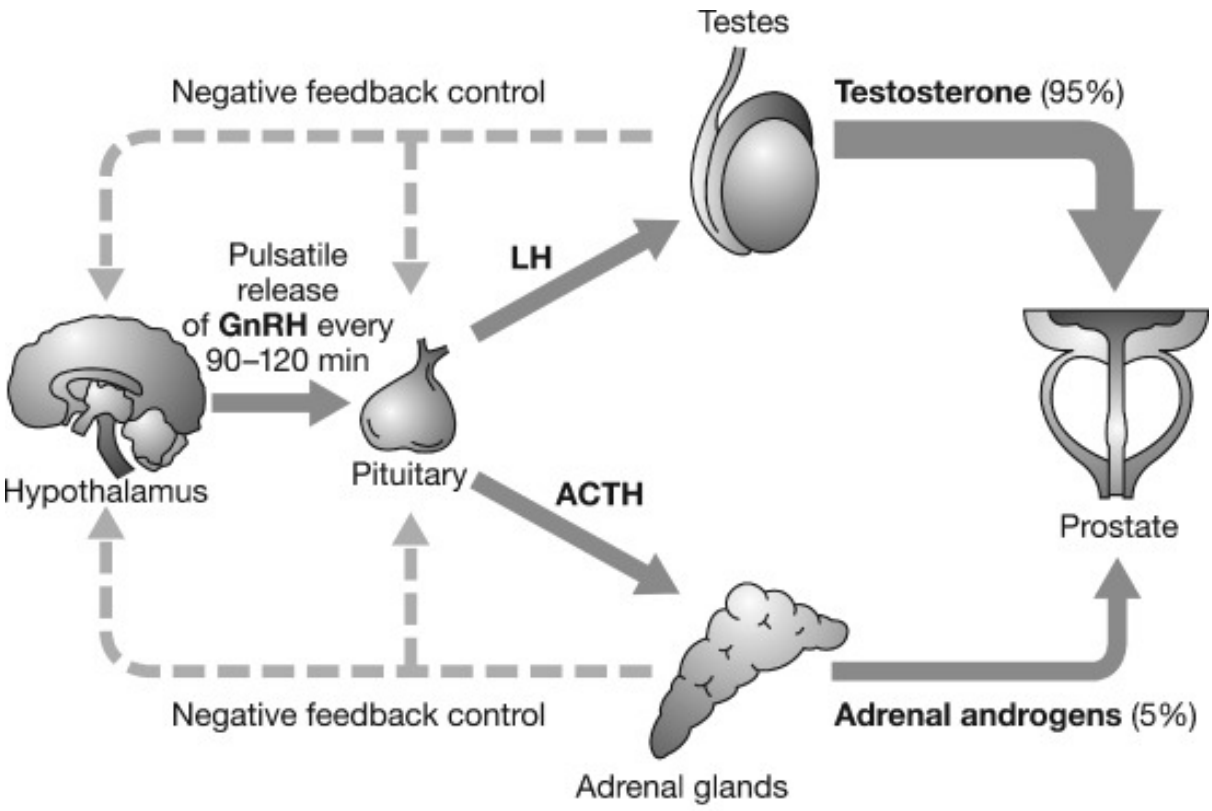

GnRH, gonadotrophin-releasing hormone; LH, luteinising hormone; ACTH, adrenocorticotrophic hormone

Figure 1.5: Androgen production in the human male.

(Source: Drudge-Coates, GnRH blockers: a changing paradigm in the management of prostate cancer. Urological Nursing: 2009; 85-92)

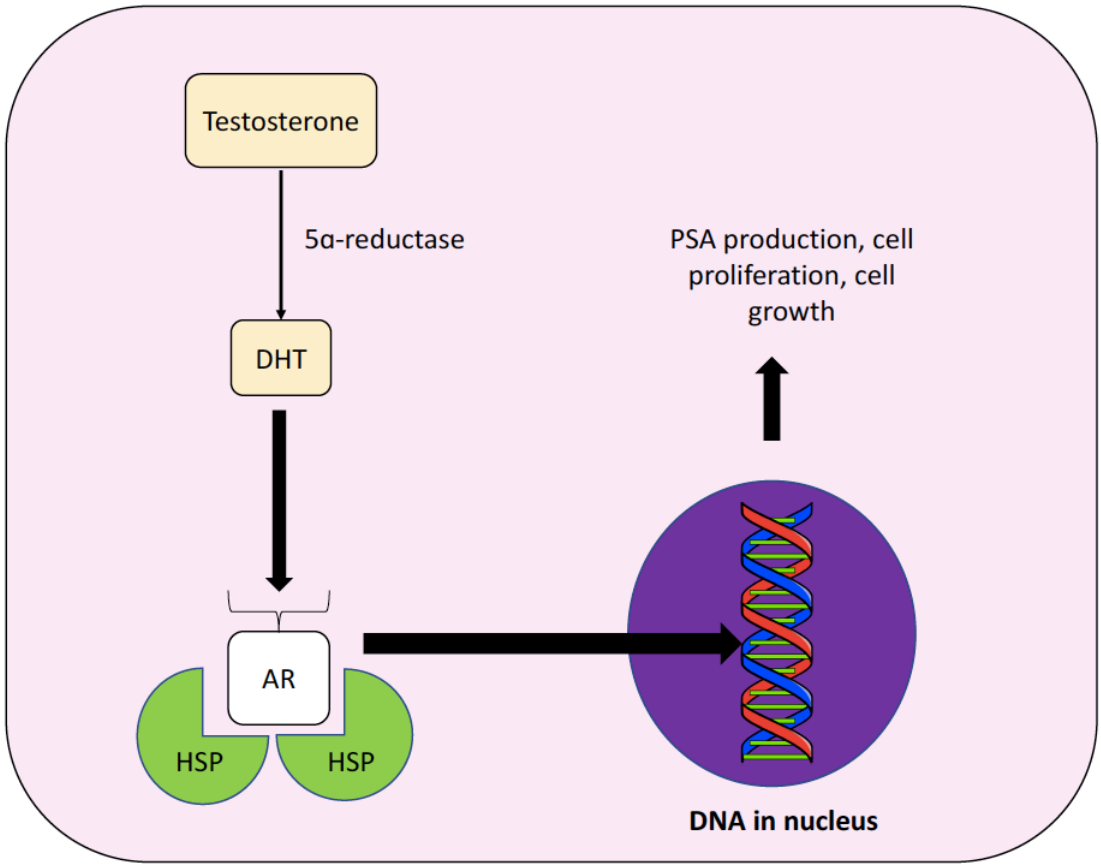

Figure 1.6: Androgen signalling in a prostate epithelial cell.

Testosterone is converted to DHT, which binds to the AR. This causes uncoupling from heat shock proteins and translocation of the AR into the nucleus where it binds to DNA causing transcription of target genes.

AR: Androgen Receptor, DHT: Dihydrotestosterone, HSP: Heat shock protein, PSA: Prostate specific antigen

1.4 Molecular Pathology of Prostate Cancer

Recent advances in molecular techniques have increased our understanding of the molecular underpinnings of PCa development. While much of this research confirmed the central role of androgen signalling in PCa, other discoveries have shown that PCa is a molecularly complex and heterogeneous disease involving numerous other genetic pathways.

Gene fusions

Over 15 years ago, gene fusions were thought to mainly occur in sarcomas and haematopoietic malignancies and were rare in carcinomas. However, a landmark paper

in 2005 demonstrated that recurrent gene fusions involving the E26 transformation-specific (ETS) family of transcription factors occur in over 50% of patients with PCa [28]. These fusions usually result in an androgen-specific promoter juxtaposed with an oncogene. By far the most common recurrent fusion, is the fusion of the 5' promoter element of the Transmembrane Serine Protease 2 (*TMPRSS2*) gene with the 3' element of the ETS-related Gene (*ERG*) [29]. Other 5' partners have been described (Homocysteine Inducible ER Protein with Ubiquitin-like domain 1 [*HERPUD1*], Solute Carrier Family 45 Member 3 [*SLC45A3*] and N-Myc Downstream Regulated 1 [*NDRG1*]) as well as other ETS family 3' partners (ETS Variant 1, 4 and 5 [*ETV1, ETV4, ETV5*] and ETS transcription factor [*ELK4*]) [29]. *TMPRSS2-ERG* fusions are present in the precursor lesion high-grade prostatic intraepithelial neoplasia (PIN) but do not occur in adjacent benign epithelial cells or stromal cells suggesting an early role in carcinogenesis [29]. The underlying cause for this recurrent non-random fusion is unclear but is thought to be related to androgen signalling and the actions of enzymes inducing DNA double-strand breaks. It has been shown *in vitro* that androgen signalling induces proximity of the *TMPRSS2* and *ERG* loci, and also enhances recruitment of enzymes that cause specific DNA double stranded breaks at these loci [30-32]. Although rare, non-ETS related gene fusions can occur in PCa. RAF kinase fusions have been identified in about 1% of PCa and are sensitive to sorafenib, a RAF inhibitor [33].

Other common mutations

A number of other mutations are common in PCa, some of which are almost exclusive to ETS-related gene fusions (Table 1.1).

The Phosphoinositide 3-kinase Protein kinase B (PI3K-AKT) pathway plays an important role in PCa and alterations in this pathway have been identified in up to 40% of primary tumours and 50% of CRPCs [34-36]. The phosphatase and tensin homolog (*PTEN*) gene has a critical role in regulating the PI3K-AKT pathway such that loss leads to downstream activation. *PTEN* inactivation is present in up to 40% of CRPC [37] and correlates with poor prognosis and higher Gleason score [38-41] .

Speckle type POZ protein (*SPOP*) gene mutations occur in approximately 10% of PCa and drive prostate neoplasia through deregulation of the PI3K/AKT and AR pathways [34]. *SPOP* mutations rarely occur in ETS fusion PCa [34].

Serine protease inhibitor Kazal-type 1 (*SPINK1*) encodes a serine protease inhibitor and is overexpressed in around 10% of PCa [42]. *SPINK1* overexpression may be a predictor of biochemical recurrence after resection although there is conflicting evidence regarding this [43]. *SPINK1* tends to occur in ETS-fusion negative PCa, although it can occur in ETS-fusion positive PCa [43].

Chromodomain helicase DNA binding protein 1 (*CHD1*) mutations and deletions occur in about 5-15% of PCa and rarely occur in ETS-fusion positive PCa [44, 45]. *CHD1* plays a role in homologous recombination such that loss of *CHD1* leads to genetic instability. Tumours with *CHD1* loss are sensitive to DNA-damaging therapies such as carboplatin and olaparib [46].

The *TP53* gene is the most commonly mutated gene in human tumours and encodes a transcription factor that activates gene programmes required for cell-cycle arrest, DNA repair and apoptosis [47]. It is mutated in 40% of CRPCs, both ETS fusion positive and negative [48], and is of prognostic significance independent of grade, stage and margin status [49-51].

NKX3.1 is expressed at high levels in normal prostate and is androgen sensitive. *NKX3.1* loss is associated with PCa suggesting it has a tumor-suppressor role [52].

Table 1.1: Common mutations in PCa.

Gene	Can occur in ETS-fusion PCa	Role in PCa
PTEN	Yes	Loss in 40% of CRPC and associated with poor prognosis [39]
SPOP	Rarely	Mutated in 10% of PCa. Deregulates the PI3K/AKT and AR pathways [34]
SPINK1	Rarely	Overexpressed in 10% of PCa [42]
CHD1	Rarely	Mutated in 5-15% of PCa. Plays a role in homologous recombination [46]
TP53	Yes	Mutated in 40% of CRPC [11]
NKX3.1	Yes	Tumor suppressor role [52]

1.5 Treatment of Prostate Cancer

PCa is a clinically heterogeneous disease. On one end of the spectrum are patients with low grade microscopic disease, usually identified after a PSA screening test, who are highly unlikely to suffer any consequences from their cancer [53]. On the other end of the spectrum are patients with aggressive cancer that will spread beyond the prostate if not removed in time [53]. These patients often develop metastatic disease and are hard to treat due to the development of resistance to current therapies. Therefore, the goal for one set of patients is to avoid unnecessary investigation and surgery, while the goal in the other set of patients is to remove the prostate before cancer cells spread beyond it. While Gleason grading and tumour volume help to stratify patients into low and high risk groups, there is currently no reliable way to separate those with low risk disease from high risk disease.

Surgery and radiotherapy

PCa that is confined to the prostate gland is usually managed with surgical excision of the prostate and, depending on biopsy and radiological findings, may also include removal of regional lymph nodes and radiotherapy [54]. Radiotherapy can also be used to treat patients with PCa that has spread into the tissues adjacent to the prostate but has not spread to distant sites (locally advanced PCa) [54].

Androgen deprivation therapy (ADT)

The first major breakthrough in the treatment of PCa came from Nobel prize-winning work in the 1940s showing that PCa could be treated by removing the testes, proving that PCa cells are dependent on androgen production for growth and survival [55]. Blocking androgen synthesis continues to be the mainstay of treatment in patients with advanced PCa, although this is now achieved through chemical rather than surgical means [56]. Luteinising hormone-releasing hormone (LHRH) agonists and LHRH antagonists suppress luteinising hormone (LH) production through different feedback mechanisms resulting in suppression of testosterone production by the testes. This leads to decreased androgen stimulation of the prostate, lower levels of PSA and improvement in symptoms [57]. ADT may be given post-operatively to patients with high Gleason grade, locally advanced PCa or positive surgical margins [54]. ADT also forms the basis for the treatment of patients with metastatic or recurrent PCa [56]. Some patients with metastatic disease at presentation may also be offered docetaxel chemotherapy [58]. Although initially effective, resistance inevitably develops to ADT in nearly all patients.

Abiraterone and Enzalutamide

Abiraterone and enzalutamide are newer "second generation" anti-androgens developed to overcome the resistance to LHRH agonists and antagonists. Abiraterone inhibits the Cytochrome P450 family 17 (*CYP17*) gene, which results in the blockage of the synthesis of androgens in the tumour as well as in the testis and adrenal glands [59]. Enzalutamide binds to the ligand-binding domain of the AR competing with, and displacing testosterone and DHT. This inhibits the translocation of AR into the nucleus and prevents transcriptional activation of androgen-responsive target genes [60]. Studies have shown improved survival for men with PCa treated with these drugs [59, 60]. However, like first generation anti-androgens, resistance to abiraterone and enzalutamide develops in nearly all men. Approximately 30-40% of men will be intrinsically resistant to these therapies whereas the remainder acquire resistance over the course of their treatment (secondary resistance).

Resistance to ADT and second generation anti-androgens

Understanding the mechanisms underpinning the development of resistance to anti-androgen therapies is a key area in PCa research. It was previously thought that resistance occurred due to PCa cell growth becoming non-responsive to AR signalling. However, recent research has shown that CRPC remains strongly dependent on AR signalling in most cases [11]. There are a number of proposed mechanisms for how the AR continues to signal despite castration levels of androgens:

1. Androgens are produced from other sources apart from the testes negating the effects of LHRH agonists and antagonists. The adrenal gland produces androgens, which can be converted into DHT resulting in AR signalling. Also, PCa cells themselves have been shown to produce androgens [61, 62].

2. The AR becomes more sensitive to low levels of androgens. AR gene amplification in the setting of ADT results in increased expression of the AR protein and increased activation by lower levels of androgens. AR gene amplification is present in approximately 20-30% of CRPC but is not observed in hormone dependent disease [63, 64].

3. AR mutations may enhance the number of mediators that can bind to the AR. Other steroids, such as oestrogen, may therefore be able to bind to the mutated AR allowing continued AR signalling. Some AR mutations alter the effect of enzalutamide causing a switch from an antagonist to an agonist effect [65]. AR mutations are present in up to 50% of CRPC but absent in localised disease [66].

4. AR splice variants are alternatively spliced variants of AR mRNA resulting in the encoding of alternative forms of the AR protein. AR splice variant-7 (AR-V7) is an AR splice variant that encodes a protein lacking the ligand-binding domain but retaining the transcriptionally active domain [67]. Therefore, AR-V7 protein may be constitutively active in a ligand-independent manner, driving CRPC growth despite enzalutamide or abiraterone treatment [68]. The detection of AR-V7 in circulating tumour cells (CTCs) is associated with resistance to enzalutamide and abiraterone in CRPC [67]. Also, patients

with detectable AR-V7 mRNA or protein do not benefit from enzalutamide or abiraterone treatment [69, 70].

5. True AR independence may occur in a subset of patients with CRPC. AR-independent PCa is usually very aggressive and is associated with neuroendocrine features. There is still debate about whether AR-independent PCa is the result of transdifferentiation of AR-positive PCa cells or due to proliferation of an AR-negative PCa clone [71].

Epigenetic alterations are also thought to play a role in the development of resistance in PCa [72]. Mechanisms through which this occurs include chromatin remodelling, DNA methylation and regulation of the RNA splicing machinery [72]. Non-coding RNAs impart some of their functions through regulation of chromatin and cell trafficking [73] and have increasingly been associated with drug resistance in many other types of cancer [74-76].

1.6 Long non-coding RNAs

Approximately 70-90% of the human genome is transcribed into RNA but only roughly 2% of the genome encodes for protein [77]. This means that the vast majority of human RNA transcripts are non-coding. Initially thought to be mostly “junk” RNA, recent discoveries have demonstrated roles for non-coding RNAs in almost all aspects of cell biology [78]. Non-coding RNAs are broadly divided into two categories: small non-coding RNAs, <200 nucleotides long, and long non-coding RNAs (lncRNAs), > 200 nucleotides long [79]. The most studied class of non-coding RNAs are microRNAs (miRNAs), a subclass of small non-coding RNAs of 18 to 25 bases in length, which play a key role regulating post-translational gene expression [80].

LncRNAs are a much less studied class of non-coding RNA. Over 100,000 lncRNAs have been identified in the human genome to date [81], but the number of functional lncRNAs, and what those functions are, remains largely unknown. LncRNAs are roughly divided into five categories: sense lncRNAs that overlap exons of another transcript on the same strand, antisense lncRNAs that overlap exons on the opposite strand, intergenic lncRNAs that lie between two genes, bidirectional lncRNAs that are transcribed

simultaneously to coding transcripts on the opposite strand and intronic lncRNAs that are located within the introns of a coding transcript [78, 79].

Upon transcription, lncRNAs can fold into three dimensional structures allowing interaction with proteins, RNA and lipids [82]. LncRNAs exhibit both nuclear and cytoplasmic localisation and are involved in the regulation of key cellular processes including transcription, translation, cell cycle regulation, cellular differentiation and nuclear-cytoplasmic trafficking (Figure 1.7) [73, 83]. The mechanisms through which this regulation is achieved are incompletely understood but include transcriptional interference, recruitment of chromatin remodelling complexes to specific gene loci and by acting as competing endogenous RNAs [78]. Competing endogenous RNAs bind with miRNAs and liberate miRNA targets from negative regulation. Given that miRNAs play a key role in regulating human mRNAs, the activity of competing endogenous RNAs may indirectly regulate a significant proportion of human protein-coding genes [80]. Aberrant expression of lncRNAs also appears to play a considerable role in human tumorigenesis [84, 85]. LncRNAs have been shown to regulate key functions in cancer cells including sustained proliferative signalling, replicative immortality, invasion and metastasis, evasion of growth suppressors, induction of angiogenesis and resistance to apoptosis [86].

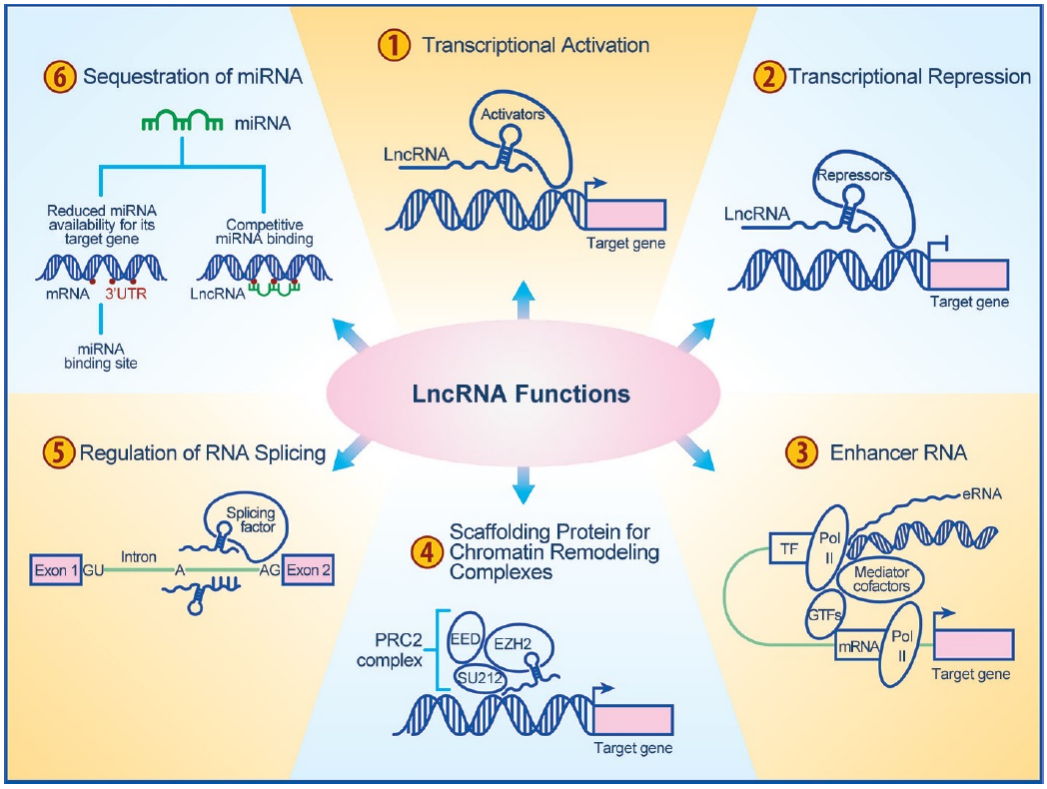

Figure 1.7: Overview of lncRNA functions.

(Source: Malik *et. al,* Long noncoding RNAs in prostate cancer: overview and clinical implications. Asian Journal of Andrology; 2016)

1.7 Long non-coding RNAs in Prostate Cancer

Although the field of lncRNA research is in its early stages, many lncRNAs have been identified that appear to play a role in prostate carcinogenesis. A literature review revealed 86 lncRNAs associated with PCa or the AR (Table 1.2). This section will highlight a selection of lncRNAs that might contribute to drug resistance in PCa (extensively reviewed in Aird *et. al* [87]).

A number of lncRNAs have been associated with the upregulation of the AR, including HOX Transcript Antisense RNA (*HOTAIR*), C-terminal binding protein 1 antisense (*CTBP1-AS)*, Prostate cancer gene expression marker 1 (*PCGEM1)* and *PlncRNA1* (Figure 1.8). *HOTAIR* is repressed by androgens and is therefore upregulated after ADT [88]. *HOTAIR* binds to the N-terminal domain of the AR, preventing the ubiquitination and degradation of the AR, thus resulting in increased AR expression [88]. *HOTAIR* overexpression can also induce an AR-binding profile similar to that induced by androgens, resulting in AR

signalling in the absence of androgens [88]. *CTBP1-AS* indirectly regulates the AR by interacting with the protein coding gene C-terminal binding protein 1 (*CTBP1)* [89]. *CTBP1* negatively regulates the AR by inhibiting AR-mediated demethylation [89]. *CTBP1-AS* upregulation (which can occur after ADT) results in downregulation of *CTBP1* leading to upregulation of the AR [89]. *PlncRNA1* protects the AR from miRNA-mediated suppression by acting as a sponge for certain AR targeting miRNAs such as miR-34c and miR-297 [90]. The lncRNA Growth arrest specific 5 (*GAS-5*) negatively regulates the AR by binding to the DNA-binding domain of the AR, thus preventing it from binding to target genes [91]. Overexpression of *GAS-5* is associated with decreased PCa cell progression *in vitro* and reduced tumour growth *in vivo* through inactivation of the PI3K-AKT pathway [92].

The AR itself also regulates the expression of lncRNAs. AR activation upregulates lncRNAs Prostate cancer associated transcript 18 (*PCAT18*) and Suppressor of cytokine signalling 2 antisense (*SOCS2-AS1*) resulting in enhanced PCa cell proliferation, migration and invasion [93, 94]. AR signalling downregulates the expression of lncRNAs such as Downregulated RNA in androgen independent cells (*DRAIC*), Prostate cancer associated transcript 14 (*PCAT14*) and Prostate cancer associated transcript 29 (*PCAT29*), lncRNAs that are associated with favourable outcomes in PCa [93, 95, 96].

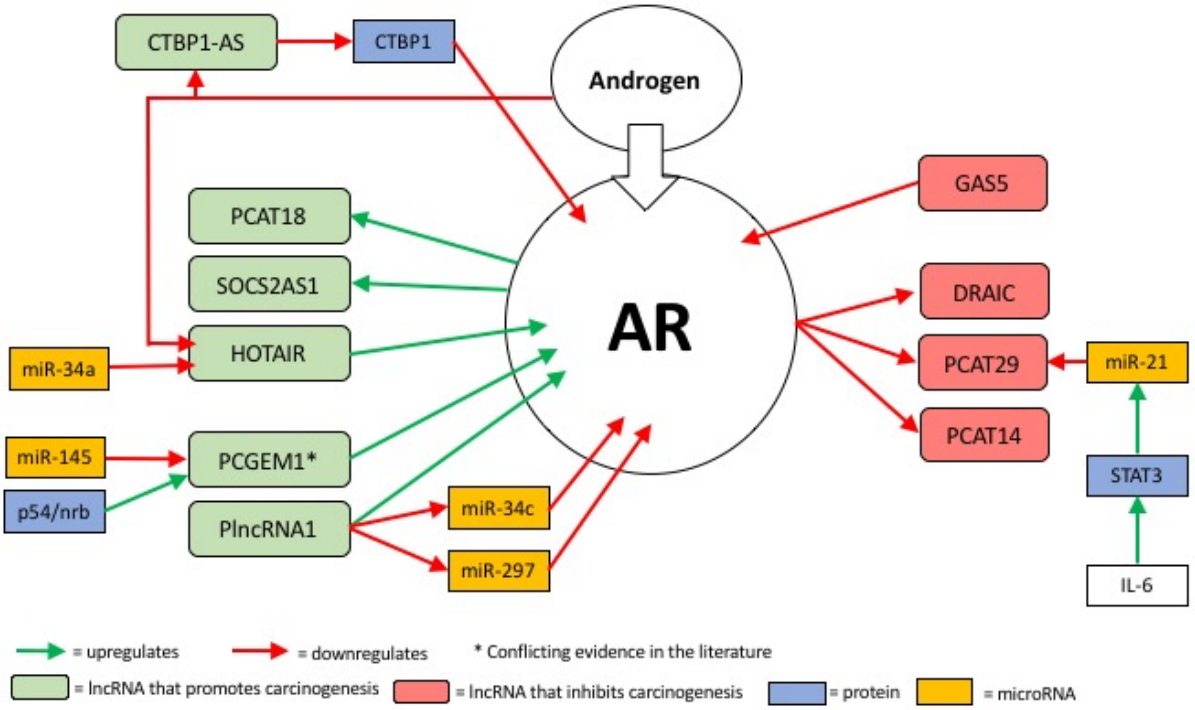

Figure 1.8: lncRNAs associated with the androgen receptor.

(Source: Aird *et. al,* Carcinogenesis in prostate cancer: the role of long non-coding RNA. Noncoding RNA Res. 2018 Mar; 3(1): 29–38.)

Table 1.2: lncRNAs associated with Prostate Cancer.

lncRNA	Association with PCa
AFAP1-AS1	Promotes PCa cell proliferation [97]
ANRIL	Promotes PCa cell proliferation [98]
ARLNC1	Associated with AR signalling [99]
ARNILA	Downregulated by the AR [100]
BCAR4	Upregulated in CRPC [101]
BDNF-AS	Downregulated in PCa [102]
BRE-AS1	Downregulated in PCa [103]
CCAT2	Upregulated in PCa [104]
CHRF	Promotes EMT and cell proliferation [105]
CTBP1-AS	Upregulates the AR [89]
DANCR	Upregulated in PCa [106]
DRAIC	Prevents the migration of PCa cells [95]
FALEC	Upregulated in PCa [107]
FENDRR	Downregulated in PCa [108]
FEZF1-AS1	Activates Notch signalling pathway [109]
FOXC2-AS1	Upregulated in PCa [110]
FOXP4-AS1	Upregulated in PCa [111]
GAS5	Downregulated in PCa [112]
GASL1	Inhibits growth in PCa [113]
GHET1	Promotes PCa cell proliferation [114]
HCG11	Downregulated in PCa [115]
HOTAIR	Promotes AR signalling [88]
HOTTIP	Promotes PCa cell proliferation [116]
HULC	Promotes EMT in PCa [117]
IGF2AS	Tumor suppressor role [118]
LEF1-AS1	Promotes AR expression [119]
LINC00304	AR regulated, promotes proliferation [120]
LINC00518	Promotes paclitaxel resistance [121]
LINC00662	Promotes PCa growth [122]
LINC00683	Downregulated in PCa [123]
LINC00844	Promotes PCa through AR signalling [124]
LINC01296	Promotes PCa cell proliferation [125]
LINC01638	Promotes PCa cell proliferation [126]
LINP1	Promotes PCa, regulates p53 [127]
LincRNA-p21	Suppresses PCa development [128]
LncRNA-ATB	Promotes EMT [129]
LncRNA-LBCS	AR regulator, inhibits CRPC [130]
LOC283070	Promotes PCa cell proliferation [131]
LOC400891	Promotes PCa progression [132]
LOC440040	Promotes PCa progression [133]
LOXL1-AS1	Promotes PCa cell proliferation [134]
LUCAT1	Promotes PCa cell migration [135]
MALAT-1	Suppresses PCa progression [136]
MEG3	Inhibits PCa cell proliferation [137]

Table 1.2 continued

lncRNA	Association with PCa
MIR222HG	Promotes development of CRPC [138]
MYU	Promotes PCa cell proliferation [139]
NAP1L6	Promotes PCa progression [140]
NEAT1	Promotes PCa progression [141]
PANDAR	Promotes PCa progression [142]
PART1	Modulates Toll-like receptors [143]
PCA3	Promotes PCa cell invasion and metastasis [144]
PCAT1	Promotes PCa cell proliferation [145]
PCAT5	ERG regulated and upregulated in CRPC [146]
PCAT14	Low expression associated with poor outcomes [147]
PCAT18	AR regulated and upregulated in PCa [93]
PCAT19	Promotes PCa growth and metastasis [148]
PCAT29	Tumor suppressor, repressed by the AR [149]
PCAT92	Upregulated in PCa [150]
PCGEM1	AR regulated and upregulated in PCa [151]
PCSEAT	Upregulated in PCa, associated with EZH2 [152]
PlncRNA-1	Causes upregulation of the AR [90]
POTEF-AS1	AR regulated and promotes PCa cell growth [153]
PRNCR1	Upregulated in PCa [154]
PSLNR	Inhibits PCa progression through p53 pathway [155]
PVT1	Upregulated in PCa, regulates tumour growth [156]
RNCR3	Promotes PCa progression [157]
SAP30L-AS1	Promotes PCa growth by repressing *SAP30L [158]*
SARCC	Modulates the AR in renal cell carcinoma [159]
SChLAP1	Upregulation associated with poor outcomes [160]
SLNCR	Binds to the AR in melanoma [161]
SNHG1	Promotes PCa cell proliferation [162]
SNHG6	Upregulation predicts poor prognosis [163]
SNHG7	Promotes PCa cell proliferation [164]
SNHG12	Promotes PCa cell proliferation [165]
SNHG15	Promotes PCa cell proliferation and EMT [166]
SOCS2-AS1	AR regulated and overexpressed in CRPC [94]
SPRY4-IT1	Enhances PCa cell invasion and proliferation [167]
TINCR	Tumour suppressor role, modulates *TRIP13 [168]*
TMPO-AS1	Overexpression correlates with poor prognosis [169]
TRPM2-AS	Overexpression correlates with poor prognosis [170]
TTTY15	Upregulated in PCa tissue [171]
TUC338	Overexpressed in PCa [172]
TUG1	Promotes PCa cell invasion [173]
UCA1	Upregulation associated with poor prognosis [174]
XIST	Tumour suppressor, modulates *RKIP* expression [175]
ZEB1-AS1	Promotes PCa cell proliferation and migration [176]

1.8 Aims and Objectives

The overall aim of this project is to utilise a human prostate cancer isogenic cell model of enzalutamide resistance to identify molecular events occurring in the development of resistance to enzalutamide. By using this model, we hope to identify novel lncRNAs and mRNAs associated with enzalutamide resistance. Enzalutamide resistance is a major problem in the treatment of PCa, eventually occurring in all patients. The mechanisms underlying enzalutamide resistance are only partially understood and there is currently no way to prevent it. Identifying novel lncRNAs and mRNAs will add to the body of knowledge on enzalutamide resistance and may form the basis of treatment strategies to circumvent enzalutamide resistance. This would have profound implications on the treatment of patients with PCa.

Another clinically relevant outcome from this project may be the development of a biomarker for enzalutamide resistance. At present, it is difficult to tell when a patient has become resistant to enzalutamide and impossible to identify patients who do not benefit from enzalutamide treatment whatsoever (primary resistance). The development of a blood or urine test for enzalutamide resistance would be very beneficial as it would allow clinicians to switch to a more useful drug and reduce the futile use of an expensive medication.

The specific aims of this project are:

- To compare the expression of lncRNAs and mRNAs in enzalutamide sensitive and enzalutamide resistant cells using microarray technology

- To validate highly ranked mRNA and lncRNA microarray patterns at the transcript level

- To determine the effect of modifying the expression of selected lncRNAs on enzalutamide sensitivity

Chapter 2
Materials and Methods

2.1 Preparation and handling of materials

Reagents and chemicals used in the laboratory were of analytical grade and stored in accordance with manufacturers' instructions. All chemicals and waste resulting from any experiments was disposed of according to local guidelines.

2.2 Cell lines

The main cell lines used in this project were LNCaP clones displaying varied resistance to enzalutamide (obtained from Novartis, Dublin, Ireland). RNA from a panel of seven human prostate cell lines (RWPE-1, PWR-1E, BPH-1, VCaP, DU 145, 22Rv1 and PC3; obtained from the American Tissue Culture Collection [ATCC-LGC Standards, Middlesex, UK]) and three non-prostate cell lines (MCF7, H1975 and HuH7) were also used, described below. H1975 was a kind gift from Dr. John D. Minna (UT South Western, USA), MCF7 was a kind gift from Dr. Paul Spiers (Trinity College, Dublin, Ireland) and HuH7 was obtained from the Japanese Collection of Research Bioresources Cell Bank.

LNCaP cell line

LNCaP cells are PCa cells derived from the left supraclavicular lymph metastasis of a 50 year old Caucasian man in 1977. They are sensitive to androgens, grow readily *in vitro* (doubling time of approximately 60 h) and tumour development correlates with serum androgen levels in mice [177].

LNCaP clones displaying varied resistance to enzalutamide

We obtained an isogenic cell line model of LNCaP cells with varied resistance to enzalutamide, previously described by *Korpal et. al* [65]. Long-term culture (90 days) of LNCaP cells with 1 µmol/L of enzalutamide led to the emergence of resistant clones. These clones were isolated and expanded. Testing revealed clones that were strongly resistant to enzalutamide and clones that were weakly resistant to enzalutamide. There was no significant change in AR expression levels or AR nuclear localisation between the resistant clones and the controls. The resistant clones could also maintain AR pathway activity. The main difference between the groups identified by *Korpal et. al* was the presence of a specific mutation in the AR (F876L mutation) in all strongly resistant clones but not in the weakly resistant clones or in the controls. In addition, they showed that

this AR mutation confers agonist activity to enzalutamide. This finding was corroborated by *Joseph et. al* and *Balbas et. al* [178, 179]. The F876L mutation (now called the F877L mutation) leads to an amino acid substitution in the ligand binding domain of the AR. We obtained three cell lines - Control (enzalutamide sensitive), Clone 9 (weakly resistant to enzalutamide) and Clone 1 (strongly resistant to enzalutamide). Cells were cultured in complete RPMI-1640 Medium (Sigma Aldrich, Missouri, USA) supplemented with 10% (v/v) foetal bovine serum (FBS), penicillin-streptomycin (10,000 units penicillin and 10 mg/mL streptomycin) and L-glutamine (200 mM). Supplements were obtained from Sigma Aldrich.

RWPE-1

RWPE-1 is a human prostate epithelial cell line derived from the peripheral zone of a histologically normal adult human prostate. The cells were transfected with a single copy of the human papilloma virus 18 (HPV-18) to establish the cell line [180].

PWR-1E

PWR-1E is a human prostate epithelial cell line derived from a normal prostate with mild hyperplasia. The cells were immortalised with an adenovirus 12-SV40 hybrid virus (Ad12-SV40) [181].

BPH-1

BPH-1 is an epithelial cell line developed from benign human prostate tissue obtained by transurethral resection.

VCaP

This line was established in 1997 from a vertebral bone metastasis from a patient with hormone refractory PCa. It was passaged as xenografts in mice then cultured *in vitro*. It is androgen sensitive *in vitro* and *in vivo*.

DU 145

DU 145 is human prostate carcinoma epithelial cell line that is not hormone sensitive and is only weakly positive for acid phosphatase. The cells do not express PSA.

22Rv1

22Rv1 is a human prostate carcinoma epithelial cell line derived from a xenograft that was serially propagated in mice after castration-induced regression and relapse of the parental, androgen-dependent CWR22 xenograft.

PC-3

The PC-3 cell line was initiated from a bone metastasis of a grade IV prostatic adenocarcinoma from a 62-year-old male Caucasian. It does not express androgens.

MCF7

MCF7 is a human breast cancer cell line (invasive ductal carcinoma) isolated in 1970 from a 69-year-old Caucasian woman. The cells are positive for oestrogen receptor (ER) and progesterone receptor (PR) but do not have *HER2* overexpression.

H1975

H1975 is a human lung adenocarcinoma cell line established in 1988 from a non-smoking female. H1975 cells are positive for the T790M epidermal growth factor receptor (EGFR) mutation, which confers resistance to tyrosine kinase inhibitor therapies.

HuH7

HuH7 is a well differentiated hepatocellular carcinoma cell line, originally taken from the liver of a 57-year-old Japanese male in 1982. Androgen signalling is important in hepatocellular carcinoma and HuH7 cells express the AR [182]. The cells also have a point mutation in the *TP53* gene.

2.3 Cell culture

Cell culture conditions

Cell culture work was performed aseptically in accordance with good laboratory practice in a laminar air flow unit (LAF). The LAF was allowed to run for at least 20 min prior to use and sanitised using 70% industrial methylated spirits (IMS) in dH_2O. Cell culture

reagents were warmed in a 37°C incubator for approximately 30 min prior to use, unless stated otherwise. All cells were cultured in a 5% CO_2 humidified atmosphere (Forma™ Steri-Cycle™ CO_2 Incubator, Thermo Fisher Scientific, Massachusetts, USA).

Propagation of cells from storage

Complete media was warmed to 37°C. Cells were removed from storage and thawed rapidly in a 37°C water bath for 2 min. Once thawed, the cells were added to 9 mL complete media in a 15 mL tube. The cells were then centrifuged at 300 χ g for 5 min. The supernatant was decanted and the cell pellet was re-suspended in 1 mL warmed complete media. The cells were added to a tissue culture flask with the required volume of media. The cells were incubated in a humidified atmosphere at 37°C with 5% CO_2.

Cell sub-culture

Cells were visualised daily using an inverted phase-contrasted microscope (Nikon Corp., Tokyo, Japan). Sub-culturing was performed when cell cultures reached 80-90% confluency. Cell culture medium was decanted and the cells were washed with 5 mL 1X Dulbecco's Phosphate Buffered Saline (PBS) (Sigma-Aldrich) to remove residual FBS. One mL trypsin ethylene-diamine tetra-acetic acid (EDTA) (Sigma-Aldrich) was added to the flasks. Flasks were incubated at 37°C for approximately 5 min to remove adherent cells from the surface. Nine mL complete medium was then added to the flasks to inactivate the trypsin. Cells were transferred to a sterile 15 mL tube and pelleted by centrifugation at 1300 χ g for 3 min in a Thermo IEC Centra GP8-R centrifuge (Thermo Fisher Scientific). The supernatant was discarded and the cell pellet re-suspended in 10 mL complete medium. This suspension was used to seed fresh flasks at a number of different densities.

Cell counting

Cells were seeded at specific densities depending on experimental set up. A bright line haemocytometer (Paul Marienfeld GmbH & Co. KG, Lauda-Königshofen, Germany) was used in conjunction with Trypan Blue (0.4% v/v) (Sigma-Aldrich) for cell counting and viability. Cells were pelleted as above and re-suspended in a specific volume of media until a single cell suspension was obtained. A 20 µL aliquot of this suspension was added

to 180 µL Trypan Blue and mixed. A coverslip was placed on the haemocytometer. The edge of the cover slip was touched gently by a pipette tip and the chamber filled by capillary action. The number of cells/mL was calculated using the following equation:

Average no. of cells counted x 10,000 x 10 = no. of cells/mL

10,000 equals the µL volume under the cover slip and 10 equals the dilution factor.

Cryopreservation

Cells were trypsinised and counted as described previously, and re-suspended in Cellbanker® cryopreservation media (AMS Biotechnology, Abingdon, UK) at a concentration of 1-1.5 x 10^6 cells/mL. Aliquots were stored at -80°C.

Mycoplasma testing

At 70-80% cell confluence, media was removed from T75 cm^3 flasks for mycoplasma testing. Prior to use, the cell supernatant was centrifuged at 300 χ g to remove cellular debris. A polymerase chain reaction (PCR) based assay adapted from Young *et al.* [183], was used to determine the presence/absence of mycoplasma. The primers were designed to encompass common mycoplasma species:

FWD 5´ - GGGAGCAAACAGGATTAGATACCCT-3´;

REV 5´ - TGCACCATCTGTCACTCTGT TAACCTC-3´

The PCR reaction consisted of the following: 12.5 µL Green 2X DreamTaq PCR Master Mix (Thermo Fisher Scientific), 0.5 µL FWD primer (10 µM) (Merck KGaA, Darmstadt, Germany), 0.5 µL REV primer (10 µM) (Merck KGaA) and 10.5 µL DNase free water (Thermo Fisher Scientific). The total reaction volume was 25 µL, which included 1 µL cell supernatant. The PCR reaction was run under the conditions laid out in Table 2.1. The resulting PCR products were electrophoresed on a 2.5% agarose gel. A PCR negative control and a known mycoplasma positive control were included. A band at 270 bp was indicative of a positive result. All cell lines were examined for mycoplasma infection after propagation from storage and every 3 months thereafter.

Table 2.1: PCR conditions for Mycoplasma testing.

Temperature	Time
95°C	5 min
94°C	30 s
55°C	30 s
72°C	1 min
	40 cycles
72°C	10

2.4 RNA isolation and quantification

Homogenisation

The cell culture supernatant was decanted and adhered cells were directly lysed by adding 1 mL TRI Reagent® (Sigma-Aldrich) to the flask surface and cells were dislodged with a cell scraper (Thermo Fisher Scientific). The cell lysate was mixed several times using a pipette tip.

Phase separation

One hundred µL 1-bromo-3-chloropropane (Sigma-Aldrich) was added to the cell lysate, vortexed vigorously for 15 s and then incubated at room temperature for 5 min. The samples were centrifuged at 12,000 χ g for 15 min at 4°C resulting in separation into an interphase and red phenol phase (containing DNA and protein), and an upper aqueous phase containing RNA.

RNA precipitation

The upper aqueous phase was carefully transferred into a fresh tube without disturbing the interphase. To precipitate the RNA from the aqueous phase, 500 µL isopropanol (Merck KGaA) was added to the sample. The sample was mixed and incubated for 5 min at room temperature. The sample was centrifuged at 12,000 χ g for 15 min at 4°C.

RNA wash

The precipitate was removed and the RNA pellet was washed with 1 mL 70% Ethanol (EtOH) (Merck KGaA). The sample was then centrifuged at 12,000 χ g for 10 min at 4°C.

RNA solubilisation

The EtOH was removed and a repeat pulse centrifuge step was performed. Surplus EtOH was removed and the pellet was allowed to air dry for 20 min. The sample was re-suspended in molecular grade water and stored at –80°C.

RNA quantification

RNA was quantified using a NanoDrop 1000 spectrophotometer (Thermo Fisher Scientific). The instrument was first initialised and blanked with 1 µL molecular grade water (Thermo Fisher Scientific). One µL of each sample was loaded individually onto the NanoDrop. The instrument was cleaned between each sample. The NanoDrop returned the nucleic acid concentration in ng/µL and also the 260:280 and 260:230 purity ratios. A 260/280 ratio of ~1.8 is generally accepted as "pure" for DNA; a ratio of ~2.0 is generally accepted as "pure" for RNA.

RNA integrity testing

RNA integrity was confirmed with agarose gel electrophoresis.

2.5 Gene expression analysis

DNase treatment

DNase I (Sigma-Aldrich) is designed to remove contaminating DNA from RNA preparations, and to subsequently remove the DNase and divalent cations from the sample. One µL 10X reaction buffer and 1 µL DNase I, amplification grade, 1 unit/µL was added to 2500 ng RNA in 8 µL molecular grade water. Samples were mixed gently and incubated at room temperature for 15 min. One µL Stop Solution was added to bind calcium and magnesium ions and to inactivate the DNase I. The sample was then heated at 70°C for 10 min.

cDNA synthesis for gene expression analysis

cDNA was synthesised on ice using an All-in-One cDNA Synthesis SuperMix kit (Bimake, Houston, TX, USA). After DNase treatment, 2.75 µL 5X qRT SuperMix was added to the RNA. The tube contents were mixed gently and incubated at 25°C for 10 min, 42°C for 90 min, and then 85°C for 10 min. The tube was chilled on ice until the contents reached

room temperature. Samples were diluted to a final volume of 40 µL using molecular grade water and stored at -20°C until use.

End-point PCR

End-point PCR reactions consisted of the following: 10 µL Green 2X DreamTaq PCR Master Mix (Thermo Fisher Scientific), 1 µL FWD primer (5 µM), 1 µL REV primer (5 µM) and 7 µL molecular grade water (Thermo Fisher Scientific). The total reaction volume was 20 µL, which included 1 µL cDNA. The negative control for each reaction consisted of 1 µL molecular grade water substituted for cDNA. The PCR reaction was run under the conditions laid out in Table 2.2 unless otherwise specified. The resulting PCR products were electrophoresed on a 2% agarose gel.

Table 2.2: PCR conditions for end-point PCR reactions

Temperature	Time
95°C	5 min
95°C 62°C 72°C	10 s 45 s 30 s 35 cycles
72°C	7 min

Agarose gel electrophoresis

PCR products were visualised on 2% agarose gels using the LABREPCO Horizon® 58 Agarose Gel Electrophoresis Apparatus (Lab Rep Co, Horsham, PA, USA). Agarose (Sigma-Aldrich) was dissolved in Tris-Acetate-EDTA (TAE) buffer (40 mM Trizma base, 20 mM acetic acid, 1 mM EDTA) by boiling in a microwave for 2- 3 min. Four µL ethidium bromide was added to the cooled solution. The solution was poured into a gel tray with well forming combs and allowed to set. One volume of 6X DNA Loading Dye (Thermo Fisher Scientific) was added to the PCR sample and loaded on to the gel if required. A DNA ladder (Thermo Fisher Scientific) was also added to the gel. Electrophoresis of the samples was carried out using 1X TAE as running buffer. The voltage was kept constant at 80 V and gels electrophoresed for approximately 30 min. The bands were visualised and

photographed under UV light using a Fusion Fx System (Vilber Lourmat, Collegien, France).

Quantitative reverse transcription PCR (RT-qPCR)

cDNA was generated using the protocol previously described (Section 2.5). RT-qPCR was carried out on the PCRmax Eco 48 Real-Time qPCR System (PCR max, Staffordshire, UK). The expression of target gene transcripts was determined using SYBR Green PCR Master Mix (Thermo Fisher Scientific). Each PCR reaction was carried out in a final volume of 20 µL containing 10 µL 2X SYBR Green Master Mix, 1 µL (5 µM) FWD and REV primers, 7 µL molecular grade water and 1 µL cDNA. PCR amplification was performed according to the conditions laid out in Table 2.3. Data were analysed using the ΔΔCt method with values normalised to 18S rRNA levels.

Table 2.3: PCR conditions for RT-qPCR reactions.

Temperature	Time
95°C	5 min
95°C 62°C	10 s 45 s } 35 cycles

2.6 Primers

Custom designed primers were used for validation of microarray data and for cloning experiments. The designs were based on sequences provided by Arraystar Inc. or in published studies (Table 2.4). Primers were purchased from Sigma-Aldrich and Integrated DNA Technologies, Leuven, Belgium. On receipt, the primers were pulsed on a vortex and re-suspended in molecular grade water to a concentration of 100 µM. Primers were further diluted to 5 µM before use.

Table 2.4: Primer designs.

Primer Name	Sequence (5’ to 3’)
AR-FL Forward	CAGCCTATTGCGAGAGAGCTG
AR-FL Reverse	GAAAGGATCTTGGGCACTTGC
AR-V7 Forward	CCATCTTGTCGTCTTCGGAAATGTTA
AR-V7 Reverse	TTTGAATGAGGCAAGTCAGCCTTTCT
CTAG1B Forward	CCAGGGGTGCTTCTGAAGGA
CTAG1B Reverse	GCACTGCGTGATCCACATCA
DGCR5 Forward	CCGATCAGCAGGTGAAAGCG
DGCR5 Reverse	GTGCGCTCACCATCGACGTAT
DGUOK-AS1 Forward	CCTTGCTAGAGGAGGAAGCCC
DGUOK-AS1 Reverse	TGCACATCCAATTATGCTTCCTG
DPP10-AS1 Forward	CCGAATCCAGCCCAGATTCT
DPP10-AS1 Reverse	AGTGCCTTCAGGTGGCTGT
FLJ26850 Forward	TGATGGGCACCTGGTACCTG
FLJ26850 Reverse	TCGGGTTGTGTGGGTTCAAAT
PCDH7 Forward	CCGTACAAGATCTACCACCAGC
PCDH7 Reverse	CAGTAATGTATGGATGTAGACGCAT
PEG10 Forward	GCTGGCTGAGCACACATGAT
PEG10 Reverse	CTACTGGATAATAGAGTGGCGGTTG
PITX2 Forward	CTTGCGAGCAAGGGAGTGTA
PITX2 Reverse	ACACAGGGTAGGTTGTACATAGCAG
RP11-1C8.7 Forward	AAGTGGCACCTGGGAAAACA
RP11-1C8.7 Reverse	GGGTCTGTCATCACTTCCATTTG
RP11-222K16.2 Forward	AGGCGAATGGGAAAGGAAAG
RP11-222K16.2 Reverse	AATCTCTGCGGGTGTCATGG
SARCC Forward	AAAACCATGATGTTGCCGCT
SARCC Reverse	AGCAGATTTCACAGGCTCCT
SARCC Cloning Forward	GCTCGGATCCATGATGATTGAAGTATGTTTATTGTAAG
SARCC Cloning Reverse	TAGACTCGAGCTACCATGTTTCATAGTTTTATTGAGTC
SPINK1 Forward	AACACTGGAGCTGACTCCCTG
SPINK1 Reverse	GGCCCAGATTTTTGAATGAGG
SPRY4-IT1 Forward	AGCCACATAAATTCAGCAGA
SPRY4-IT1 Reverse	CGATGTAGTAGGATTCCTTTCA

2.7 Microarray

General background:

RNA was shipped to Arraystar Incorporated, Maryland, USA for evaluation. Arraystar microarrays are designed for global gene expression profiling of both lncRNAs and mRNAs on the same array. Arraystar Human LncRNA Microarray v4.0 detects 40,173 lncRNAs. The lncRNAs are constructed using public transcriptome databases (Refseq, UCSC knowngenes, GENCODE, LncRNAdb, RNAdb, NRED, lincRNA catalogues [184-186], ENCODE CAGE Clusters), Arraystar lncRNA collection pipelines and landmark publications up until 2015. The microarray also includes an entire collection of 20,730 protein coding mRNAs. Each RNA transcript is detected by a splice junction-specific probe or a unique exon sequence, such that the individual transcripts are reliably and accurately detected. Positive probes for housekeeping genes and negative probes are printed on the array for hybridisation quality control.

RNA preparation

Control, Clone 9 and Clone 1 cell lines were cultured as previously described (Section 2.3). One µL dimethyl sulfoxide (DMSO) was added to Control 1 cells for 24 h prior to RNA extraction. DMSO served as the vehicle control. One µM enzalutamide was added to both Clone 1 and Clone 9 for 24 h prior to RNA extraction. Total RNA was extracted as previously described (Section 2.4), dried down using RNAStable (Biomatrica, California, USA) and sent to Arraystar.

Labelling and Hybridisation

Each sample was amplified and transcribed to fluorescent cRNA along the entire length of the transcripts with 3' bias utilising a random priming method (Arraystar Flash RNA Labelling Kit, Arraystar). The labelled cRNAs were hybridized onto the Human LncRNA Array v4.0 (8 x 60K, Arraystar). Hybridisation was performed in Agilent SureHyb Hybridization Chambers.

Data Collection and Normalisation

After washing the slides, the arrays were scanned by the Agilent Scanner G2505C. Agilent Feature Extraction software (version 11.0.1.1.) was used to analyse the acquired array

images. Quantile normalisation and subsequent data processing were performed using GeneSpring GX v12.1 software package (Agilent Technologies).

To identify differentially expressed lncRNAs and mRNAs with statistical significance, Volcano Plot filtering was performed between two compared groups (either Control versus Clone 1 or Control versus Clone 9). The threshold was a fold change of ≥ 2.0 and a p-value of ≤ 0.05. False discovery rates were adjusted from all the p-values by the Benjamini-Hochberg method for multiple testing correction. The fold change between log2 transformed normalised intensities was calculated as $FC = 2^{|norm1-norm0|}$ where FC is the fold change.

2.8 Cloning Experiments

A summary diagram of the cloning experiments is given in Appendix I.

Amplification of SARCC gene by PCR

Primers for the *SARCC* gene were manually designed and ordered from Integrated DNA Technologies (Table 2.4). Binding sites for BamH I and Xho I were incorporated upstream and downstream of the gene. cDNA from Clone 1 cells was used to amplify the insert. PCR conditions are set out in Table 2.5.

Table 2.5: PCR conditions for *SARCC* amplification.

Temperature	Time
95°C	10 min
95°C	1 min
58°C	1 min
72°C	1 min
	35 cycles
72°C	10 min

Clean-up of PCR products:

PCR products were purified using the Wizard® SV Gel and PCR Clean-Up System (Promega) according to the manufacturer's instructions. Briefly, membrane binding solution was added to the PCR products in equal volumes. This was added to a mini-column assembly, incubated at room temperature for 1 min and centrifuged at 16,000 χ

g for 1 min. The flow-through was discarded, 700 µL Membrane Wash Solution was added to the column, and the mini-column centrifuged at 16,000 χ g for 1 min. The flow-through was discarded, 500 µL Membrane Wash Solution was added and the mini-column was centrifuged at 16,000 χ g for 5 min. The flow-through was discarded and the mini-column centrifuged at 16,000 χ g for 1 min with the lid open to allow evaporation of any residual EtOH. The mini-column was transferred to a clean 1.5 mL microcentrifuge tube and 50 µL nuclease-free water added. This was incubated at room temperature for 1 min and centrifuged at 16,000 χ g for 1 min. The purified DNA was then stored at -20°C until required.

TOPO Cloning

TOPO cloning was performed using the TOPO® TA Cloning® Kit and the pCR™2.1-TOPO® plasmid (Invitrogen, ThermoFisher Scientific). The pCR™2.1-TOPO® plasmid is supplied linearised with single 3'-thymidine overhangs and topoisomerase I covalently bound to the vector. The thymidine overhangs bind to the adenine overhangs of the PCR products produced by *Taq* polymerase during the PCR process. In total, 3 µL PCR product was added to 1 µL salt solution and molecular grade water was added to a total volume of 5 µL. One µL pCR™2.1-TOPO® was added for a final volume of 6 µL. The reaction was mixed gently and incubated at room temperature for 5 min. The reaction was then placed on ice until transformation was performed.

Transformation

Transformation was carried out using DH5α E. coli chemically competent cells (ThermoFisher Scientific). The cells were removed from -80°C and let thaw on ice. Three µL DNA was added to 50 µL cell suspension. The tube(s) were incubated on ice for 30 min and then placed into a 42°C water bath for 30 s. The tube(s) were placed back on ice for 2 min. The solution was diluted to 1 mL by the addition of 950 µL SOC medium (2% tryptone, 0.5% yeast extract, 0.4% glucose, 10 mM NaCl, 2.5 mM KCl, 10 mM $MgCl_2$ and 10 mM $MgSO_4$. The tube(s) were then shaken at approximately 200 rpm for 60 min at 37°C. The solution was streaked out onto agar plates containing Fast-Media® Amp Agar X-Gal (InvivoGen, California, USA) and incubated overnight at 37°C. Blue/white selection was carried out on the colonies with 10 white colonies selected. These colonies were

added to tubes containing liquid medium Fast-Media® Amp TB (InvivoGen). The tubes were incubated at 37°C and shaken at approximately 200 rpm overnight.

Plasmid DNA isolation

Plasmid DNA was isolated using the PureYield™ Plasmid Miniprep System (Promega, Wisconsin, USA) according to the manufacturer's instructions. Briefly, 1.5 mL bacterial culture was centrifuged at 15,000 χ g for 30 s and the supernatant discarded. An additional 1.5 mL of bacterial culture was added to the same tube, centrifuged at 15,000 χ g for 30 s and the supernatant discarded. The cell pellet was re-suspended in 600 µL molecular grade water. One hundred µL cell lysis buffer was added and the samples mixed by inversion. Subsequently, 350 µL cold (4–8°C) neutralisation solution was added and samples mixed thoroughly by inverting. The samples were centrifuged at 15,000 χ g for 3 min. The supernatant was transferred to a PureYield™ mini-column without disturbing the cell pellet. The mini-column was placed into a collection tube and centrifuged at 15,000 χ g for 15 s. The flow-through was discarded and the mini-column was placed into the same collection tube. Two hundred µL Endotoxin Removal Wash was added to the mini-column and centrifuged at 15,000 χ g for 15 s, followed by 400 µL Column Wash Solution and centrifuged at 15,000 χ g for 30 s. The mini-column was transferred to a clean 1.5 mL micro-centrifuge tube, 30 µL elution buffer added and the mini-column let stand for 1 min at room temperature. This was centrifuged at 15,000 χ g for 15 s to elute the plasmid DNA, which was stored at -20°C.

Restriction enzyme digest

Five samples of pCR2.1-TOPO SARCC DNA were selected for double digest using BamH I and Xho I restriction enzymes as these sites were present at each end of the insert and did not cut the insert itself. Restriction enzymes BamH I and Xho I were obtained from ThermoFisher Scientific and used as per manufacturer's instructions. Buffers were chosen based on available restriction enzyme buffer reference tables. Ten µL plasmid DNA was added to 40 µL molecular grade water. This was added to 2.5 µL BamH I, 2.5 µL Xho I, 10 µL 10X buffer and 35 µL molecular grade water giving a final volume of 100 µL. This was incubated overnight at 37°C. The digest was stopped by heat inactivating at 65°C for 15 min. End-point PCR was performed using the original SARCC primers (Table

2.4) and 1 µL DNA from the digestion, to confirm the presence of the SARCC gene. Two samples identified to have the SARCC gene present were chosen for band isolation.

Band isolation

Target DNA was electrophoresed on an agarose gel as previously described (Section 2.5). The target band was visualised using a long-wavelength UV lamp. To reduce nicking, the gel was irradiated for the absolute minimum time possible. The DNA fragment of interest was excised using a clean scalpel. The gel slice was transferred to a previously weighed microcentrifuge tube and the weight of the gel obtained. The DNA was then purified using the Wizard® SV Gel and PCR Clean-Up System (Promega). Membrane binding solution was added at a ratio of 10 µL solution per 10 mg of agarose gel. The mixture was vortexed and incubated at 55°C for 10 min or until the gel slice had completely dissolved. The dissolved gel mixture was transferred to mini-columns and purified as per manufacturer's instructions. In parallel, DNA from a new plasmid, pcDNA3.1(+) (Invitrogen) was also digested using BamH I and Xho I and band isolation performed.

Ligation and transformation

Ligation of the SARCC insert into the new plamid, pcDNA3.1(+) was performed using a molar ratio of 1:3 (vector:insert) as per Table 2.6. T4 DNA Ligase (ThermoFisher Scientific) was added last and the solution was mixed gently by pipetting up and down. The solution was incubated at room temperature for 10 min and then chilled on ice until transformed in to bacterial cells. The pcDNA3.1(+) plasmid containing the *SARCC* insert and the control pcDNA3.1(+) plasmid were transformed into DH5α E. coli chemically competent cells as previously described (Section 2.8). Five µL ligation solution was added to 50 µL DH5α E. coli chemically competent cells. The solution was streaked onto agar plates containing Fast-Media® Amp Agar (InvivoGen) and incubated overnight at 37°C. Ten colonies were added to tubes containing liquid medium Fast-Media® Amp TB (InvivoGen) and incubated overnight at 37°C. The plasmid DNA was isolated using the PureYield™ Plasmid Miniprep System (Promega Corporation).

Table 2.6: Components of the ligation reaction.

Sample	Volume
10X T4 DNA Ligase Buffer	2 µL
Vector DNA (3kb)	50 ng (0.025 pmol)
Insert DNA (1 kb)	50 ng (0.076 pmol)
T4 DNA Ligase	1 µL
Molecular grade water	up to 20 µL

Transfection

Transfection was performed using TurboFect Transfection Reagent (ThermoFisher Scientific). At the time of transfection, the target cells had a confluency of 70-90%. The cells were seeded into a 6-well plate ($0.8 – 2.4 \times 10^5$ cells per well). Four µg plasmid DNA was diluted in 400 µL serum free media (the volume of DNA was at least $1/10^{th}$ the volume of media). The transfection reagent was vortexed and then 6 µL was added to the diluted DNA. This was mixed immediately by pipetting and incubated at room temperature for 15 min. The solution was added dropwise to the wells containing cells and the plate rocked gently to achieve even distribution. The cells were incubated at 37°C in a humidified CO_2 incubator. Selection of transfected cells was achieved by treatment with G418 disulfate antibiotic (Invivogen) as resistance to G418 is conferred by the Neomycin gene. Prior to transfection, an antibiotic killing curve was undertaken on target cells to determine the minimum concentration of antibiotic that killed the majority of cells within 14 days (media and antibiotic was replaced every 2 days). Transfected cells were then treated for at least 14 days based on this concentration.

2.9 Cell Blocks and Immunohistochemistry

Preparation of formalin fixed paraffin embedded (FFPE) cell blocks

Cells were recovered from the culture flasks as previously described (Section 2.3). The cell suspension was diluted with 50 mL complete media and centrifuged at 200 χ g for 5 min. Bovine thrombin (Instrumentation Laboratory, Munich, Germany) and human plasma (Instrumentation Laboratory) reagents were reconstituted with molecular grade water. One drop of reconstituted plasma reagent was added to the pellet, followed by 3 drops of reconstituted thrombin. The sample was incubated for 3 min to allow a clot to form, placed into a white cell safe biopsy capsule, and then placed into an appropriately labelled cassette. The cassette was closed with a metal clip and placed in a specimen pot containing 10% buffered formalin (Thermo Fisher Scientific). This was processed and embedded using standard laboratory protocols. The FFPE blocks were stored at room temperature.

FFPE block sectioning

The FFPE blocks were sectioned at 4 µm using a HM325 rotary microtome (Thermo Fisher Scientific). The sections were floated in a 56°C waterbath and mounted onto TOMO® adhesion slides (Matsunami Glass, Osaka, Japan). The sections were dried overnight by placing the slides on a heating block at 40°C. Slides were used immediately or stored at RT.

Immunohistochemistry (IHC)

Immunohistochemical staining with antibodies to synaptophysin, chromogranin and AR protein was undertaken at the Department of Histopathology, St James's Hospital, Dublin, according to standardised protocols. The following antibodies were used: anti-Chromogranin A, mouse monoclonal antibody, LK2H10 clone, prediluted (Ventana Medical Systems, Arizona, USA); anti-Synaptophysin, rabbit monoclonal antibody, MRQ-40 clone (Cell Marque, California, USA); anti-Androgen receptor, rabbit monoclonal antibody, SP107 clone (Cell Marque). All three antibodies were stained on the Ventana Benchmark Ultra platform with OptiView DAB detection system (Ventana). There was no antigen retrieval stage for chromogranin A staining and the antibody was incubated for 16 min. Synaptophysin staining protocol included heat mediated antigen retrieval with

Cell Conditioning solution CC1 (Ventana) for 40 min and antibody incubation for 32 min. Androgen receptor staining protocol included heat mediated antigen retrieval with Cell Conditioning solution CC1 (Ventana) for 40 min and antibody incubation for 20 min.

2.10 Cell Doubling and Cell Proliferation Assay

Cell doubling

Cells were counted as previously described (Section 2.3) and 200,000 viable cells were seeded into each well of a 6-well plate. Cells were counted again after 72 h of culture. Doubling time was calculated according to the formula:

Doubling Time = [T × (ln2)] / [ln (Xe / Xb)]

where T equals the length of time in culture, Xe equals the number of cells at the end and Xb equals the initial number of cells.

Assessment of enzalutamide resistance by cell proliferation assay

Cell proliferation was evaluated using an assay based on the measurement of 5-bromo-2'-deoxyuridine (BrdU) incorporation during DNA synthesis. The Cell Proliferation ELISA BrdU Assay (Roche Diagnostics, Basel, Switzerland) was used. Cells and drugs were added simultaneously to a flat bottomed 96 well plate – 1,000 viable cells were seeded per well in a final volume of 200 µL. Enzalutamide was diluted in media to provide the following concentrations: 1 µM, 2.5 µM, 5 µM, 7.5 µM, 10 µM, 15 µM, 20 µM and 40 µM. Controls were untreated cells (no DMSO or enzalutamide) and cells treated with DMSO only. The plate was incubated at 37°C for one week. Following treatment, 20 µL BrdU labelling solution (1:100 dilution in sterile culture media) was added to each well and incubated at 37°C for 4 h. All liquid was removed from the plate and the plate was allowed to dry at 37°C for a further 10 min. Cells were fixed with 200 µL FixDenat solution per well for 30 min at room temperature and then the solution was removed. One hundred µL anti-BrdU-POD (1:100 anti-BrdU-POD stock with antibody dilution solution) was added to each well and incubated at room temperature for 90 min. The antibody conjugate was removed and the wells washed three times with 200 µL washing solution per well. The washing solution was removed and 100 µL substrate solution was added to each well. The plate was incubated at room temperature for 5-10 min or until colour change was detected. Twenty-five µL 1 mM H_2SO_4 was added to each well to stop the reaction. The

plate was read on an LT4500 Absorbance Microplate Reader (Labtech, East Sussex, UK) within 5 min of adding the stop solution. The plates were read at 450 nm with reference wavelength 690 nm.

2.11 Statistics

Independent experiments were completed a minimum of three times. Graphpad PRISM 7 software (Graphpad, California, USA) was used for statistical analysis. Significance was determined via one-way analysis of variance (ANOVA), where the number of groups in the experiment was three or more, or an appropriate student's *t* test, where the number of groups was two. A probability of $p \leq 0.05$ was considered to represent a significant difference between the groups. A *post hoc* test was performed following ANOVA to determine which groups were significantly different to each other. Post-test analysis was conducted using Tukey, Dunnett or Bonferroni multiple comparisons test (as appropriate).

Chapter 3
lncRNAs and mRNAs associated with enzalutamide resistance

3.1 Quality control of material for microarray analysis

Cell lines were tested for Mycoplasma prior to use and were negative (Figure 3.1). RNA was extracted as previously described (Section 2.4). Total RNA from each sample was quantified using a NanoDrop ND-1000 spectrophotometer (Thermo Fisher Scientific) and RNA integrity was assessed by standard electrophoresis (Figure 3.2). The integrity and concentration of the RNA was determined prior to shipment and by Arraystar Inc. upon receipt.

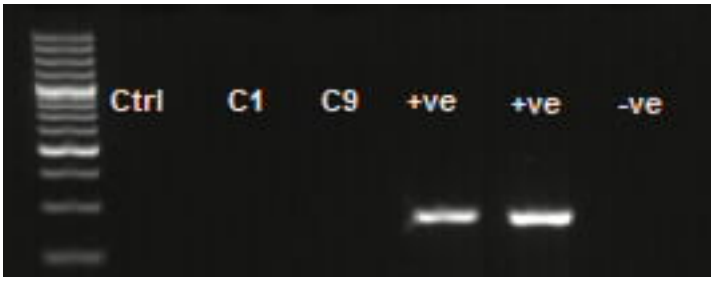

Figure 3.1: Mycoplasma testing

Mycoplasma was not detected in the three cell lines. C1 = Clone1, C9 = Clone 9, +ve = positive control, -ve = negative control.

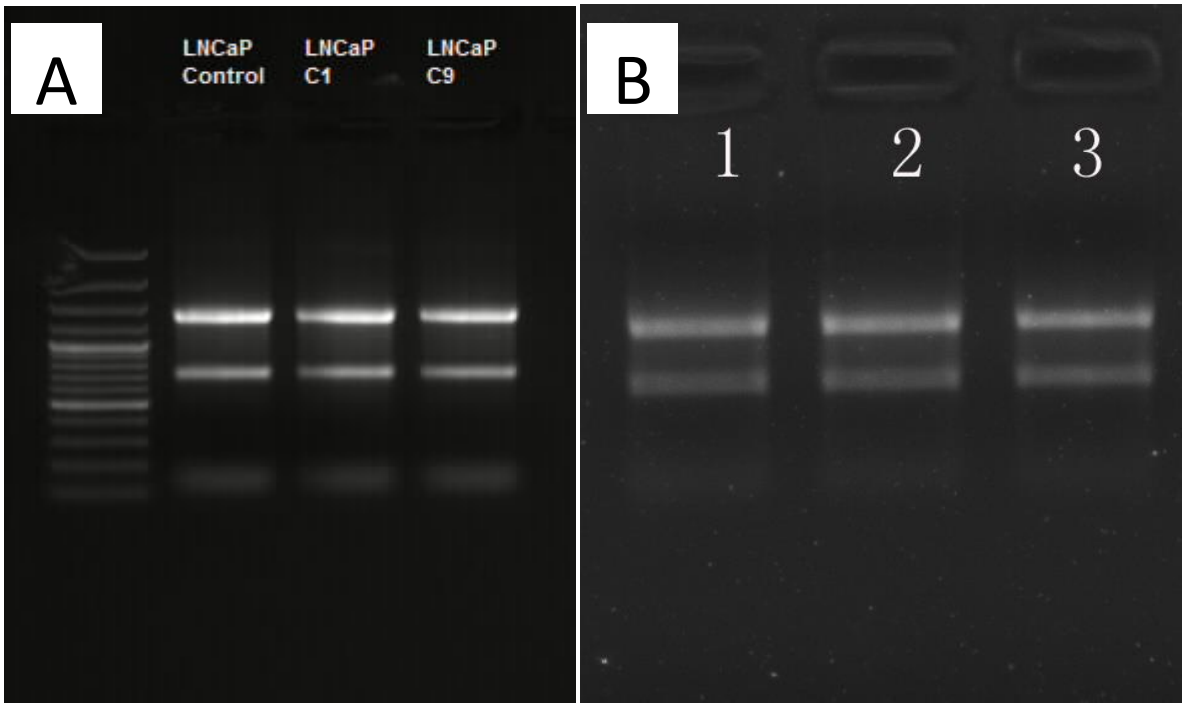

Figure 3.2: Assessment of RNA integrity

Assessment of RNA integrity, prior to sending (A) and by Arraystar Inc. (B).

Lane 1 = Control, Lane 2 = Clone 1, Lane 3 = Clone 9. The 28S and 18S ribosomal bands are sharp intense bands with the intensity of the upper band about twice that of the lower band, indicating good RNA integrity.

3.2 Quality assessment of data after filtering

The RNA was evaluated by Arraystar as previously described (Section 2.7). The data on lncRNA and mRNA expression was evaluated after quantile normalisation. The distribution of intensities from all three samples was similar after normalisation (Figure 3.3). After normalisation of the raw data, lncRNAs flagged as “present” or “marginal” in at least 1 out of 3 samples were chosen for further data analysis.

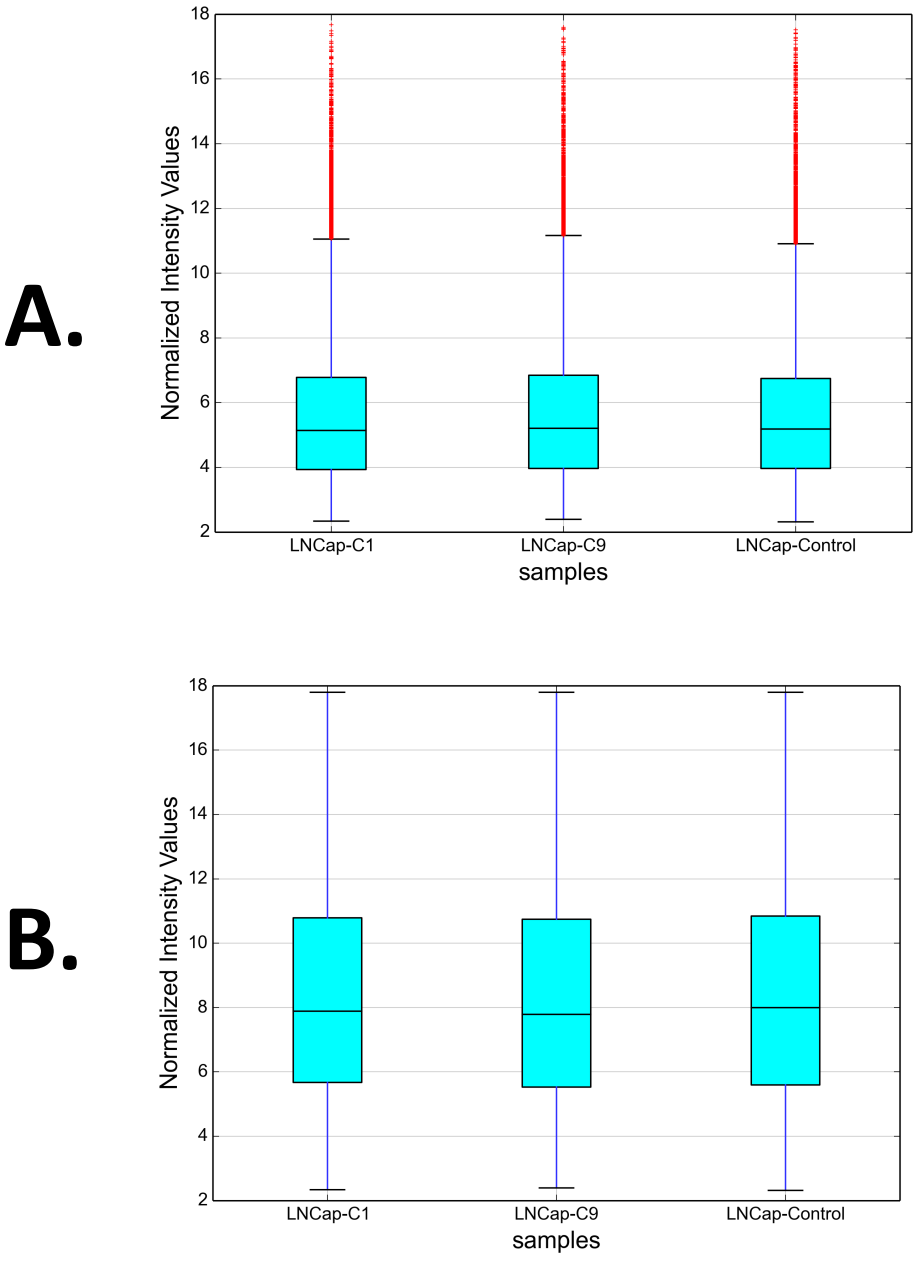

Figure 3.3: Quality assessment of data after filtering.

A = lncRNA data. B = mRNA data. The distributions of log2-ratios for the samples were consistent after normalisation. n=1.

3.3 Differentially expressed lncRNAs

Grouped analysis between the different groups according to FC is shown using a principle component analysis (PCA), allowing the direct visualisation of the different levels of lncRNA expression between groups (Figure 3.4).

In total, 3,150 upregulated lncRNAs and 3,713 downregulated lncRNAs were identified when comparing clone 1 (strongly enzalutamide resistant) to the control (enzalutamide sensitive). Data is shown as a scatter-plot and heat-map in Figure 3.5.
In total, 2,923 upregulated lncRNAs and 2680 downregulated lncRNAs were identified when comparing clone 9 (weakly enzalutamide resistant) to the control (enzalutamide sensitive). Data is shown as a scatter-plot and heat-map in Figure 3.6.

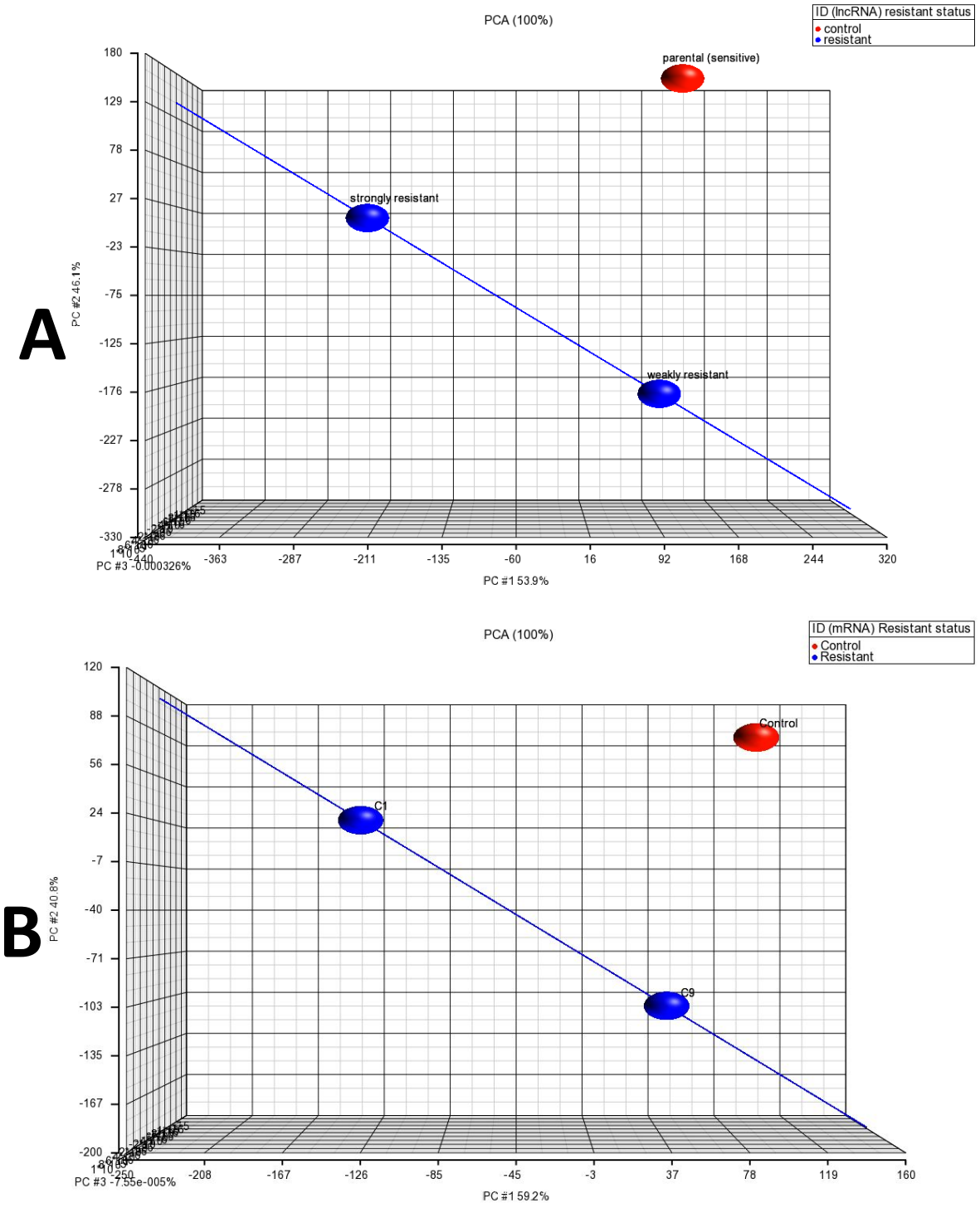

Figure 3.4: Principle component analysis.

Principle component analysis indicates that the grouping of all three samples are different. A = lncRNAs. B = mRNAs. C1 = Clone 1, C9 = Clone 9.

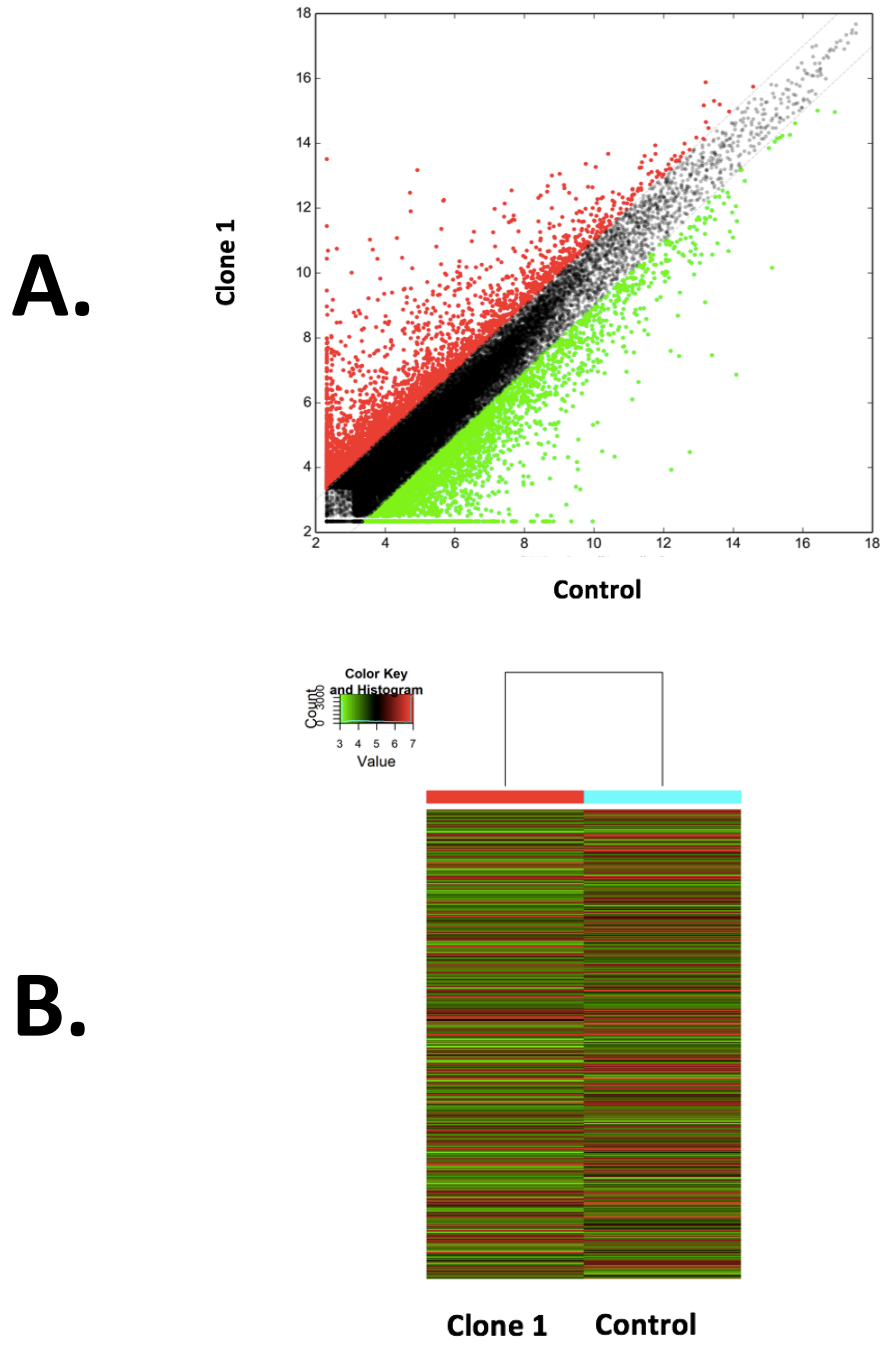

Figure 3.5: Expression levels for clone 1 versus control cells.

The values of the X and Y axes in the scatter-plot (A) are the averaged normalised signal values of the groups (log2 scaled). Upregulated lncRNAs of more than 2.0 fold change are marked red and downregulated lncRNAs marked green. The heat-map (B) shows the relationship among lncRNA expression patterns of samples. Red indicates high and green indicates low relative expression.

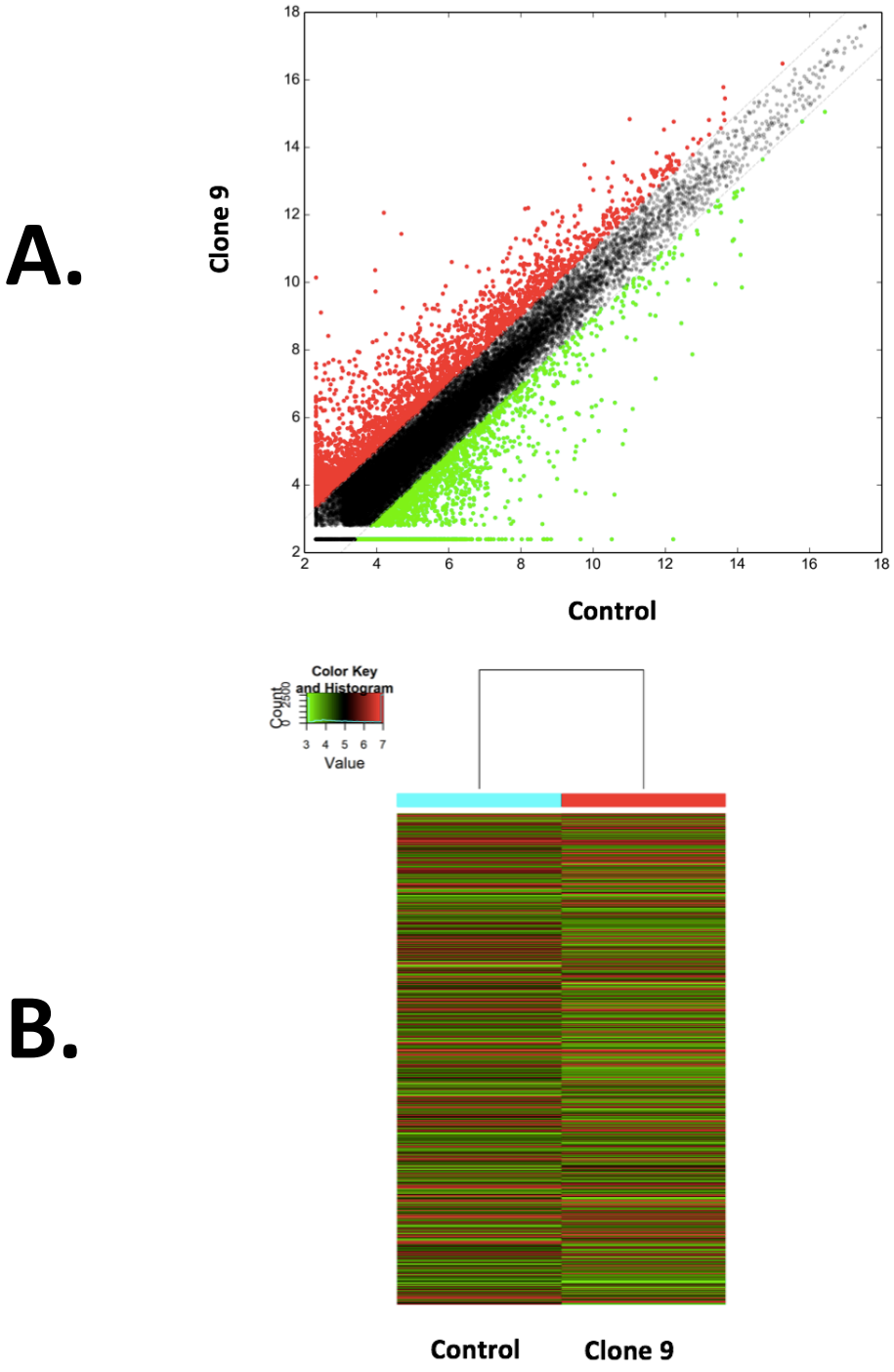

Figure 3.6: Expression levels for clone 9 versus control cells.

The values of the X and Y axes in the scatter-plot (A) are the averaged normalised signal values of the groups (log2 scaled). Upregulated lncRNAs of more than 2.0 fold change are marked red and downregulated lncRNAs marked green. The heat-map (B) shows the relationship among lncRNA expression patterns of samples. Red indicates high and green indicates low relative expression.

3.4 Upregulated lncRNAs

3.4.1 The top ten upregulated lncRNAs

The top ten upregulated lncRNAs by FC in Clone 1 and Clone 9 compared to the control are shown in Table 3.1. A thorough literature review did not reveal any previously reported associations to PCa or the AR. Many of the genes were poorly characterised or had no known cancer associations reported.

Table 3.1: Top ten upregulated lncRNAs in Clone1 and Clone 9 versus control.

Upregulated in Clone 1 versus Control		Upregulated in Clone 9 versus Control	
Fold Change	**Gene Symbol**	**Fold Change**	**Gene Symbol**
2340	*DPP10-AS1*	233	*RP11-119D18.1*
559	*RP11-1C8.7*	226	*G064429**
323	*FLJ26850*	108	*RP11-426J5.2*
305	*LOC101928891*	101	*RP5-827C21.6*
282	*RP11-222K16.2*	84	*G062386**
278	*RP11-385E5.5*	54	*G074428**
217	*LOC283352*	54	*G089220**
177	*DGCR5*	39	*G018651**
144	*DGUOK-AS1*	35	*G012915**
141	*RP11-384L8.1*	32	*G077283**

***RNA-seq data sourced by Arraystar from Iyer *et. al* 2015 [186]**

3.4.2 Upregulated lncRNAs with known associations to PCa or the AR

A literature review revealed 86 lncRNAs with a reported association to PCa or the AR (Provided in Table 1.2). Fifteen of these lncRNAs were upregulated with a FC greater than 2.0 (Table 3.2).

Table 3.2: Upregulated lncRNAs with previously reported associations to PCa or the AR.

Upregulated lncRNA	Fold change (Clone 1 *vs.* Control 1)	Reported association to PCa or the AR
RP11-38P22.2 (SARCC)	51.5	Binds to the AR and AR protein in renal cell carcinoma [159, 187]
SPRY4-IT1	41.8	Enhances PCa cell invasion and proliferation *in vitro* [167]
AFAP1-AS1	14.3	Enhances PCa cell proliferation and metastasis *in vitro* via targeting *RBM5*, an inhibitor of the Wnt signalling pathway [97]
PART-1	9.1	Highly expressed in normal prostate and is regulated by androgens [188]. It modulates Toll-like receptor pathways in PCa cells *in vitro* [143].
LINC00844	5.2	Regulated by androgens and facilitates AR binding to chromatin [124]. Tumour suppressor role in PCa cells *in vitro* by reducing proliferation and metastasis [124].
HOTAIR	4.0	Binds to the AR, preventing its degradation [88]. Can induce an AR-binding profile similar to that induced by androgens, resulting in AR signalling in the absence of androgens [88].
SNHG7	4.0	Overexpressed in PCa, promotes PCa migration and invasion by modulating EMT [189]. Acts as a sponge for miRNA-324-3p causing upregulation of *WNT2B*, a protein in the Wnt signalling pathway [189]. Also sponges miR-503 leading to PCa cell proliferation [164]
FEZF1-AS1	3.8	Activates the Notch signalling pathway, associated with metastasis and poorer prognosis in PCa [109]
HOTTIP	3.5	Knockdown inhibits PCa cell proliferation and enhances cell sensitivity to cisplatin by suppressing the Wnt pathway [116]

Table 3.2 continued

Upregulated lncRNA	Fold change (Clone 1 *vs*. Control 1)	Reported association to PCa or the AR
LUCAT1	2.7	Promotes the migration and invasion of prostate cancer cells by inhibiting *KISS1* expression which has a tumor suppressor role in a number of cancers [135].
LEF1-AS1	2.5	Associated with the initiation and development of PCa by acting as a sponge of miR-330-5p leading to upregulation of *LEF1* [119]. *LEF1* is associated with increased AR expression and CRPC [190]
SNHG12	2.5	Promotes tumorigenesis by acting as a sponge on miR-133b [191] and activates the Wnt signalling pathway through sponging miRNA-195 [165]
MEG3	2.4	Inhibits cell proliferation and induces apoptosis in PCa by reducing the protein expression of *BCL-2* [137]
SNHG15	2.3	Associated with PCa cell migration, invasion and EMT and acts as a sponge on miR-338-3p causing upregulation of *FKBP1A* [166].
LINC00683	2.1	Associated with an unfavorable prognosis in PCa based on TCGA analysis [123]

3.4.3 Selection of upregulated lncRNAs for validation

LncRNAs were selected for validation based on their degree of differential expression and whether they were previously linked to mechanisms that may contribute to enzalutamide resistance. We selected *DGCR5, DPP10-AS1, FLJ26850, RP11-1C8.7, RP11-222K16.2, SARCC* and *SPRY4-IT1* for validation. Control, Clone 1 and Clone 9 cells were cultured in triplicate and RNA isolated and quantified as previously described (Section 2.3 and 2.4). cDNA was synthesised and RT-qPCR performed as previously described (Section 2.5).

3.4.4 LncRNA *DPP10-AS1* is significantly overexpressed in enzalutamide resistant cells

DPP10 antisense RNA 1 (*DPP10-AS1*) showed a FC of 2340 in Clone 1 compared to Control based on Arraystar data. RT-qPCR confirmed that *DPP10-AS1* was significantly overexpressed in Clone 1 (Figure 3.7). There are no previous reports evaluating the role of *DPP10-AS1* or Dipeptidyl peptidase like 10 (*DPP10*) in PCa or AR signalling.

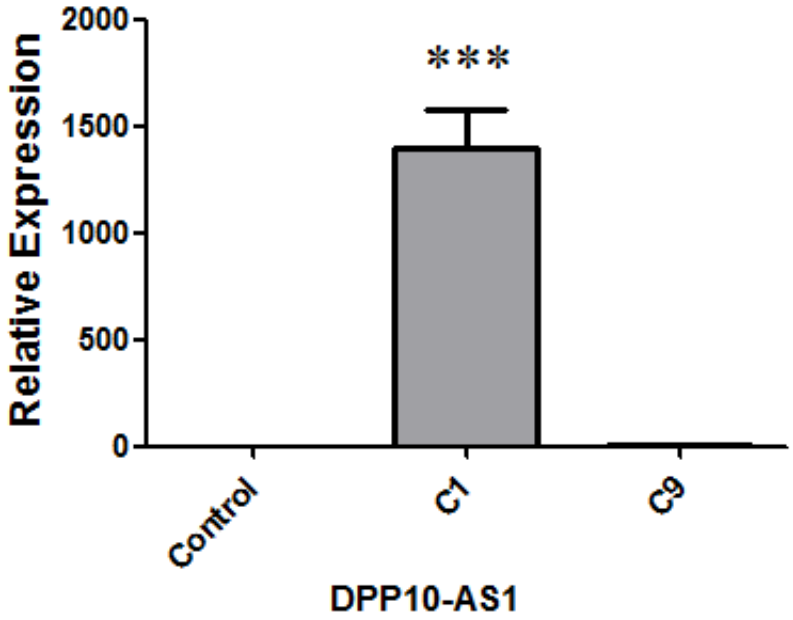

Figure 3.7: LncRNA *DPP10-AS1* is significantly overexpressed in Clone 1 versus Control. Data graphed as mean ± SEM (n=3). Statistical analysis performed using ordinary one-way ANOVA, *post-hoc* Dunnett's test (Clone 1 *vs* Control, *** p≤0.001). C1 = Clone 1, C9 = Clone 9.

3.4.5 LncRNA *FLJ26850* is significantly overexpressed in enzalutamide resistant cells

FLJ26850 showed a fold change of 323 in Clone 1 compared to Control 1 based on Arraystar data. RT-qPCR confirmed that *FLJ26850* was significantly overexpressed in Clone 1 (Figure 3.8). There are no previous reports evaluating the role of *FLJ26850* in PCa or AR signalling.

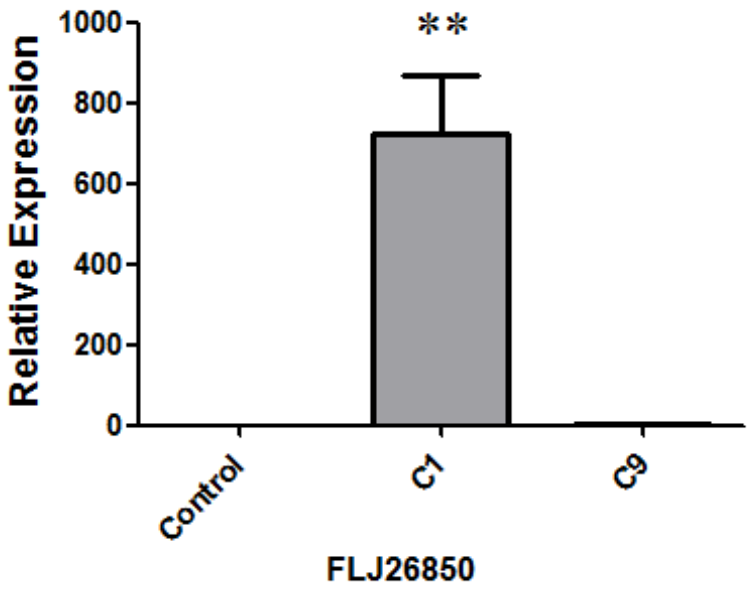

Figure 3.8: LncRNA *FLJ26850* is significantly overexpressed in Clone 1 versus Control. Data graphed as mean ± SEM (n=3). Statistical analysis performed using ordinary one-way ANOVA, *post-hoc* Dunnett's test (Clone 1 *vs* Control, ** p≤0.01). C1 = Clone 1, C9 = Clone 9.

3.4.6 LncRNA *RP11-222K16.2* is significantly overexpressed in enzalutamide resistant cells

RP11-222K16.2 showed a fold change of 282 in Clone 1 compared to Control 1 based on Arraystar data. RT-qPCR confirmed that *RP11-222K16.2* was significantly overexpressed in Clone 1 (Figure 3.9). There are no previous reports evaluating the role of *RP11-222K16.2* or *EOMES* in PCa or AR signalling.

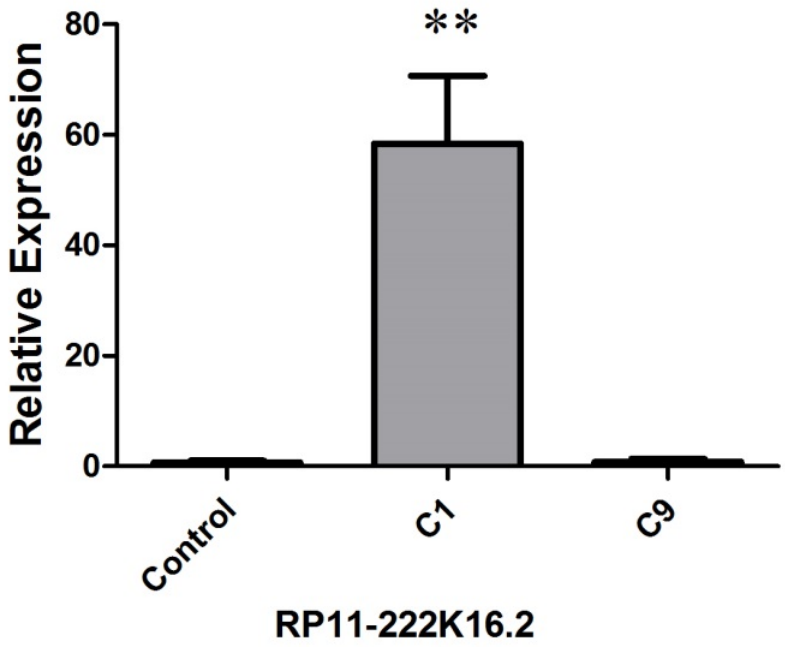

Figure 3.9: LncRNA *RP11-222K16.2* is overexpressed in Clone 1 versus Control.

Data graphed as mean ± SEM (n=3). Statistical analysis performed using ordinary one-way ANOVA, *post-hoc* Dunnett's test (Clone 1 *vs* Control, ** p≤0.01).

C1 = Clone 1, C9 = Clone 9.

3.4.7 LncRNA *SARCC* is significantly overexpressed in enzalutamide resistant cells

Suppressing Androgen Receptor in Renal Cell Carcinoma (*SARCC*) showed a fold change of 51.5 in Clone 1 compared to Control 1 based on Arraystar data. RT-qPCR confirmed that *SARCC* was significantly overexpressed in Clone 1 (Figure 3.10). Also known as *RP11-38P22.2, lnc-P2RY1-1* and *ENST00000460407*, *SARCC* binds directly to the AR and to AR protein in renal cell carcinoma (RCC) [159, 187]. Given the high relative expression and its reported association to the AR, we selected this lncRNA for further evaluation (discussed in Chapter 4).

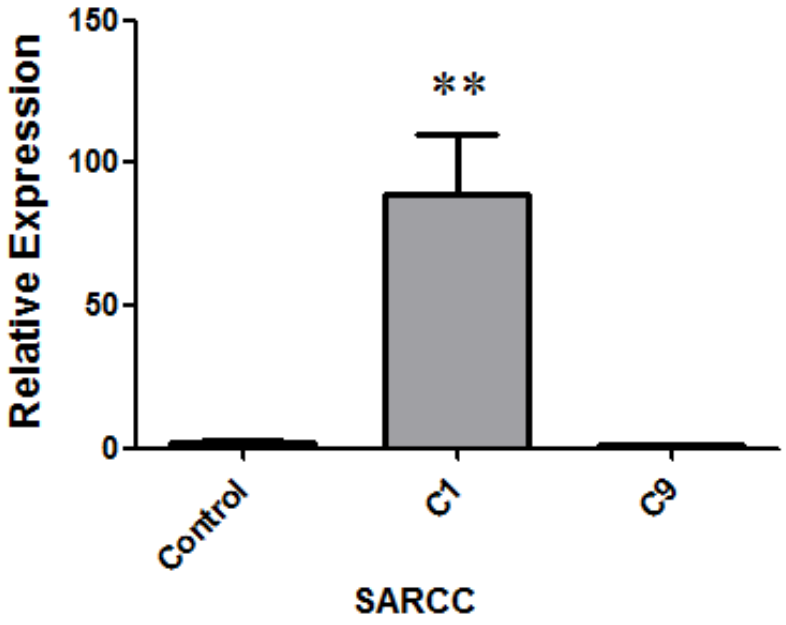

Figure 3.10: LncRNA *SARCC* is significantly overexpressed in Clone 1 versus Control. Data graphed as mean ± SEM (n=3). Statistical analysis performed using ordinary one-way ANOVA, *post-hoc* Dunnett's test (Clone 1 *vs* Control, ** p≤0.01). C1 = Clone 1, C9 = Clone 9.

3.4.8 LncRNA *SPRY4-IT1* is significantly overexpressed in enzalutamide resistant cells

SPRY4 intronic transcript 1 (*SPRY4-IT1*) showed a fold change of 41.8 in Clone 1 compared to Control 1 based on Arraystar data. RT-qPCR confirmed that *SPRY4-IT1* was significantly overexpressed in Clone 1 (Figure 3.11).

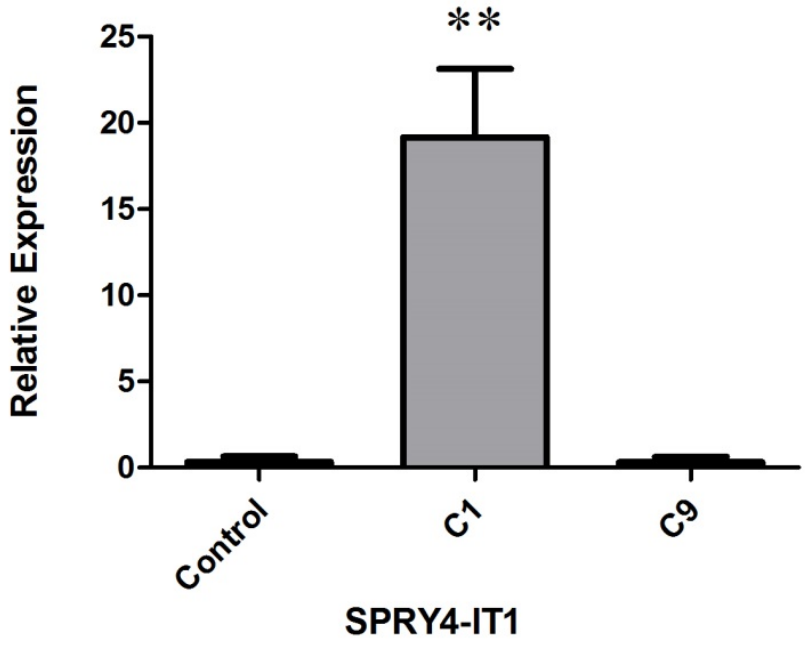

Figure 3.11: LncRNA *SPRY4-IT1* is significantly overexpressed in Clone 1 versus Control. Data graphed as mean ± SEM (n=3). Statistical analysis performed using ordinary one-way ANOVA, *post-hoc* Dunnett's test (Clone 1 *vs* Control, ** p≤0.01). C1 = Clone 1, C9 = Clone 9.

3.4.9 LncRNA *RP11-1C8.7* is significantly overexpressed in enzalutamide resistant cells

RP11-1C8.7 showed a fold change of 559 in Clone 1 compared to Control 1 based on Arraystar data. RT-qPCR confirmed that *RP11-1C8.7* was significantly overexpressed in Clone 1 (Figure 3.12). There are no previous reports evaluating the role of *RP11-1C8.7* in PCa or AR signalling.

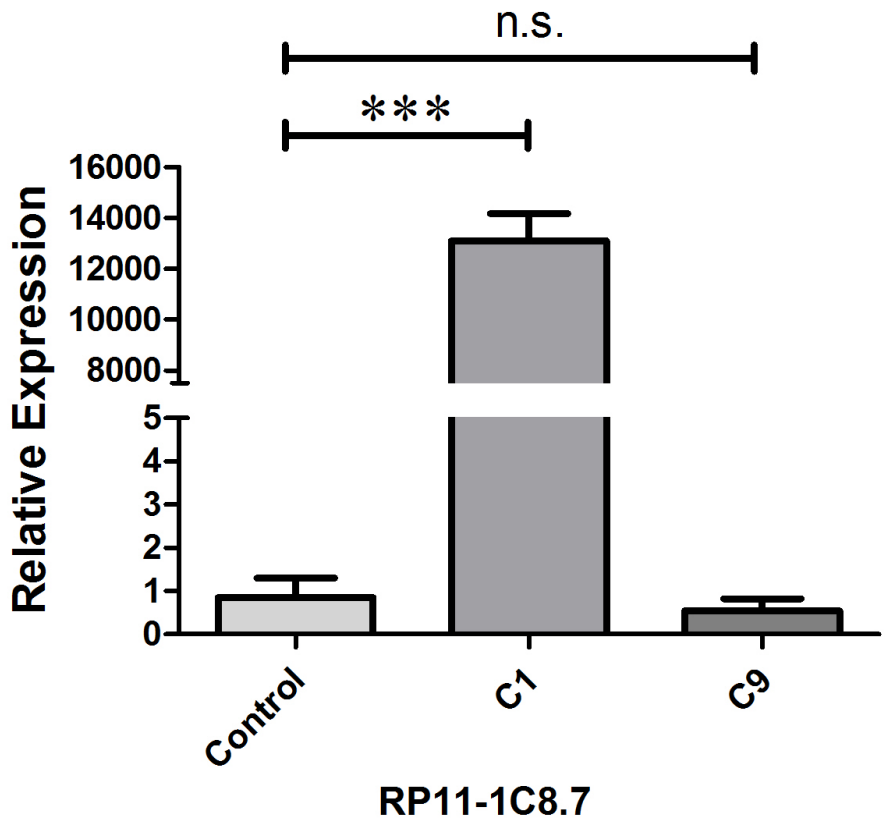

Figure 3.12: LncRNA *RP11.C8.7* is significantly overexpressed in Clone 1 versus Control. Data graphed as mean ± SEM (n=3). Statistical analysis performed using ordinary one-way ANOVA, *post-hoc* Dunnett's test (Clone 1 *vs* Control, *** p≤0.001). C1 = Clone 1, C9 = Clone 9, n.s. = not significant.

3.4.10 Validation of lncRNA *DGCR5*

DiGeorge syndrome critical region gene 5 (*DGCR5*) showed a fold change of 177 in Clone 1 compared to Control 1 based on Arraystar data. RT-qPCR showed there was no significant change in expression of *DGCR5* (Figure 3.13).

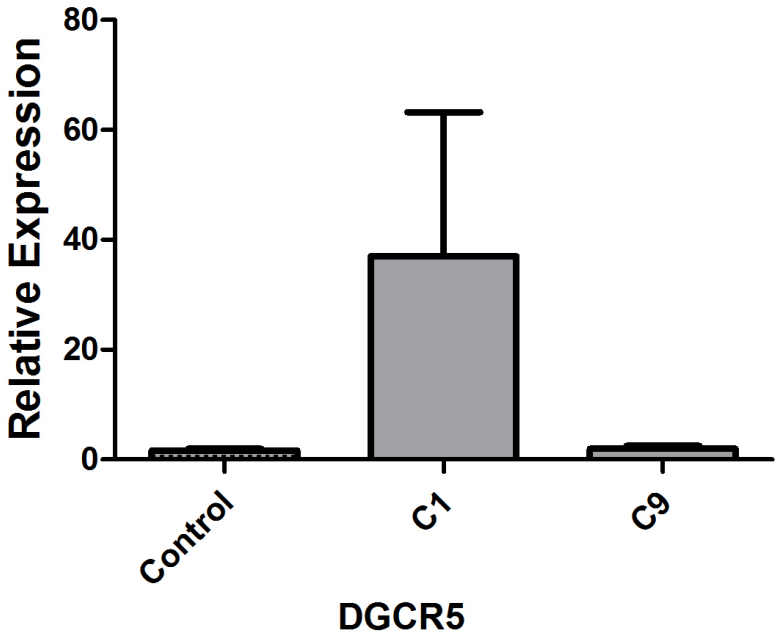

Figure 3.13: *DGCR5* relative gene expression by RT-qPCR.

Data graphed as mean ± SEM (n=3). Statistical analysis performed using ordinary one-way ANOVA, *post-hoc* Dunnett's test (Clone 1 *vs* Control, not statistically significant). C1 = Clone 1, C9 = Clone 9.

3.5 Downregulated lncRNAs

3.5.1 The top ten downregulated lncRNAs

The top ten downregulated lncRNAs by FC in Clone 1 and Clone 9 compared to Control are shown in Table 3.3. The only association with PCa in the literature was that *LOC440040* upregulation promoted tumor progression and predicted poor prognosis in patients with PCa [133]. Silencing of *RP11-476D10.1* enhances apoptosis and autophagy while inhibiting proliferation of papillary thyroid carcinoma cells [192]. The remainder of the genes were either poorly characterised or had no known association to cancer.

Table 3.3: Top ten down-regulated lncRNAs in Clone1 and Clone 9 versus control.

Downregulated in Clone 1 versus Control		Downregulated in Clone 9 versus Control	
Fold Change	**Gene Symbol**	**Fold Change**	**Gene Symbol**
311	*XLOC 013193**	903	*XLOC 013193*
308	*G003081***	277	*LOC650226*
196	*G026537***	152	*XLOC 007124*
149	*G019273***	117	*G030769*
128	*RP11-476D10.1*	86	*G058502*
90	*G058502*	81	*G009267*
83	*G002978*	80	*G002978*
81	*RP11-989E6.3*	76	*G082708*
79	*G082708*	75	*NKAIN3-IT1*
78	*NKAIN3-IT1*	65	*LOC440040*

***Sourced by Arraystar from RNA-seq data by Cabili *et. al* 2011**

****Sourced by Arraystar from RNA-seq data by Iyer *et. al* 2015**

3.5.2 Downregulated lncRNAs with known associations to PCa or the AR

We evaluated whether any of the 86 lncRNAs previously associated with PCa or the AR (Given in Table 1.2) were downregulated in Clone 1 compared to the control. Sixteen lncRNAs showed a FC greater than 2.0 (Table 3.4).

Table 3.4: Downregulated lncRNAs with known associations to PCa or the AR.

Downregulated lncRNA	Fold change between Clone 1 and Control	Reported association to PCa or the AR
PCAT-1	77	Promotes PCa cell proliferation and regulates *BRCA2* [145, 193]
LINC00662	22	Promotes PCa tumorigenesis by sponging miR-34a [122]
SChLAP1	8	Overexpressed in PCa, especially CRPC [194, 195]
NEAT1	6.1	Promotes cell proliferation and invasion [141]
TUG1	4.9	Promotes cancer progression by sponging miR-26a [173]
PRNCR1	4.3	Physically binds to the AR [196]
LincRNA-p21	4.1	Suppresses the development of PCa [128]
HCG11	3.0	Downregulation predicts a poor prognosis [115]
HULC	2.9	Promotes tumor progression by regulating EMT [117]
BCAR4	2.8	Upregulated in CRPC [101]
CTBP1-AS	2.8	Associated with PCa and AR overexpression [89]
TTTY15	2.8	Promotes PCa by sponging *LET-7* [171]
GHET1	2.6	Higher expression in PCa tissue [114]
PCA3	2.2	Overexpressed in PCa and involved in EMT [197, 198]
FOXP4-AS1	2.1	Promotes PCa by upregulating *FOXP4* [111]
ARNILA	2.1	Downregulated by the AR in breast cancer [100]

3.6 Differentially expressed mRNAs

A total of 2,423 upregulated mRNAs and 3,228 downregulated mRNAs were identified when comparing clone 1 (strongly enzalutamide resistant) to the control (enzalutamide sensitive). Data is shown as a scatter-plot and heat-map in Figure 3.14. A total of 1,342 up-regulated mRNAs and 2,043 down-regulated mRNAs were identified when comparing clone 9 (weakly enzalutamide resistant) to the control (enzalutamide sensitive). Data is shown as a scatter-plot and heat-map in Figure 3.15.

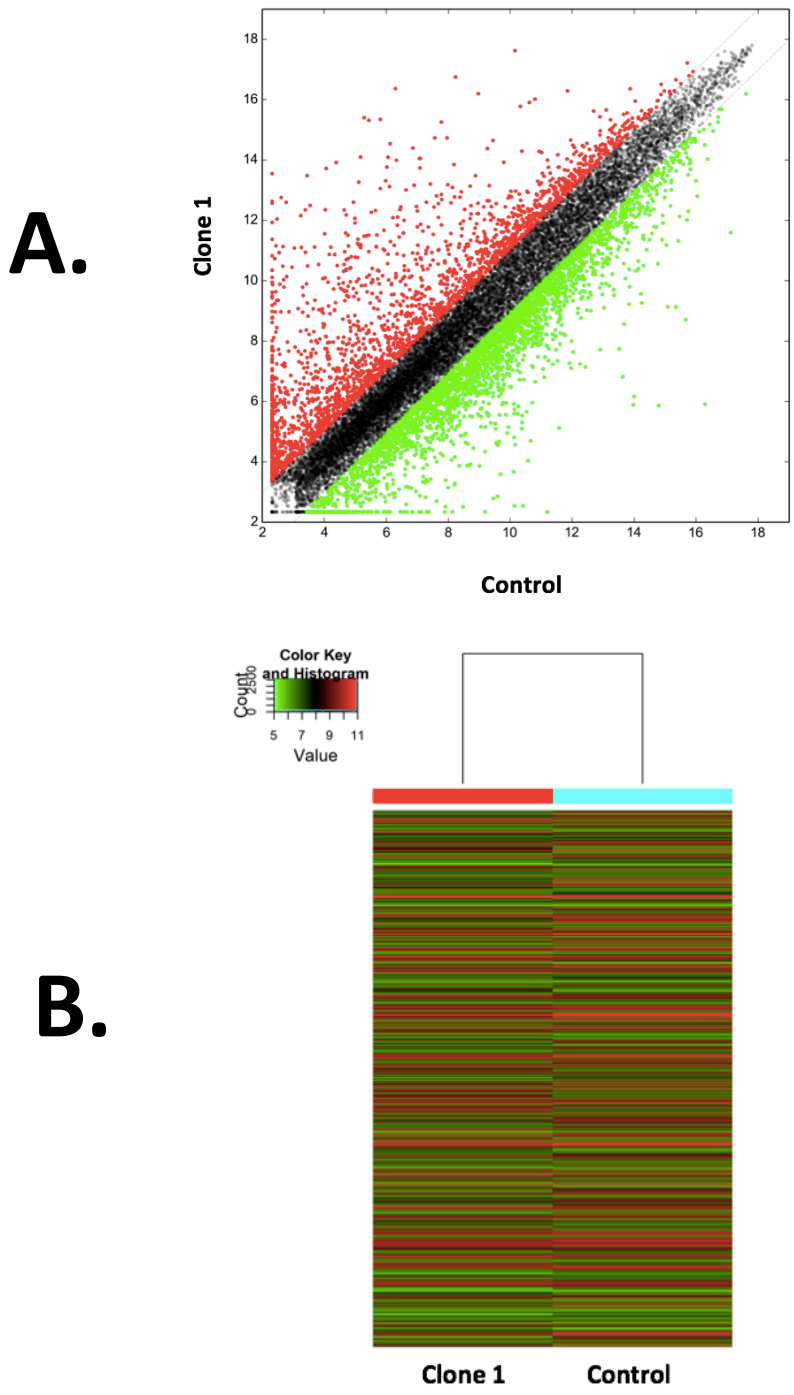

Figure 3.14: mRNA expression levels for Clone 1 versus Control cells.

The values of the X and Y axes in the scatter-plot (A) are the averaged normalised signal values of the groups (log2 scaled). Upregulated mRNAs of more than 2.0 fold change are marked red and downregulated mRNAs marked green. The heat-map (B) shows the relationship among mRNA expression patterns of samples. Red indicates high and green indicates low relative expression.

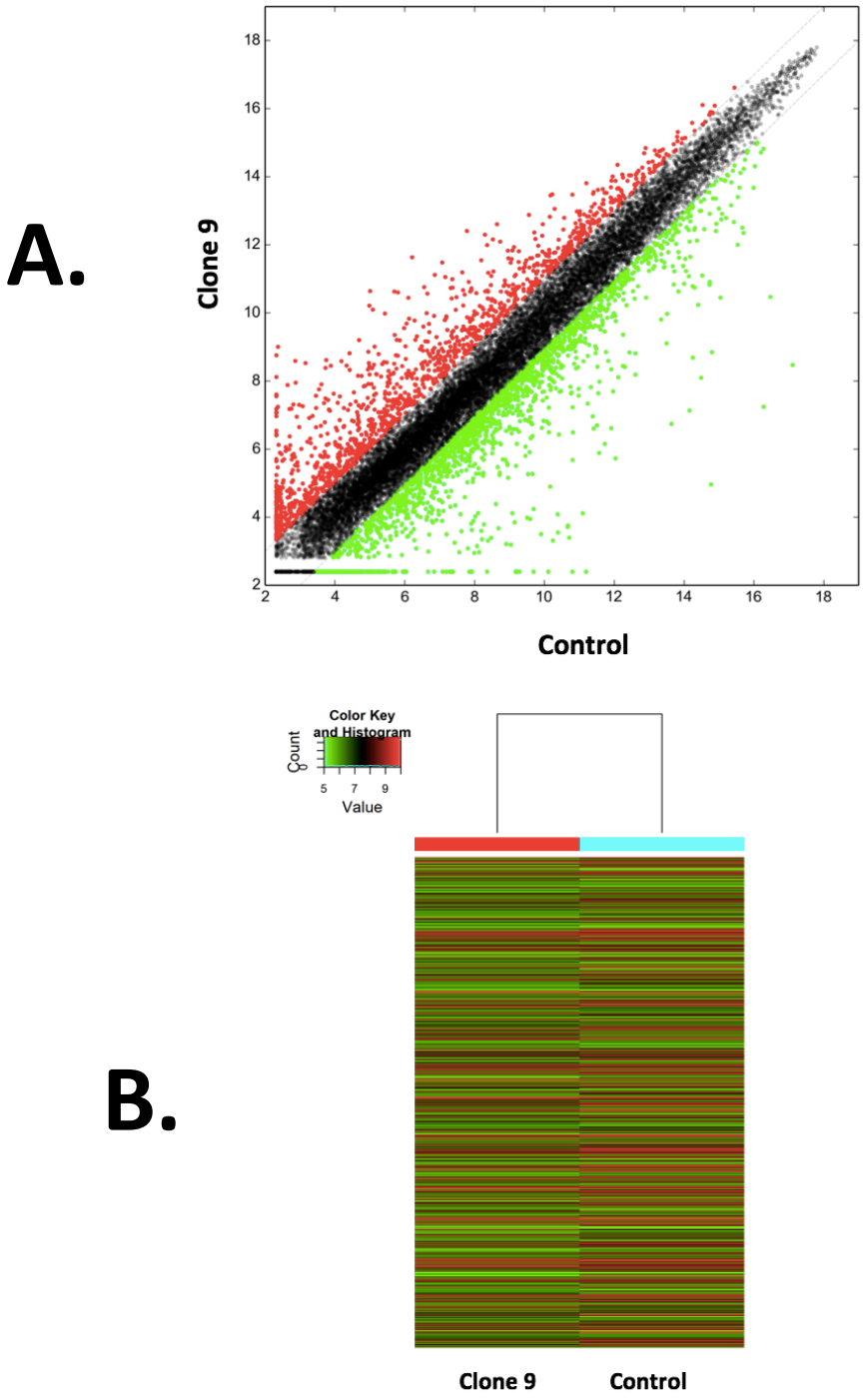

Figure 3.15: mRNA expression levels for Clone 9 versus Control cells.

The values of the X and Y axes in the scatter-plot (A) are the averaged normalised signal values of the groups (log2 scaled). Upregulated mRNAs of more than 2.0 fold change are marked red and downregulated mRNAs marked green. The heat-map (B) shows the relationship among mRNA expression patterns of samples. Red indicates high and green indicates low relative expression.

3.7 Upregulated mRNAs

3.7.1 Gene Ontology Analysis

The Gene Ontology (GO) project provides a controlled vocabulary to describe gene and gene product attributes in any organism (http://www.geneontology.org). The ontology covers three domains: biological process, cellular component and molecular function. Fisher's exact test was used to determine if there was more overlap between the differentially expressed list of mRNAs and the GO annotation list than would be expected by chance. Figure 3.16 shows upregulated mRNAs grouped by their molecular function. The largest group concerns receptor binding (194 genes).

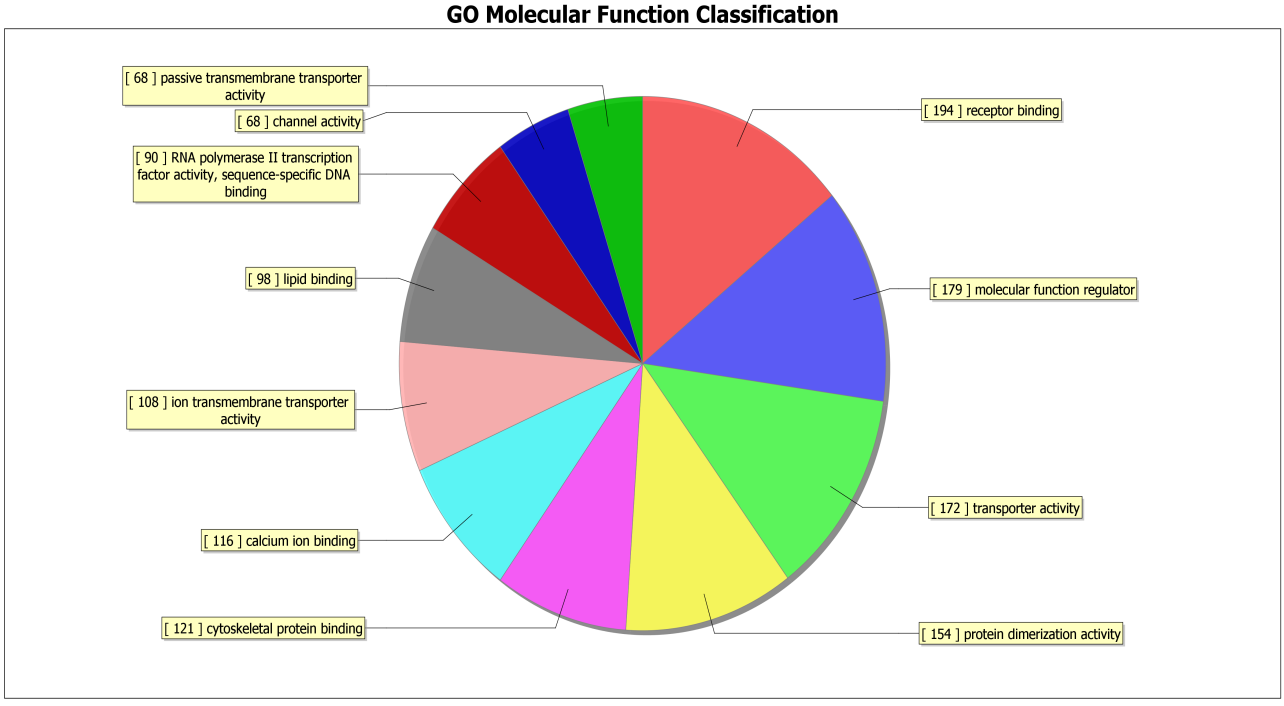

Figure 3.16: Upregulated mRNAs grouped by molecular function.

Number of genes given in brackets.

3.7.2 Pathway Analysis

Pathway analysis is a functional analysis mapping genes to Kyoto Encyclopedia of Genes and Genomes (KEGG) pathways. The p-value (EASE-score, Fisher p-value or hypergeometric p-value) denotes the significance of the pathway correlated to the conditions. Figure 3.17 shows upregulated mRNAs grouped by pathways. The largest group concerns purine metabolism (35 genes).

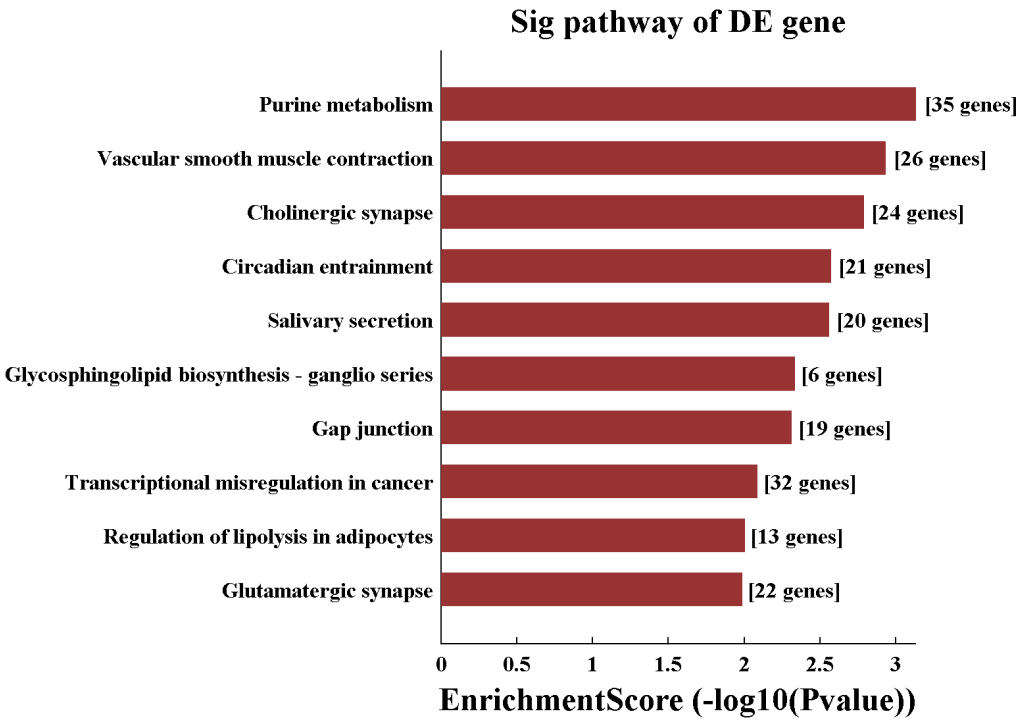

Figure 3.17: KEGG pathway analysis of upregulated mRNAs.

3.7.3 The top ten upregulated mRNAs

The top ten upregulated mRNAs in Clone 1 compared to the control are listed in Table 3.5 including reported associations to PCa or the AR.

Table 3.5: Top ten upregulated mRNAs in Clone 1 compared to Control.

Upregulated mRNA	Fold change Clone 1 *vs*. Control 1	Reported association to PCa or the AR
SERPINB1	2400	Protects cells from proteases released during stress or infection. Reduced expression in locally advanced and metastatic PCa [199]
SCG3	1271	Encodes a neuroendocrine secretory protein [200]. No reported association to PCa or the AR.
RGS2	1221	Regulates G protein-coupled receptor signalling. Inhibits androgen-independent activation of the AR[201]. High levels in advanced PCa correlate to poor patient survival and metastasis [202]
FUNDC1	1132	Activator of hypoxia-induced mitophagy [203]. No reported association to PCa or the AR.
MATK	1111	Plays a significant role in the signal transduction of hematopoietic cells [204]. No reported association to PCa or the AR.
CTAG1B (NY-ESO-1)	1078	Absent expression in benign prostate but associated with ERG fusion PCa and PCa with PTEN loss [205].
HYI	1052	Involved in carbohydrate transport and metabolism [206]. No reported association to PCa or the AR.
GPAT2	942	Highly expressed in PCa, melanoma, lung and breast cancer[207].
PEG10	910	AR repressed gene, upregulated in neuroendocrine PCa in response to AR interference[208, 209]
SGCE	810	Encodes a cellular membrane protein of unknown function. Often co-expressed with *PEG10* [210].

3.7.4 Upregulated mRNAs with important associations to PCa or the AR

We evaluated genes known to be involved in the development of PCa and CRPC to determine if they were significantly upregulated in Clone 1 compared to control cells (Table 3.6).

Table 3.6: Selected upregulated mRNAs previously associated with PCa or the AR.

Upregulated mRNA	Fold change Clone 1 *vs*. Control
SPINK1	343
PCDH7	229
PITX2	119
AR	2.3
SPOP	< 2.0

3.7.5 Selection of mRNAs for validation

mRNAs were selected for validation based on their degree of differential expression and whether they were previously linked to mechanisms that may contribute to enzalutamide resistance. We selected *CTAG1B, PITX2, SPINK1, PCDH7* and *PEG10* for validation. Cells from Control, Clone 1 and Clone 9 were cultured and RNA isolated and quantified as previously described (Sections 2.3 and 2.4). cDNA was synthesised and RT-qPCR performed as previously described (Section 2.5).

3.7.6 *CTAG1B* is significantly upregulated in enzalutamide resistant cells

Cancer/testis antigen 1B (*CTAG1B*), also known as New York esophageal squamous cell carcinoma (*NY-ESO-1*), showed a fold change of 1078 between Clone 1 and Control. RT-qPCR confirmed that *CTAG1B* was significantly overexpressed in Clone 1 (Figure 3.18).

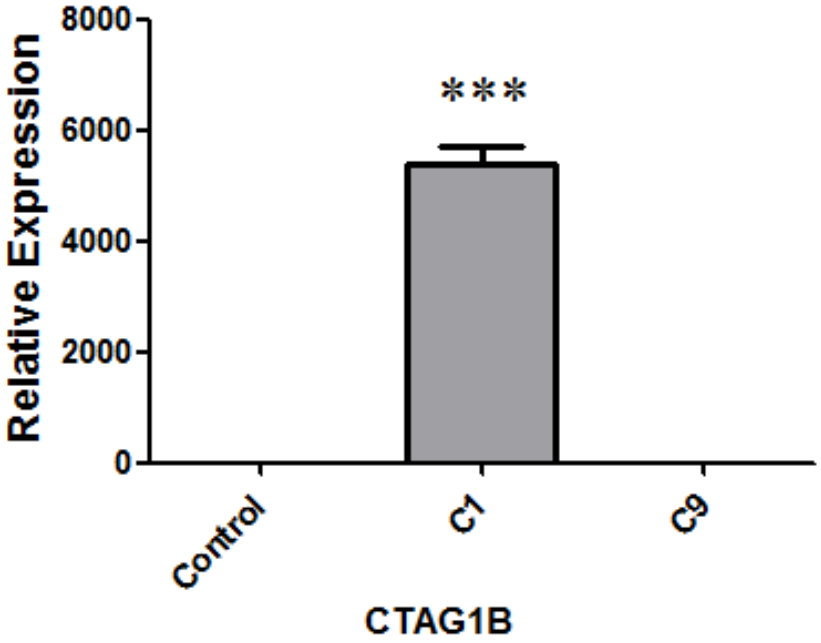

Figure 3.18: *CTAG1B* is significantly overexpressed in Clone 1 versus Control.

Data graphed as mean ± SEM (n=3). Statistical analysis performed using ordinary one-way ANOVA, *post-hoc* Dunnett's test (Clone 1 *vs* Control, *** p≤0.001).

C1 = Clone 1, C9 = Clone 9.

3.7.7 *PEG10* is significantly upregulated in enzalutamide resistant cells

Paternally expressed gene 10 (*PEG10*) showed a fold change of 910 between Clone 1 and Control. RT-qPCR confirmed that *PEG10* was significantly overexpressed in Clone 1 (Figure 3.19).

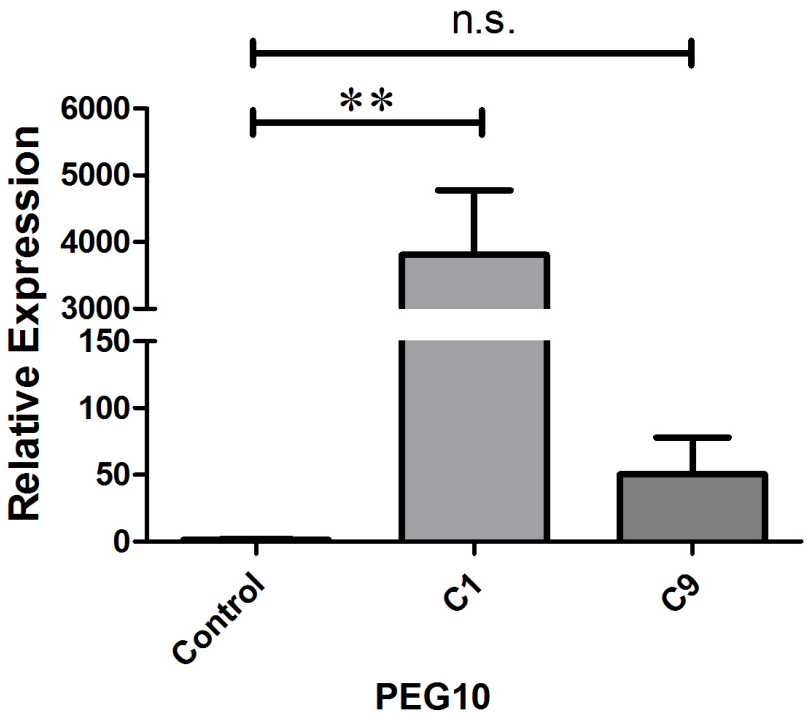

Figure 3.19: *PEG10* is significantly overexpressed in Clone 1 versus Control.

Data graphed as mean ± SEM (n=3). Statistical analysis performed using ordinary one-way ANOVA, *post-hoc* Dunnett's test (Clone 1 *vs* Control, *** p≤0.001).

C1 = Clone 1, C9 = Clone 9, n.s. = not significant.

3.7.8 *SPINK1* is significantly upregulated in enzalutamide resistant cells

SPINK1 showed a fold change of 343 between Clone 1 and Control. RT-qPCR confirmed that *SPINK1* was significantly overexpressed in Clone 1 (Figure 3.20).

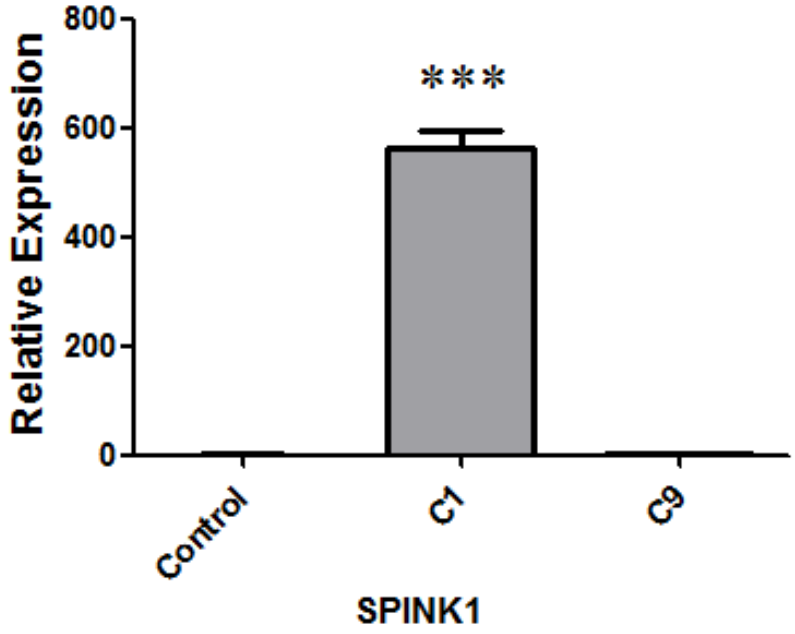

Figure 3.20: *SPINK1* is significantly overexpressed in Clone 1 versus Control.

Data graphed as mean ± SEM (n=3). Statistical analysis performed using ordinary one-way ANOVA, *post-hoc* Dunnett's test (Clone 1 *vs* Control, *** p≤0.001).

C1 = Clone 1, C9 = Clone 9.

3.7.9 *PITX2* is significantly upregulated in enzalutamide resistant cells

Paired like homeodomain 2 (*PITX2*) showed a fold change of 119 between Clone 1 and Control. RT-qPCR confirmed that *PITX2* was significantly overexpressed in Clone 1 (Figure 3.21).

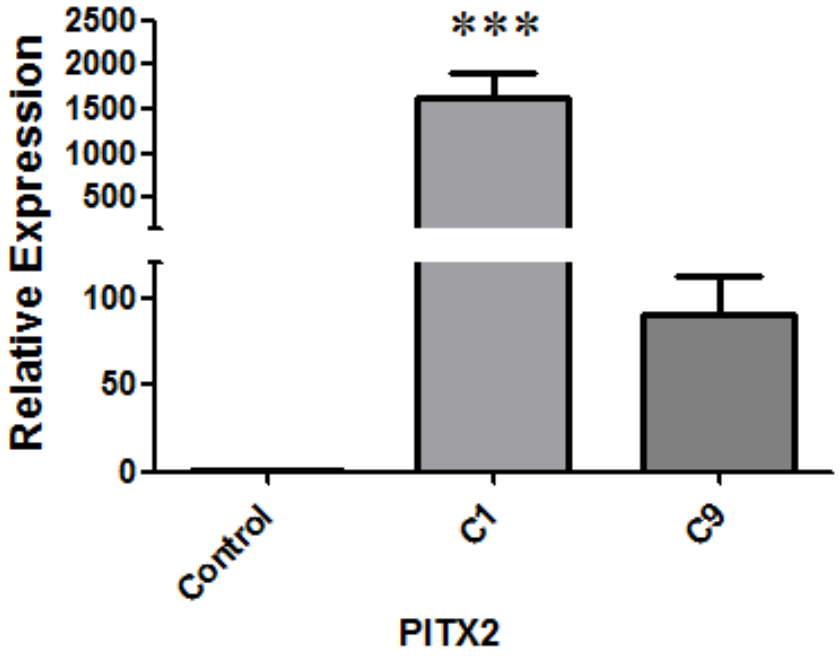

Figure 3.21: *PITX2* is significantly overexpressed in Clone 1 versus Control.

Data graphed as mean ± SEM (n=3). Statistical analysis performed using ordinary one-way ANOVA, *post-hoc* Dunnett's test (Clone 1 *vs* Control, *** p≤0.001).

C1 = Clone 1, C9 = Clone 9.

3.7.10 *PCDH7* is significantly upregulated in enzalutamide resistant cells

Protocadherin 7 (*PCDH7*) showed a fold change of 229 between Clone 1 and Control. RT-qPCR confirmed that *PCDH7* was significantly overexpressed in Clone 1 (Figure 3.22).

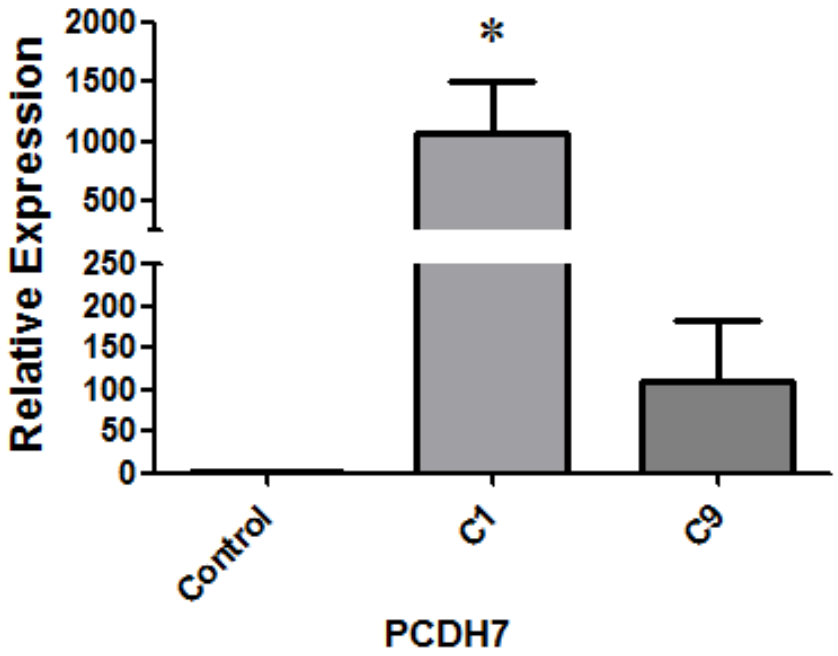

Figure 3.22: *PCDH7* is significantly overexpressed in Clone 1 versus Control.

Data graphed as mean ± SEM (n=3). Statistical analysis performed using ordinary one-way ANOVA, *post-hoc* Dunnett's test (Clone 1 *vs* Control, * p≤0.05).

C1 = Clone 1, C9 = Clone 9.

3.8 Downregulated mRNAs

3.8.1 The top ten downregulated mRNAs

The top ten downregulated mRNAs in Clone 1 compared to Control 1 are listed in Table 3.7 including reported associations to PCa or the AR.

Table 3.7: Top ten downregulated mRNAs.

Downregulated mRNA	Fold change Clone 1 *vs*. Control	Reported association to PCa or the AR
H2AFJ	1321	Encodes a variant H2A histone [211]. No reported associations to PCa or the AR
PEG3	488	Transcription factor, regulates foetal growth rates [212]. Promotes PCa cell growth in rats [213]. Downregulated by androgens *in vitro [214]*
SLC22A3	462	Associated with prostate carcinogenesis [215]
UGT2B17	270	Associated with androgen metabolism, deletion is association with an increased risk of PCa [216]
TM4SF1	234	AR regulated, overexpressed in PCa, involved in cell migration [217]
UGT2B11	228	Associated with androgen metabolism and expression regulated by androgens in PCa cells *in vitro [218]*
PXDN	194	Overexpressed in PCa tissue, inhibits oxidative stress leading to decreased apoptosis [219]
TSPY3	124	Normal expression restricted to the testis [220], no reported associations to PCa or the AR
CTNNA3	115	Encodes α-T-catenin involved in cell–cell adhesion [221]. No reported associations to PCa or the AR
TRIM49	113	Preferentially expressed in testis and involved in protein-protein interactions [222]. No reported associations to PCa or the AR

3.8.2 Downregulated mRNAs with important associations to PCa or the AR

Genes known to be involved in the development of PCa and CRPC were evaluated to see if they were significantly downregulated in Clone 1 compared to Control (Table 3.8).

Table 3.8: Selected downregulated mRNAs previously associated with PCa or the AR.

Downregulated mRNA	Fold change Clone 1 vs Control 1
PTEN	< 2.0
SPOP	< 2.0
CHD1	< 2.0
TP53	2.1

3.9 Assessment of lncRNAs and mRNAs in a panel of cell lines

The expression of validated lncRNAs and mRNAs was assessed by end-point PCR in a panel of cell lines as previously described (Section 2.2) and summarised in Table 3.9. Validated lncRNAs and mRNAs were expressed in both benign and malignant cell lines but were more likely to be expressed in more aggressive PCa cell lines 22Rv1, PC-3 and DU 145 (Figure 3.23)

Table 3.9: Panel of cancer cell lines used in experiments.

Group	Cell Line	Source
Benign prostate	RWPE-1	Human prostate tissue
	PWR-1E	Prostatic epithelial cells
	BPH-1	Human prostate tissue
AR positive	VCaP	Vertebral bone metastasis
	22Rv1	Androgen-dependent xenograft
	LNCaP-FGC	Lymph node metastasis
AR negative	PC-3	Bone metastasis
	DU 145	Brain metastasis
Other cancer type	MCF7	Breast cancer
	H1975	Lung adenocarcinoma
	HuH7	Hepatocellular carcinoma

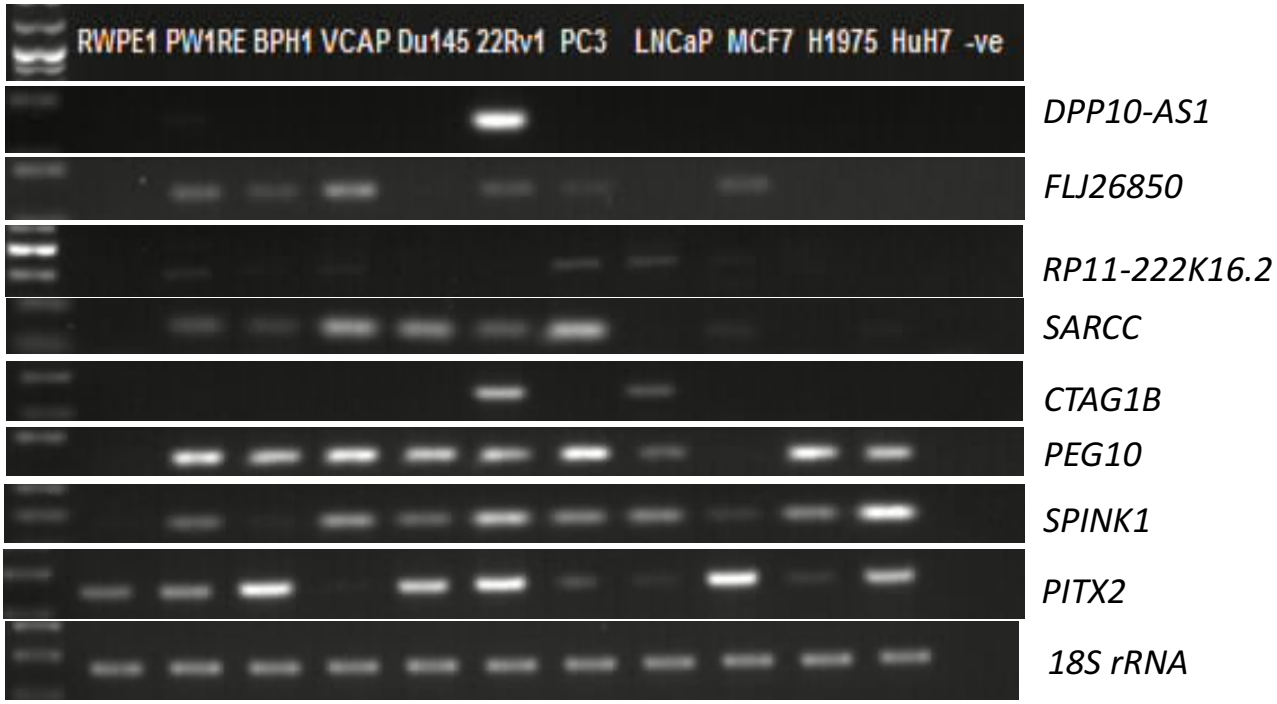

Figure 3.23: Expression of lncRNAs and mRNAs in a panel of cell lines. End-point PCR, n=1. 18S rRNA used as loading control.

3.10 Evaluation of the AR signalling pathway

Given the central importance of the AR signalling pathway in PCa and enzalutamide resistance, we evaluated the differential expression of the AR and AR-V7 [67]. Cells from Control, Clone 1 and Clone 9 were cultured in triplicate and RNA isolated and quantified as previously described (Section 2.3 and 2.4). cDNA was constructed and RT-qPCR performed as previously described (Section 2.5). Primers were designed and constructed as previously described (Table 2.4). There was no significant difference in expression of the AR between the cell lines (Figure 3.24). However, AR-V7 was significantly overexpressed in Clone 1 cells (Figure 3.25).

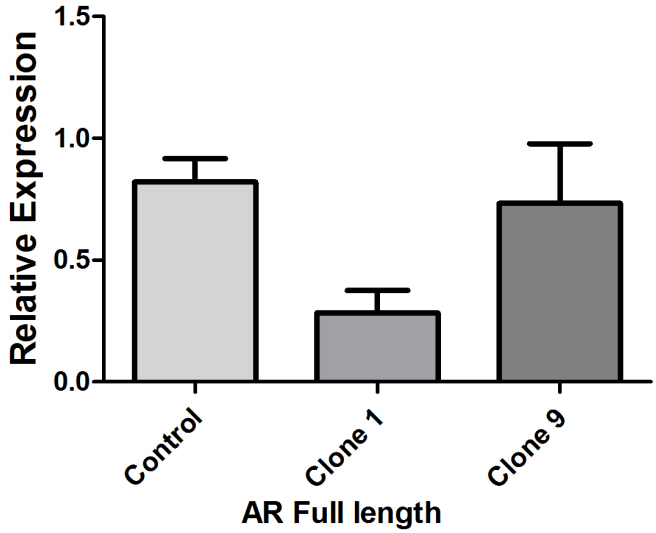

Figure 3.24: Expression of AR-FL in cells with varied enzalutamide resistance.

Data graphed as mean ± SEM (n=3). Statistical analysis performed using ordinary one-way ANOVA, *post-hoc* Dunnett's test. There is no difference in AR full length expression between enzalutamide sensitive and resistant cells.

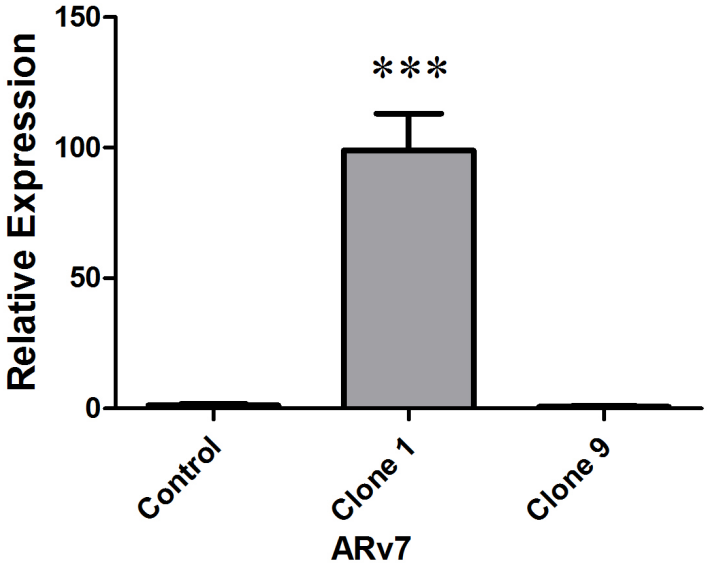

Figure 3.25: AR-V7 is significantly overexpressed in Clone 1 compared to Control.

Data graphed as mean ± SEM (n=3). Statistical analysis performed using ordinary one-way ANOVA, *post-hoc* Dunnett's test (Clone 1 *vs* Control, *** p≤0.001).

3.11 Evaluation of neuroendocrine differentiation

Neuroendocrine differentiation is an important feature of lethal CRPC. Patients with neuroendocrine PCa have a poor prognosis due to resistance to anti-androgen therapies [208]. It is unclear whether neuroendocrine PCa develops due to the growth of a separate clone of malignant neuroendocrine cells or if it is due to transdifferentiation of malignant epithelial cells. Neuroendocrine PCa is becoming more common in patients on second generation anti-androgens suggesting that targeting the AR may be associated with its development. One study reported that *PEG10* is upregulated after treatment with anti-androgens and is associated with the development of neuroendocrine PCa [208]. Given that *PEG10* is upregulated in our data, and also because neuroendocrine differentiation is a potential mechanism for the development of enzalutamide resistance, we evaluated the expression of common genes associated with neuroendocrine differentiation.

3.11.1 *BRN2* and *CgA* are not upregulated in enzalutamide resistant cells

BRN2 is highly expressed in neuroendocrine PCa and its expression is correlated with the development of neuroendocrine differentiation [223]. CgA mRNA overexpression has been used to identify neuroendocrine differentiation as it encodes for chromogranin A, a protein highly expressed in neuroendocrine tissues [224]. The relative expression of both *BRN2* and *CgA* were evaluated by RT-qPCR as previously described (Section 2.5). While both showed more expression in enzalutamide resistant cells, the difference was not significant (Figure 3.26 and 3.27).

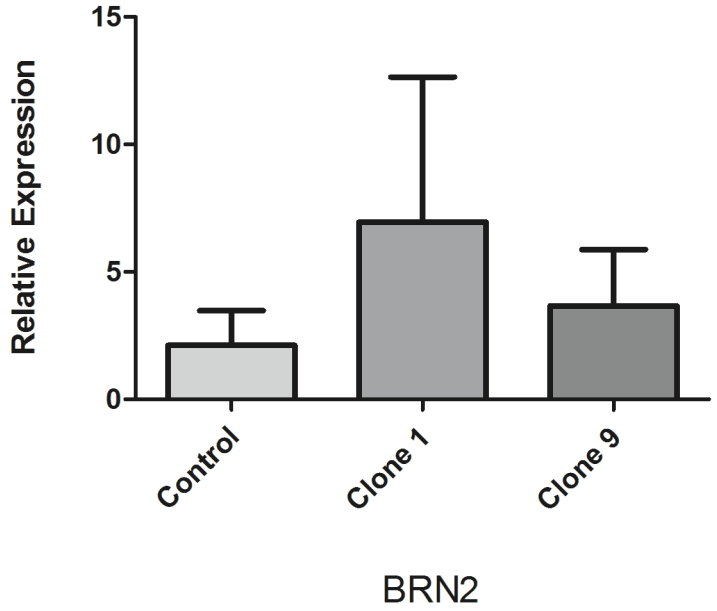

Figure 3.26: Expression of *BRN2* in Control, Clone 1 and Clone 9.

Data graphed as mean ± SEM (n=3). Statistical analysis performed using ordinary one-way ANOVA, *post-hoc* Dunnett's test. There is no difference in *BRN2* expression between enzalutamide sensitive and resistant cells.

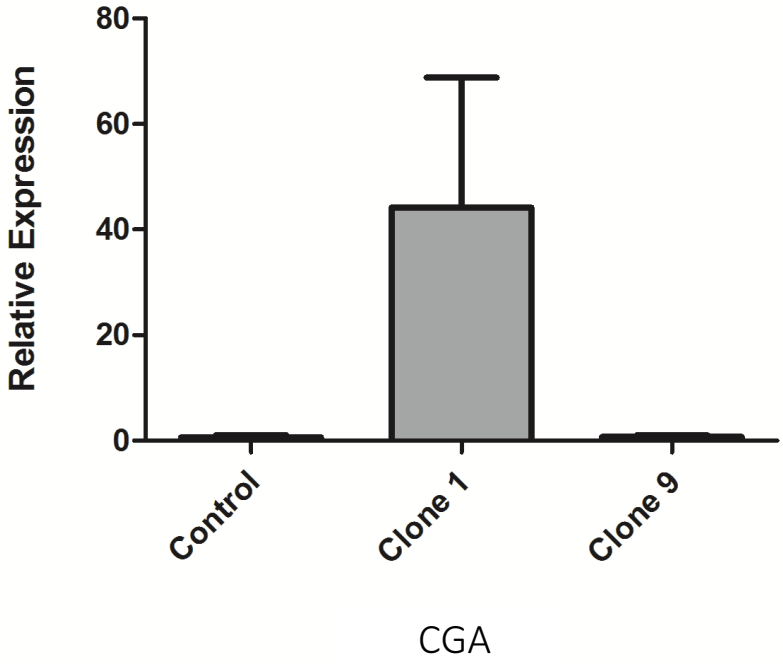

Figure 3.27: Expression of *CGA* in cells with varied enzalutamide resistance.

Data graphed as mean ± SEM (n=3). Statistical analysis performed using ordinary one-way ANOVA, *post-hoc* Dunnett's test. There is no significant difference in *CGA* expression between enzalutamide sensitive and resistant cells.

Chapter 4
Evaluation of lncRNA SARCC

4.1 *SARCC* background

Having validated a number of lncRNAs and mRNAs that were upregulated in enzalutamide resistant cells, the next step was to pick one lncRNA candidate and one mRNA candidate for further investigation. We were particularly keen to investigate a lncRNA candidate as they have been associated with drug resistance in other organ systems and are highly stable when circulating in body fluids, a useful property for a potential biomarker [225]. LncRNA SARCC and mRNA PCDH7 were chosen for further investigation although the experiments for PCDH7 were ultimately unsuccessful (see section 4.10).

LncRNA SARCC was chosen for further investigation as we had validated its overexpression in enzalutamide resistant cells compared to enzalutamide sensitive cells. Also, previous research on *SARCC* showed an association with the AR. Zhai *et. al* demonstrated that *SARCC* can physically bind to AR protein and that DHT enhanced the interaction of *SARCC* with the AR in RCC cells [159, 187]. They also showed that *SARCC* is mainly located in the nucleus and a region at the 3' end of *SARCC* binds to the ligand binding domain of the AR. Although Zhai *et. al* found *SARCC* to have a tumour suppressor role in RCC and was associated with a decrease in AR protein expression, another study reported that *SARCC* is overexpressed in RCC tissue compared to benign renal tissue arguing against a tumour suppressor role [226].

A key feature of CRPC is continued AR signalling despite undetectable circulating androgens. As lncRNA *SARCC* can bind to the AR and was upregulated in enzalutamide resistant cells, theoretically, lncRNA *SARCC* could cause continued AR signalling in the absence of androgens. This potential functional role in AR signalling made it a good candidate for further investigation. We aimed to overexpress *SARCC* in enzalutamide sensitive Control cells to determine if this would result in increased resistance to enzalutamide and also to knockdown *SARCC* in the enzalutamide resistant Clone 1 cells to examine if this would result in increased sensitivity to enzalutamide.

4.2 Overexpression of *SARCC*

A summary of the cloning strategy for overexpression of *SARCC* is given in Appendix I. Briefly, *SARCC* was amplified by PCR as previously described (Section 2.8). Agarose gel electrophoresis confirmed the presence of SARCC after PCR (Figure 4.1). TOPO cloning and transformation into E. coli bacteria was performed as previously described (Section 2.8). Plasmid DNA was isolated and samples containing *SARCC* were selected for double digest using BamH I and Xho I restriction enzymes as previously described (Section 2.8). The insert was isolated by band isolation and DNA purification was performed as previously described (Section 2.8). In parallel, DNA from a new plasmid, pcDNA3.1(+) (Invitrogen) was also digested using BamH I and Xho I and band isolation performed. Figure 4.2 is a representative gel electrophoresis image of the DNA after band isolation and purification showing the *SARCC* insert. Ligation of the *SARCC* insert into the pcDNA3.1(+) plasmid was performed as previously described (Section 2.8). An overview of the resulting recombinant plasmid DNA is shown in Appendix II. The pcDNA3.1(+) plasmid containing the *SARCC* insert and the control pcDNA3.1(+) plasmid were transformed into DH5α E. coli chemically competent cells as previously described (Section 2.8). Plasmid DNA was isolated and the presence of the SARCC insert confirmed by PCR using the original *SARCC* primers (Table 2.5) (Figure 4.3).

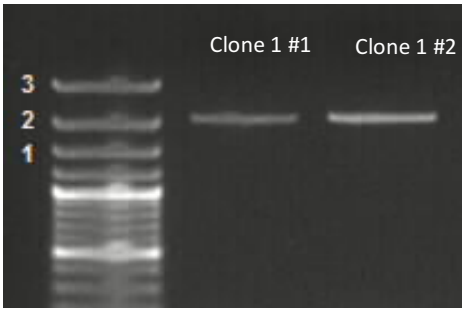

Figure 4.1: Gel electrophoresis of *SARCC* PCR products.

Bright bands at predicted size of *SARCC* insert (2150 base pairs). 1 = 1500 bp, 2 = 2000 bp, 3 = 3000 bp.

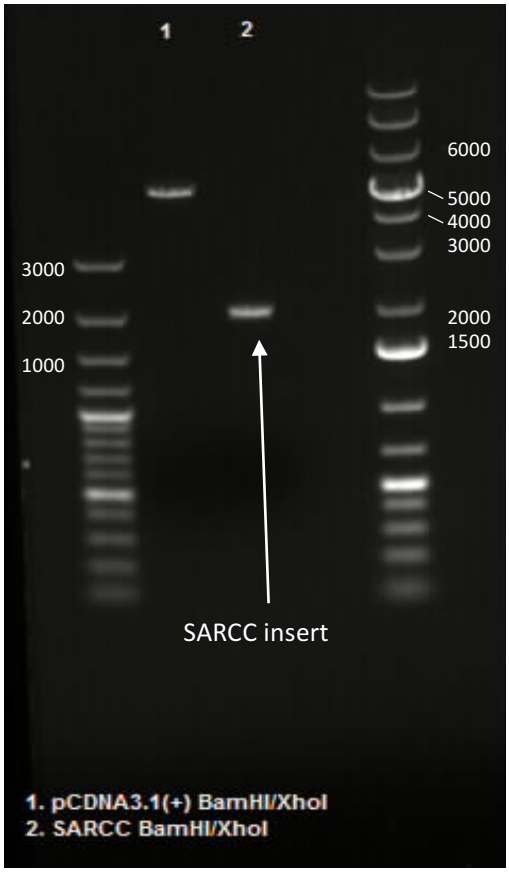

Figure 4.2: Purified DNA after restriction enzyme digest and band isolation.

Predicted length of pcDNA3.1(+) is 5428 bp and for SARCC insert is 2150 bp

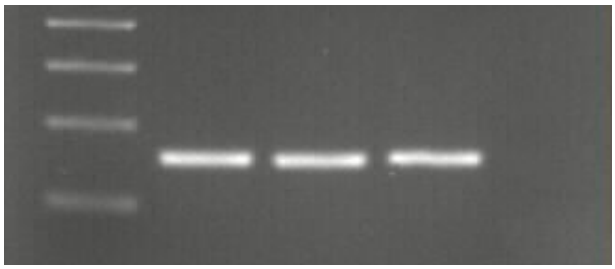

Figure 4.3: Gel electrophoresis confirming SARCC in all three samples of plasmid DNA.

Orientation of the insert

The orientation of the insert was examined using the restriction enzyme Hind III. The correct orientation of the insert is shown in part A of Figure 4.4, where digestion with Hind III would provide three fragments measuring 510, 633 and 6,435 base pairs. If, however, the insert was in the incorrect orientation (part B), digestion with Hind III would result in three fragments measuring 510, 1,025 and 6,043 base pairs. The DNA from two of the plasmids were selected and digested with Hind III. Five µL plasmid DNA, 1 µL Hind III, 2 µL 10X buffer and 12 µL molecular grade water were gently mixed together and digested overnight at 37°C. Gel electrophoresis confirmed that SARCC was in the correct orientation based on the size of the fragments (Figure 4.5).

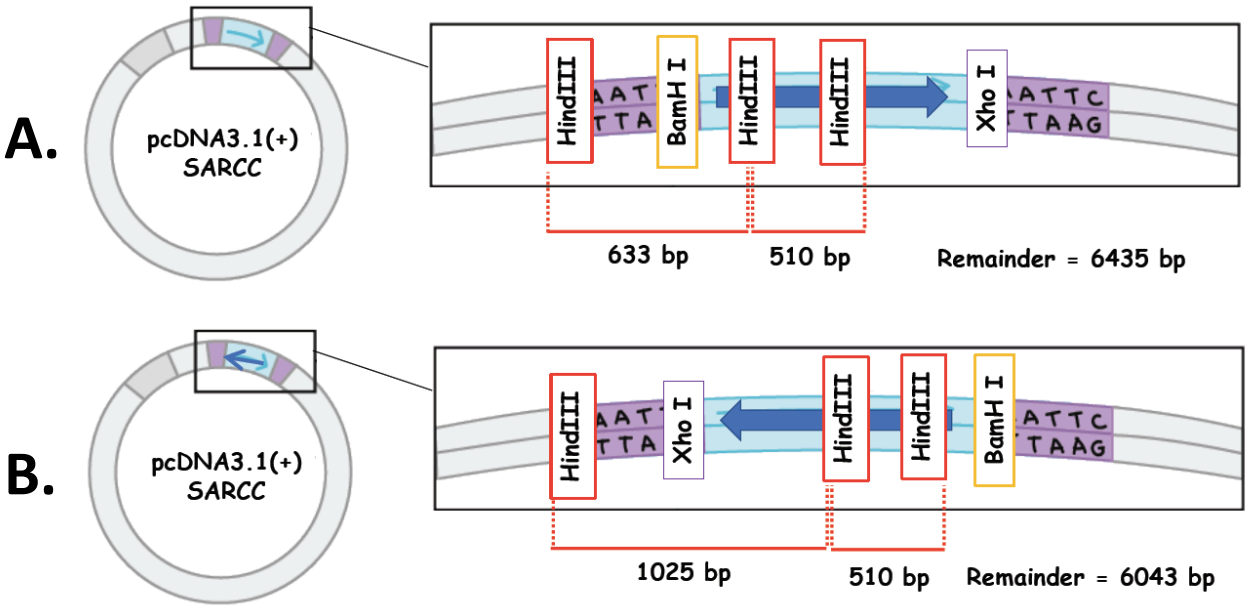

Figure 4.4: Schematic showing the restriction enzyme sites in the *SARCC* insert.

A (top) shows the correct orientation while B (bottom) shows the incorrect orientation.

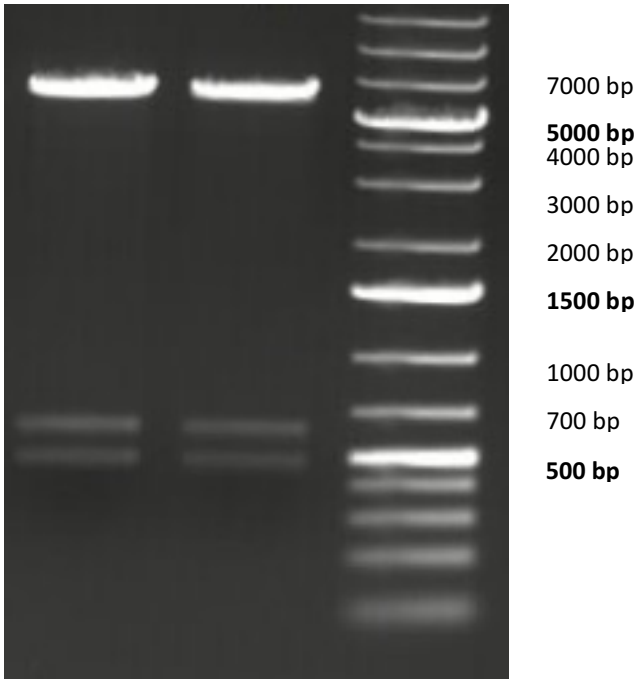

Figure 4.5: pcDNA3.1(+) *SARCC* digested by Hind III.

Both samples show three fragments at predicted lengths for correct orientation (510 bp, 633 bp and 6435 bp)

Transfection

In preparation for a double integration transfection, the plasmids were linearised with Pvu I, a restriction enzyme that cuts pcDNA3.1(+) in one location and does not cut the *SARCC* insert. Linearisation was successful but multiple attempts at transfection using various combinations of concentrations and new plasmid DNA were unsuccessful. Therefore, a single integration stable transfection was performed using TurboFect Transfection Reagent as previously described (Section 2.8). Both the vector containing the *SARCC* gene and an empty vector control were transfected. Treatment with 4 µL 100 mg/mL G418 dilsulfate was used to select the transfected cells. The media and G418 were replaced approximately every 2-3 days for 14 days.

Preparation of SARCC overexpressed cell line for analysis

Cells from the parent Clone 1 cells, the empty vector control (EVC) and the *SARCC* overexpressed cells were cultured in triplicate. RNA was isolated and cDNA synthesised as previously described (Section 2.5).

4.3 *SARCC* overexpression is confirmed in enzalutamide sensitive cells

RT-qPCR was undertaken on cDNA from the parent, EVC and *SARCC* overexpressed cells as previously described (Section 2.5) using the original *SARCC* primers (Table 2.5). *SARCC* was significantly overexpressed in the cells containing the *SARCC* insert (Figure 4.6).

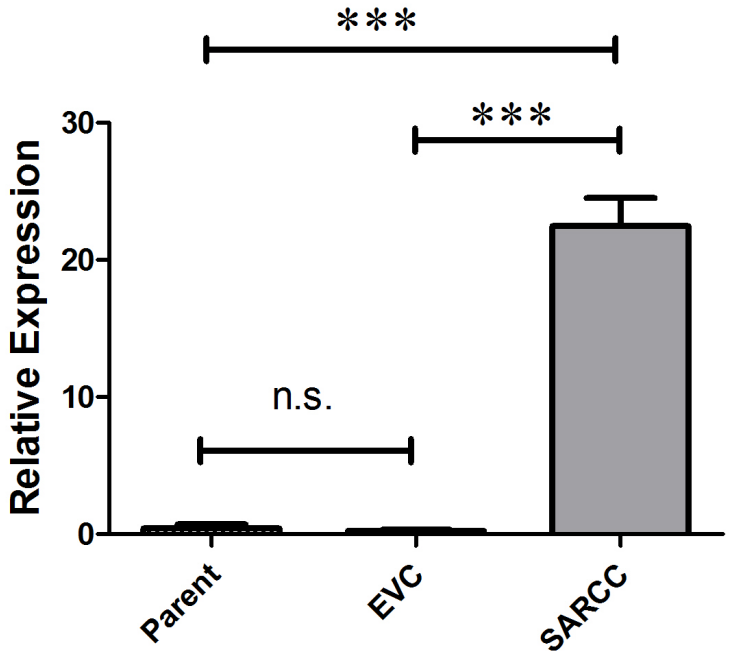

Figure 4.6: *SARCC* is overexpressed compared to Control and the EVC.

Data graphed as mean ± SEM (n=3). Statistical analysis performed using ordinary one-way ANOVA, *post-hoc* Dunnett's test (* p≤0.001). EVC = Empty Vector Control**

4.4 *SARCC* overexpression is associated with increased resistance to enzalutamide

Cells from the EVC and *SARCC* overexpressed cell lines were seeded in triplicate into a 96 well plate with varying concentrations of enzalutamide and a BrdU assay performed as previously described (Section 2.10). The *SARCC* overexpressed cells showed increased resistance to enzalutamide compared to the EVC cells (Figure 4.7).

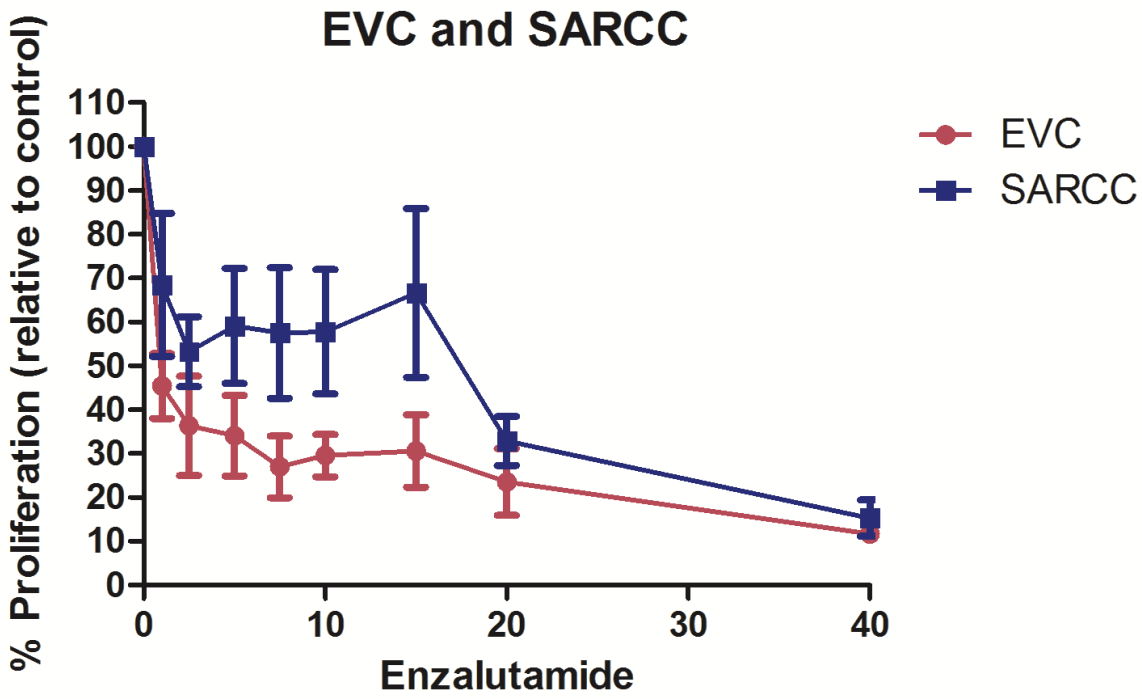

Figure 4.7: *SARCC* overexpressed cells are more resistant to enzalutamide treatment than the EVC cells

Data graphed as mean ± SEM (n=3).

4.5 *SARCC* overexpression does not result in a significant alteration in cell doubling time

Cell doubling time was evaluated in the EVC and *SARCC* overexpressed cell lines as previously described (Section 2.10). There was no significant difference in cell doubling time between the EVC cells and the *SARCC* overexpressed cells (Table 4.2).

Table 4.1: Comparison of cell doubling time

	EVC	***SARCC***
Doubling time, n = 1	50 hours	55 hours
Doubling time, n = 2	53 hours	47 hours
Doubling time, n = 3	58 hours	53 hours
Mean doubling time	53.7 hours	51.7 hours

4.6 *SARCC* overexpression does not result in significant alteration in AR expression

We assessed the expression of the AR in the EVC and *SARCC* overexpressed cell lines by RT-qPCR as previously described using primers originally described by Antonarakis *et. al* [67] (Table 2.5). We also assessed AR expression at the protein level by performing immunohistochemistry (IHC) for the AR protein (Section 2.9), on cell blocks derived from the EVC and *SARCC* overexpressed cell lines. There was no significant difference in AR mRNA expression by qPCR (Figure 4.8). There was also no appreciable difference in immunohistochemical staining - both the EVC and *SARCC* overexpressed cells showed strong nuclear staining for the AR protein (Figure 4.9).

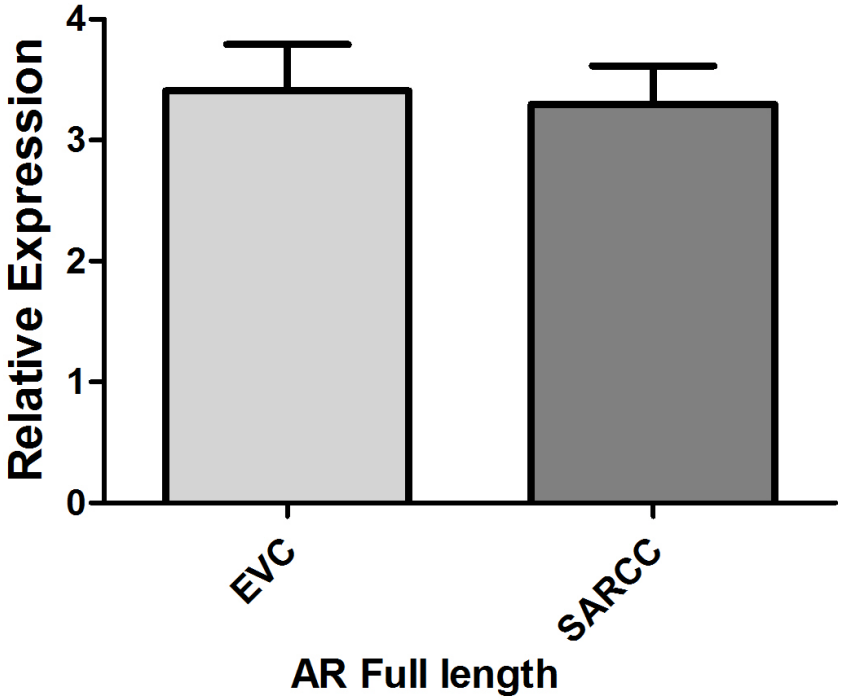

Figure 4.8: AR expression in EVC versus *SARCC* overexpressed cell lines.

Data graphed as mean ± SEM (n=3). Statistical analysis performed using ordinary one-way ANOVA, *post-hoc* Dunnett's test.

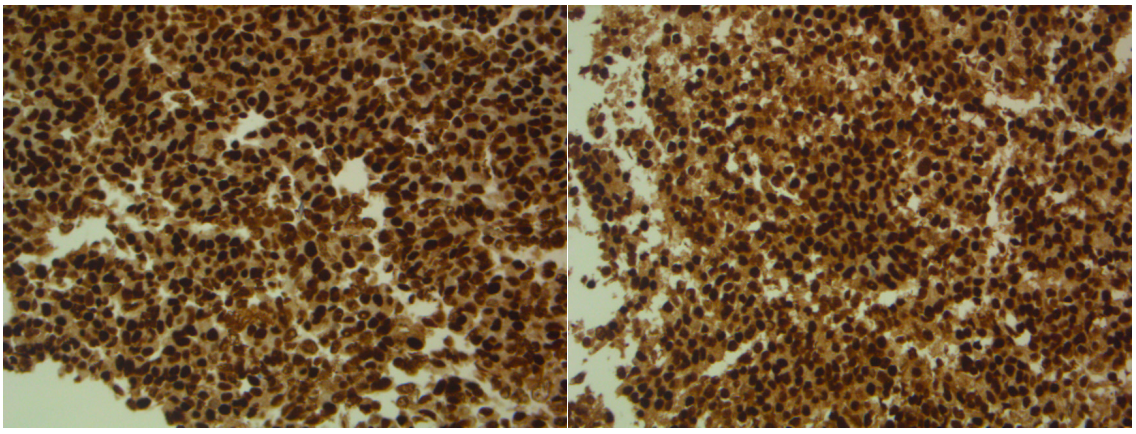

Figure 4.9: Immunohistochemistry for AR protein.

There is strong nuclear staining for the AR protein in both the EVC cells (left) and the *SARCC* overexpressed cells (right). 200X magnification.

4.7 *SARCC* overexpression does not result in significant alteration in AR-V7 expression

We assessed the expression of AR-V7 in the EVC and *SARCC* overexpressed cell lines by RT-qPCR as previously described (Section 2.5) using primers originally described by Antonarakis *et. al [67]* (Table 2.5). We did not find any significant alteration in expression (Figure 4.10).

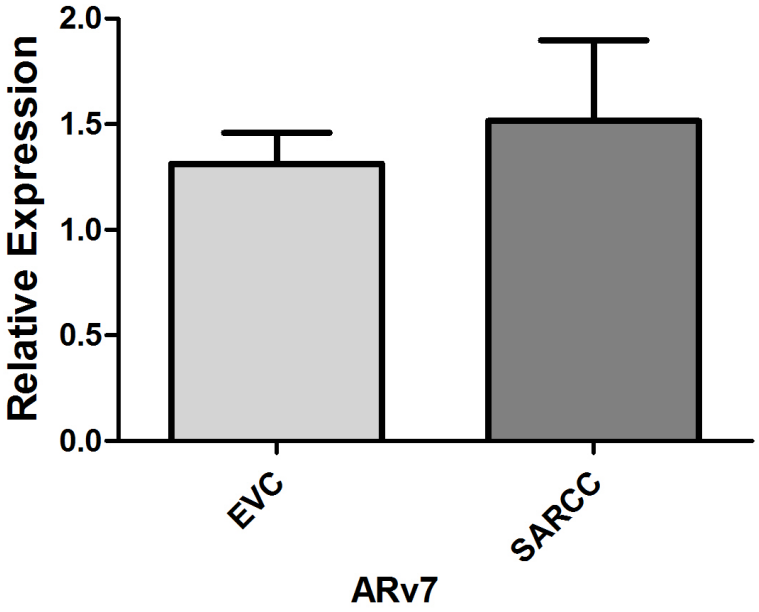

Figure 4.10: AR-V7 expression in EVC compared to *SARCC* overexpressed cells. RT-qPCR showed no significant difference in AR--V7 expression between the EVC and *SARCC* overexpressed cell lines. Data graphed as mean ± SEM (n=3). Statistical analysis performed using ordinary one-way ANOVA, *post-hoc* Dunnett's test.

4.8 *SARCC* overexpression does not result in significant alteration in neuroendocrine expression

The expression of neuroendocrine markers synaptophysin and chromogranin was assessed by immunohistochemistry on cell blocks derived from the EVC and *SARCC* overexpressed cell lines, as previously described (Section 2.9). There was no appreciable difference in staining with both cell lines showing an absence of staining (Figure 4.11).

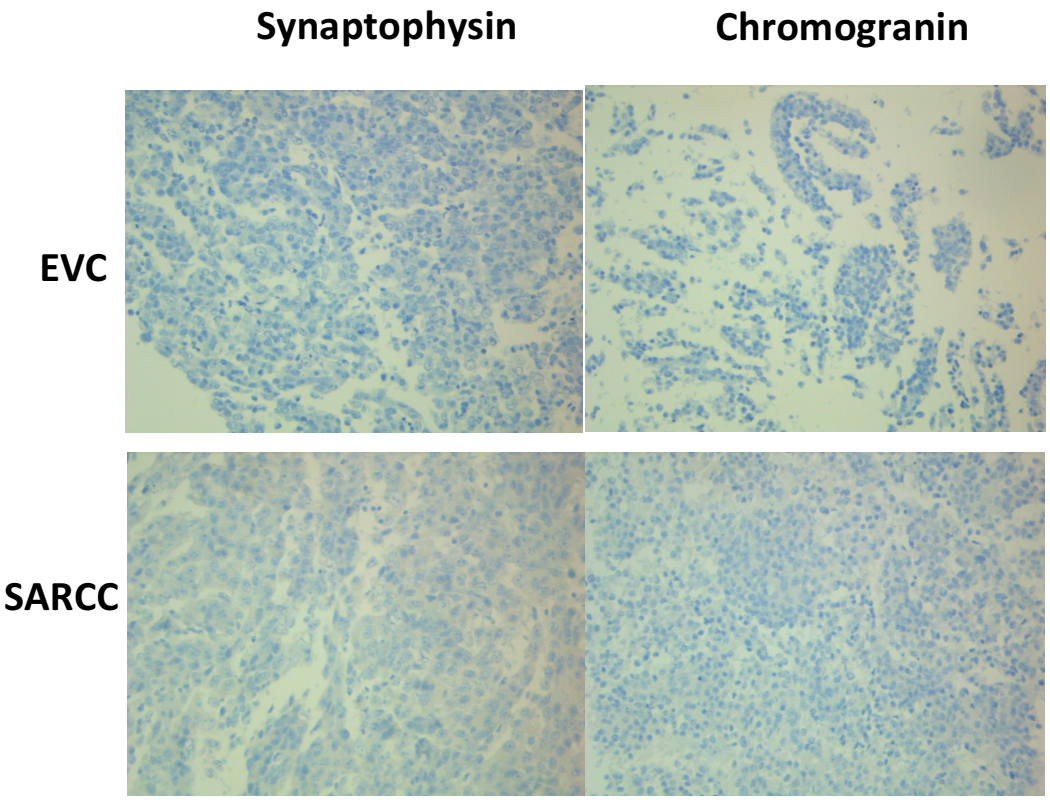

Figure 4.11: Immunohistochemistry for synaptophysin and chromogranin. Staining for synaptophysin (left column) and chromogranin (right column) is negative in the EVC cells (top row) and the *SARCC* overexpressed cells (bottom row). 200X magnification.

4.9 Knockdown of *SARCC*

Knockdown of the *SARCC* gene was attempted using short hairpin RNA (shRNA). We used the plasmid pLK0.1 TRC (Sigma Aldrich) and primers as described by Zhai *et. al* [159, 187]. Transformation of the insert into the plasmid was successful but repeated attempts at transfection into Clone 1 cells using various concentrations of plasmid DNA, Turbofect and different cultures of Clone 1 cells were unsuccessful. We repeated the cloning experiments using a different digestion approach with the same plasmid but, again, transfection was unsuccessful.

4.10 Evaluation of *PCDH7*

PCDH7 was chosen for further evaluation as it was significantly overexpressed in enzalutamide resistant cells (from mRNA screen) and previous reports describe an association with CRPC and enzalutamide resistance [227]. We attempted to overexpress and knockdown *PCDH7* in a similar manner to SARCC and then assess its effect on enzalutamide resistance. We used the TOPO® TA Cloning® Kit and the pCR™2.1-TOPO® plasmid (Invitrogen, ThermoFisher Scientific) as previously described (Section 2.8). We also attempted cloning using the plasmid pcDNA3.1(+) (Invitrogen) and the plasmid PLX303 (Addgene). Despite multiple attempts, we were unable to purify a sufficient quantity of the *PCDH7* plasmid DNA from E. coli bacteria for transfection. Knockdown of *PCDH7* was attempted using shRNA and the plasmid pLK0.1 TRC (Sigma Aldrich). Although plasmid DNA was isolated after transformation, attempts at transfection were unsuccessful.

Chapter 5
Discussion and Future Directions

5.1 Introduction

One of the main causes of cancer related death in PCa is the development of drug resistance to anti-androgen therapies. Despite the development of a new generation of anti-androgen therapies, drug resistance remains a key problem. Numerous studies have shown that, in most cases of drug resistance, AR signalling is maintained despite treatment with anti-androgens [11]. Structural changes in the AR, such as the F877L mutation and AR-V7 splice variant, can result in AR signalling despite ADT [65, 67]. While this recent knowledge has enhanced our understanding of the mechanisms underlying drug resistance, it has not yet led to significant changes in the treatment and monitoring of patients in the clinical setting.

The aim of this study was to evaluate the molecular changes that occur in the development of resistance to enzalutamide, a "second generation" anti-androgen. We were particularly interested in the role of lncRNAs, as they are an understudied area of molecular biology and recent papers have described how they may contribute to drug resistance in other cancers [74, 161, 228].

We used an isogenic cell line model of LNCaP cells with varied resistance to enzalutamide and evaluated differentially expressed lncRNAs and mRNAs. LNCaP cells are known to lack expression of the DNA mismatch repair proteins MSH2 and MSH6 suggesting that LNCaP cells have a high rate of spontaneous mutation [229]. For most cases of acquired drug resistance, spontaneous mutation accounts for the emergence of resistant clones. Cells with a high spontaneous mutation rate are therefore useful when trying to identify drug resistant clones as there is a higher likelihood that a resistant clone will emerge. However, LNCaP cell line models may not accurately reflect typical cases of PCa as deficiencies in mismatch repair protein expression are rare in PCa [230].

The strongly resistant cells in our study were known to have the F877L mutation compared to the sensitive cells which did not. The F877L mutation leads to an amino acid substitution in the ligand binding domain of the AR which confers resistance to enzalutamide [65]. It can also confer an antagonist to agonist switch to enzalutamide. This study showed that the resistant cells also express the AR splice variant, AR-V7. AR-

V7 encodes a truncated AR that lacks a ligand-binding domain but retains the N-terminal domain. Although the truncated AR protein is unable to bind ligand, it is capable of promoting activation of target genes and is associated with both primary and secondary resistance to enzalutamide [68].

5.2 lncRNA *SARCC*

SARCC was chosen for focused evaluation due to its known associations to the AR – the 800 nucleotide (nt) region at the 3' end of *SARCC* can bind to the DNA-binding domain and the ligand-binding domain of the AR protein [159, 187]. The N-terminal domain of the AR fails to bind to *SARCC*. *SARCC* overexpression could therefore lead to enzalutamide resistance through activating the AR by directly binding to it or by preventing enzalutamide binding. It may also facilitate translocation of the AR to the nucleus or facilitate binding to AREs.

This study showed that *SARCC* is significantly overexpressed in enzalutamide resistant LNCaP cells compared to enzalutamide sensitive cells. In addition, when *SARCC* was overexpressed in enzalutamide sensitive cells, this resulted in increased resistance to enzalutamide. This finding suggests that *SARCC* plays a functional role in the development of resistance to enzalutamide, something that has not been previously reported.

We did not observe any significant difference in AR mRNA expression when *SARCC* was overexpressed in enzalutamide sensitive cells. This finding supports previous work that showed AR mRNA expression in PCa was unaffected by *SARCC* overexpression or knockdown [159]. Previous studies in RCC reported that *SARCC* exerts its effects at the protein level, where it plays a tumour suppressor role by binding to the AR and enhancing its degradation [159, 187]. We assessed AR protein expression by immunohistochemistry and found no difference in expression when *SARCC* was overexpressed compared to the EVC. It is unclear why *SARCC* appears to degrade the AR in RCC but not in PCa. One possible explanation is that the presence of AR^{F877L} or AR-V7 alters the effect of *SARCC* as it is acting on a mutated AR rather than the full length AR present in RCC. It is also worth noting that a different study examining *SARCC* in RCC

found that it was overexpressed in RCC tissue compared to benign renal tissue arguing against a tumour suppressor role [226].

Another consideration was whether *SARCC* was affecting RNA splicing and enhancing the expression of AR-V7, thus leading to enzalutamide resistance. LncRNAs can bind to splicing factors or RNA-binding proteins and cause alternative splicing patterns [231]. For example, lncRNA *MALAT-1* can sequester splicing factors within nuclear paraspeckles to alter splicing efficiency [232]. However, when we overexpressed *SARCC* in enzalutamide sensitive cells, there was no significant difference in AR-V7 expression.

SARCC is a long intergenic non-coding RNA (lincRNA), a subtype of lncRNA that does not overlap protein-coding genes, located on chromosome 3. lincRNAs vary in their proximity to protein-coding genes with some within a few bases and others more than 3Mb away [233]. While some lincRNAs affect the expression of neighbouring genes, proximity to a protein-coding gene does not necessarily predict the function of a lincRNA. The *SARCC* gene is a single exon and is located in close proximity to the protein coding gene *P2RY1*. *P2RY1* encodes a protein belonging to the P2Y receptor family, a family of G-protein coupled receptors that respond to extracellular purine and pyrimidine nucleotides. The P2RY1 receptor functions as a receptor for extracellular ATP and ADP. *P2RY1* showed a 2.4-fold increase in expression in enzalutamide resistant cells compared to sensitive cells based on microarray data. Other members of the P2Y receptor family (P2RY2, 4, 6, 8, 10, 11, 13 and 14) did not show any significant change in expression. We did not further investigate whether *P2RY1* expression is associated with enzalutamide resistance. However, KEGG pathway analysis showed that the most upregulated pathway in enzalutamide resistant cells was a pathway associated with purine metabolism (35 genes upregulated) suggesting that purine receptors may play a role in resistance.

5.2.1 Further work – *SARCC* and enzalutamide resistance

While *SARCC* overexpression resulted in increased resistance to enzalutamide, knockdown of *SARCC* in enzalutamide resistant cells is required to determine a concomitant increase in enzalutamide sensitivity. We attempted knockdown of *SARCC*

but multiple efforts at transfection were unsuccessful. Further work could attempt *SARCC* knockdown using a different strategy such as CRISPR.

Further work could also examine *SARCC* expression *in vivo*. Evaluation of *SARCC* expression in PCa tissue has never been performed. Tissue or blood samples of patients with PCa could be assessed for *SARCC* expression by RNA-ISH. It would be important to evaluate the levels of SARCC in samples of patients with and without enzalutamide resistance.

5.2.2 Further work – *SARCC* as a biomarker of enzalutamide resistance

If the above experiments confirmed the findings in this study, the use of *SARCC* as a biomarker for enzalutamide resistance could be considered. A reliable biomarker for primary and secondary resistance to enzalutamide would be of great benefit in the clinical setting. Quantifying *SARCC* expression in patients before and during enzalutamide treatment and at the point of the development of resistance could be performed.

5.2.3 Further work – *SARCC* and the AR

As *SARCC* can bind to AR protein, further work could be performed to evaluate whether *SARCC* can promote AR signalling. The expression of AR target genes such as *NKX3.1*, *TMPRSS2*, *FKBP5, KLK3, UGT2B15*, *IGF1R* and *UBE2C* could be evaluated by qPCR in *SARCC* overexpressed cells and compared to their expression in EVC cells. A more accurate quantification of AR protein expression would also be helpful. AR protein quantification in *SARCC* overexpressed cells compared to EVC cells could be performed by Western blot analysis or mass spectrometry.

5.2.4 Further work – evaluation of *P2RY1* expression

Although *P2RY1* demonstrated just over a two fold increase in enzalutamide resistant cells, its close proximity to *SARCC* on chromosome 3 suggests that the functions of *SARCC* and *P2RY1* could be interlinked. qPCR could be used to assess the expression of *P2RY1* in enzalutamide resistant cells and in *SARCC* overexpressed cells.

5.2.5 Further work – evaluation of *SARCC* on miRNA expression

Like other lncRNAs, *SARCC* may function as a competing endogenous RNA and regulate the AR by competing for shared miRNAs. Previous work has shown that the AR can bind to an ARE in the promoter region of miR-143-3p causing a decrease in its activity and altering the expression of its target genes *AKT, MMP-13, KRAS* and *P-ERK* [159]. *SARCC* expression has also been shown to affect the expression of miR-143-3p in RCC [159]. Cell lines from *SARCC* overexpression and knockdown experiments could be used to evaluate the effect of *SARCC* expression on miR-143-3p and its target genes. Software programmes such as TargetScan could also be used to identify other miRNA binding sites on *SARCC*.

5.2.6 Further work – evaluation of the role of hypermethylation in *SARCC* expression

MethPrimer software analysis in a previous study predicted that CPG-rich islands were located at the promoter region of *SARCC* suggesting that hypermethylation could be a mechanism for silencing of *SARCC* expression [159]. Bisulfite sequencing analysis could be performed to see if hypermethylation of *SARCC* plays a role in its regulation and to see if *SARCC* is hypermethylated in enzalutamide sensitive PCa cells or hypomethylated in enzalutamide resistant PCa cells.

5.2.7 Further work – evaluation of the role of hypoxia on *SARCC* expression

Under hypoxic conditions, HIF-2α accumulates within cells and can translocate into the nucleus to form a HIF complex with HIF-1β. HIF-2α regulates numerous genes, including *C-MYC*, through binding to hypoxia response elements in their promoters [234]. Zhai *et. al* showed that HIF-2α regulates *SARCC* expression in RCC via binding to hypoxia responsive elements on its promoter [187]. Knockdown of HIF-2α increased *SARCC* expression. They also showed that the expression of *SARCC* was downregulated in LNCaP cells under hypoxic conditions. Similar experiments could be performed in the cell lines developed in this study to see if HIF-2α regulates *SARCC* expression and if it alters the resistance of PCa cells to enzalutamide.

5.3 Other lncRNAs

In this study, five other highly upregulated lncRNAs were validated by qPCR as being significantly overexpressed in enzalutamide resistant cells - *SPRY4-IT1, DPP10-AS1, FLJ26850, RP11-222K16.2* and *RP11-1C8.7*. This is the first time that these lncRNAs have been associated with enzalutamide resistance in PCa.

SPRY4-IT1 is an intronic region within the Sprouty RTK signaling antagonist 4 (*SPRY4*) gene and is associated with a number of human cancers including PCa, melanoma, colorectal cancer and lung cancer [235]. The primary transcript is cleaved to release a mature product that localizes to the cytoplasm although the structure of the primary and cleaved transcript is unknown [236]. *SPRY4-IT1* was previously shown to be highly upregulated in the human prostate cancer cell line PC3 and was detectable in the urine of PCa patients [167]. Knockdown of *SPRY4-IT1* in PC3 cells inhibited cell proliferation and invasion and increased cell apoptosis [167].

DPP10-AS1 is highly expressed in testis but not in prostate based on RNA-seq data from tissue samples of 95 people [220]. *DPP10-AS1* has been reported in association with Human epidermal growth factor receptor 2 (*HER-2*) positive breast cancer but its function is unknown [237]. There are no reported associations with other types of cancer. The protein coding *DPP10* gene encodes a type II membrane protein that is a member of the S9B family in clan SC of the serine proteases, although the protein has no detectable protease activity. It is downregulated in pancreatic cancer [238] but there have been no previous reports evaluating the role of *DPP10-AS1* or *DPP10* in PCa or AR signalling.

FLJ26850 is highly expressed in benign prostate tissue [220] and maps on chromosome 19, at 19q13.33 according to Entrez Gene. There have been no previous reports evaluating the role of *FLJ26850* in cancer or AR signalling.

RP11-222K16.2 is associated with altered expression in newly diagnosed acute myeloid leukemia [239]. Its expression was highly correlated with the expression of its neighbouring protein coding gene, Eomesodermin (*EOMES*), which is involved in the

regulation of developmental processes [240]. The microarray analysis from our study showed that *EOMES* is upregulated in enzalutamide resistant cells compared to enzalutamide sensitive cells (3.6-fold change). There have been no reports evaluating the role of *RP11-222K16.2* or *EOMES* in PCa or AR signalling.

RP11-1C8.7 is upregulated in high-grade ovarian serous carcinoma compared with non-tumor tissues [241] and may help to predict prognosis in renal papillary cell carcinoma as part of a panel of seven lncRNAs [242]. There have been no reports evaluating the role of *RP11-1C8.7* in PCa or AR signalling.

5.3.1 Further work – evaluation of the role of validated lncRNAs in enzalutamide resistance

Similar to the experiments evaluating the role of *SARCC*, the five validated lncRNAs could be overexpressed in enzalutamide sensitive cells and knocked down in enzalutamide resistant cells to determine what effect, if any, they have on enzalutamide resistance.

5.3.2 Further work – validation of other lncRNAs

A number of other lncRNAs with interesting features such as *HOTAIR* and *AFAP1-AS1* were upregulated in enzalutamide resistant cells according to the microarray analysis, but were not validated. *HOTAIR* binds to the N-terminal domain of the AR whereas *AFAP1-AS1* enhances PCa cell metastasis *in vitro* via targeting *RBM5*, an inhibitor of the Wnt signalling pathway [88, 97]. qPCR could be performed to validate the overexpression of *HOTAIR* and *AFAP1-AS1.*

5.3.3 Further work – evaluation of downregulated lncRNAs

Downregulated lncRNAs were not evaluated further due to time and financial constraints. Many of the most downregulated lncRNAs were poorly characterised with no known associations to cancer. qPCR looking at relative expression of the most downregulated lncRNAs could be performed to validate the findings of the microarray analysis. Further overexpression and knockdown experiments could be performed to evaluate their effects in enzalutamide resistance.

5.4 mRNAs and enzalutamide resistance

Microarray analysis revealed 2,423 upregulated mRNAs when comparing Clone 1 to Control. Grouping these mRNAs by molecular function revealed a large number of genes involved in receptor binding and protein dimerisation, key functions in AR signalling.

A number of significantly upregulated mRNAs were validated as being overexpressed in enzalutamide resistant cells - *CTAG1B, PEG10, SPINK1, PITX2* and *PCDH7*. This is the first time these genes have been associated with enzalutamide resistance in PCa apart from *PCDH7*.

CTAG1B is a cancer-testis antigen with expression in numerous cancer types, including PCa [243]. Much of the research into *CTAG1B* has focused on its ability to elicit immune responses and, therefore, as a target for cancer immunotherapy [243]. The role of cancer testis antigens in oncogenesis is unclear but some data points to a role in the regulation of EMT [244]. *CTAG1B* has not been reported in association with the AR although Melanoma antigen gene protein-A11 (*MAGEA11*), a related cancer testis antigen gene, increases AR transcriptional activity in PCa by direct interactions with the AR and other coactivators [245]. *MAGEA11* showed a 2.3-fold increase in expression in Clone 1 compared to Control based on our microarray analysis. A previous study of *CTAG1B* expression by immunohistochemistry on a tissue microarray of PCa tissue samples showed positive staining in 8.8% of 8,761 tumors [205]. There was a threefold higher rate of expression in *ERG* fusion positive tumors and, within this group, expression was associated with early biochemical recurrence and high Gleason grade. In *ERG*-negative PCa, *CTAG1B* expression was associated with *PTEN* loss.

Paternally expressed gene 10 (*PEG10*) is required for placental development and is highly upregulated in neuroendocrine PCa [208, 209]. *PEG10* is AR repressed, but under AR interference from enzalutamide treatment, it becomes highly upregulated and this is associated with the development of neuroendocrine PCa [208, 209]. Stimulating AR activity reverses *PEG10* and neuroendocrine marker expression *in vitro* [209].

SPINK1 encodes a protein that inhibits serine proteases, such as trypsin [246], and is overexpressed in a subset of patients with PCa[43]. Recently presented data at the American Association for Cancer Research Annual Meeting in 2019 reported that blocking AR signalling upregulates *SPINK1* expression in PCa and that this is associated with an increase in neuroendocrine markers [247].

PITX2 hypermethylation (and consequent reduced gene expression) is associated with poorer outcomes in head and neck squamous cell carcinoma, breast, lung and PCa [248-251]. *PITX2* methylation testing has been assessed as a biomarker for poorer outcome on prostate biopsies [252]. However, other data has shown that *PITX2* is overexpressed in metastatic CRPC, particularly in bone metastases, and it may play a role in cell migration and metastasis [253]. It has been identified as an upstream regulator of both the AR and the insulin-like growth factor-1 receptor (IGF-1R) [254]. *PITX2* overexpression has also been associated with cell invasion and dissemination in breast cancer [255] and with ovarian cancer progression [256].

PCDH7 encodes a cell surface protein that is required for the rounding of cells at the onset of mitosis [257]. It was previously shown to be upregulated in an androgen-independent LNCaP cell line [258]. Data presented at the AACR Annual Meeting in 2018 showed *PCDH7* was overexpressed in CRPC cell lines and the highest levels were seen in an enzalutamide resistant cell line [227].

5.4.1 Further work – evaluation of mRNA expression on enzalutamide resistance

Similar to the cloning experiments with SARCC, overexpression and knockdown of the five validated mRNAs could be performed to assess how they impact on enzalutamide resistance. In particular, given its previously reported association to enzalutamide resistance, overexpression and knockdown of PCDH7 would be important to examine. As previously discussed (Section 4.10), we attempted overexpression and knockdown of PCDH7 but were unsuccessful.

5.4.2 Further work – evaluation of protein expression for validated mRNAs

In addition to assessing the expression of mRNA transcripts, further work could be undertaken to evaluate expression levels at the protein level by Western blot or mass spectrometry.

5.4.3 Further work – *PITX2* and hypermethylation

PITX2 is a regulator of the AR and methylation is important in determining its expression. Bisulfite sequencing analysis could be performed to determine if hypermethylation of *PITX2* plays a role in its regulation and to see if *PITX2* is hypermethylated in enzalutamide sensitive PCa cells or hypomethylated in enzalutamide resistant PCa cells.

5.4.4 Further work – *PITX2* and the IGF1 receptor

The expression of the IGF1 receptor (IGF-1R) in enzalutamide resistant cells could be evaluated by qPCR as its expression is regulated by *PITX2* [208]. The IGF1 receptor can activate the AR offering a potential mechanism for AR signalling in the absence of androgens [259].

5.5 Panel of cell lines

The expression of validated lncRNAs and mRNAs were evaluated by end-point PCR in a panel of cell lines (Section 3.9). They were expressed in both benign and malignant cell lines but were more likely to be expressed in more aggressive PCa cell lines 22Rv1, PC-3 and DU 145. In particular, most of the lncRNAs and mRNAs were expressed in 22Rv1, a cell line that is known to be resistant to enzalutamide and shows high levels of AR-V7 expression [260, 261]

5.6 Neuroendocrine differentiation

Neuroendocrine differentiation in PCa is associated with an aggressive phenotype and poor prognosis. Neuroendocrine PCa is also resistant to anti-androgens and appears to be truly AR-independent i.e. cancer cell growth is not dependent on AR signalling. We assessed the expression of two neuroendocrine mRNAs, *BRN2* and *CGA*, by qPCR but did not show any significant difference in expression at the transcript level. We also examined the expression of two commonly expression neuroendocrine proteins,

synaptophysin and chromogranin, by immunohistochemistry on the SARCC overexpressed and EVC cell lines but there was no difference in expression. These findings suggest that the development of resistance in this cell population is not related to neuroendocrine differentiation.

5.7 Clinical Relevance and Conclusions

The development of resistance to anti-androgen therapies is a key problem in the treatment of PCa. While some AR mutations and AR splice variants are associated with the development of resistance, the full picture of how resistance develops is still unclear and treatment strategies to overcome resistance are lacking. In this study, we evaluated an isogenic cell line model with varied levels of resistance to enzalutamide. Microarray analysis revealed a large number of differentially expressed lncRNAs and mRNAs. We validated 6 lncRNAs and 5 mRNAs associated with enzalutamide resistance by qPCR. This is the first time that these lncRNAs and mRNAs have been reported in association with drug resistance in PCa, apart from *PCDH7*. One of the lncRNAs, *SARCC*, was selected for further evaluation due to previous reports that it could bind to the AR. Overexpression of *SARCC* in enzalutamide sensitive cells resulted in an increase in resistance to enzalutamide suggesting a functional role for *SARCC* in the development of enzalutamide resistance.

This work has identified a number of potentially important novel lncRNAs and mRNAs in enzalutamide resistance that may be targeted in patients. In particular, given *SARCCs* potential functional role in AR signalling, targeting of *SARCC* could alter the development of enzalutamide resistance. This would significantly improve PCa mortality as enzalutamide is a very effective and safe drug when used in sensitive patients. Another clinically relevant outcome from this project is the potential to use one of the lncRNAs as a biomarker for enzalutamide resistance. As lncRNAs are stable in circulating fluids, they are good biomarker candidates. Identifying patients with enzalutamide resistance would be beneficial as it would allow switching to a more effective medication and avoid wasting money.

The upregulation of CTAG1B is noteworthy as it can elicit immune responses and may be a target for immunotherapy. Thus far, there has been little success in using immunotherapy in PCa patients but this marker may identify a subgroup that are responsive to immunotherapy.

In conclusion, this project has identified *SARCC*, a lncRNA, with a potential functional role in enzalutamide resistance. In addition, a number of lncRNAs and mRNAs associated with enzalutamide resistance were identified for the first time.

References

1. McNeal, J.E., The zonal anatomy of the prostate. Prostate, 1981. **2**(1): p. 35-49.
2. Signoretti, S., D. Waltregny, J. Dilks, B. Isaac, D. Lin, L. Garraway, et al., p63 is a prostate basal cell marker and is required for prostate development. Am J Pathol, 2000. **157**(6): p. 1769-75.
3. Wang, Y., S. Hayward, M. Cao, K. Thayer, and G. Cunha, Cell differentiation lineage in the prostate. Differentiation, 2001. **68**(4-5): p. 270-9.
4. Abrahamsson, P.A., Neuroendocrine cells in tumour growth of the prostate. Endocr Relat Cancer, 1999. **6**(4): p. 503-19.
5. Toivanen, R. and M.M. Shen, Prostate organogenesis: tissue induction, hormonal regulation and cell type specification. Development, 2017. **144**(8): p. 1382-1398.
6. Kellokumpu-Lehtinen, P., R. Santti, and L.J. Pelliniemi, Correlation of early cytodifferentiation of the human fetal prostate and Leydig cells. Anat Rec, 1980. **196**(3): p. 263-73.
7. Bray, F., J. Ferlay, I. Soerjomataram, R.L. Siegel, L.A. Torre, and A. Jemal, Global cancer statistics 2018: GLOBOCAN estimates of incidence and mortality worldwide for 36 cancers in 185 countries. CA Cancer J Clin, 2018. **68**(6): p. 394-424.
8. NCRI, *Cancer in Ireland 1994-2016 with estimates for 2016-2018: Annual Report of the National Cancer Registry*, N.C.R. Ireland, Editor. 2018, NCRI: Cork, Ireland.
9. Rebbeck, T.R., S.S. Devesa, B.L. Chang, C.H. Bunker, I. Cheng, K. Cooney, et al., Global patterns of prostate cancer incidence, aggressiveness, and mortality in men of african descent. Prostate Cancer, 2013. **2013**: p. 560857.
10. Brandt, A., J. Sundquist, and K. Hemminki, Risk for incident and fatal prostate cancer in men with a family history of any incident and fatal cancer. Ann Oncol, 2012. **23**(1): p. 251-6.
11. Attard, G., C. Parker, R.A. Eeles, F. Schroder, S.A. Tomlins, I. Tannock, et al., Prostate cancer. Lancet, 2016. **387**(10013): p. 70-82.
12. Eeles, R., C. Goh, E. Castro, E. Bancroft, M. Guy, A.A. Al Olama, et al., The genetic epidemiology of prostate cancer and its clinical implications. Nat Rev Urol, 2014. **11**(1): p. 18-31.
13. Freedman, M.L., A.N. Monteiro, S.A. Gayther, G.A. Coetzee, A. Risch, C. Plass, et al., Principles for the post-GWAS functional characterization of cancer risk loci. Nat Genet, 2011. **43**(6): p. 513-8.
14. Zuccolo, L., R. Harris, D. Gunnell, S. Oliver, J.A. Lane, M. Davis, et al., Height and prostate cancer risk: a large nested case-control study (ProtecT) and meta-analysis. Cancer Epidemiol Biomarkers Prev, 2008. **17**(9): p. 2325-36.
15. Kenfield, S.A., M.J. Stampfer, J.M. Chan, and E. Giovannucci, Smoking and prostate cancer survival and recurrence. JAMA, 2011. **305**(24): p. 2548-55.
16. Coffey, D.S., Similarities of prostate and breast cancer: Evolution, diet, and estrogens. Urology, 2001. **57**(4 Suppl 1): p. 31-8.
17. Nelson, W.G., A.M. Demarzo, and S. Yegnasubramanian, The diet as a cause of human prostate cancer. Cancer Treat Res, 2014. **159**: p. 51-68.

18. Nelson, W.G., T.L. DeWeese, and A.M. DeMarzo, The diet, prostate inflammation, and the development of prostate cancer. Cancer Metastasis Rev, 2002. **21**(1): p. 3-16.
19. Sfanos, K.S., H.A. Hempel, and A.M. De Marzo, The role of inflammation in prostate cancer. Adv Exp Med Biol, 2014. **816**: p. 153-81.
20. Sfanos, K.S., B.A. Wilson, A.M. De Marzo, and W.B. Isaacs, Acute inflammatory proteins constitute the organic matrix of prostatic corpora amylacea and calculi in men with prostate cancer. Proc Natl Acad Sci U S A, 2009. **106**(9): p. 3443-8.
21. Pernar, C.H., E.M. Ebot, K.M. Wilson, and L.A. Mucci, The Epidemiology of Prostate Cancer. Cold Spring Harb Perspect Med, 2018. **8**(12).
22. Etminan, M., B. Takkouche, and F. Caamano-Isorna, The role of tomato products and lycopene in the prevention of prostate cancer: a meta-analysis of observational studies. Cancer Epidemiol Biomarkers Prev, 2004. **13**(3): p. 340-5.
23. Szymanski, K.M., D.C. Wheeler, and L.A. Mucci, Fish consumption and prostate cancer risk: a review and meta-analysis. Am J Clin Nutr, 2010. **92**(5): p. 1223-33.
24. Cao, Y. and J. Ma, Body mass index, prostate cancer-specific mortality, and biochemical recurrence: a systematic review and meta-analysis. Cancer Prev Res (Phila), 2011. **4**(4): p. 486-501.
25. Green, S.M., E.A. Mostaghel, and P.S. Nelson, Androgen action and metabolism in prostate cancer. Mol Cell Endocrinol, 2012. **360**(1-2): p. 3-13.
26. Evans, R.M., The steroid and thyroid hormone receptor superfamily. Science, 1988. **240**(4854): p. 889-95.
27. Jin, H.J., J. Kim, and J. Yu, Androgen receptor genomic regulation. Transl Androl Urol, 2013. **2**(3): p. 157-177.
28. Tomlins, S.A., D.R. Rhodes, S. Perner, S.M. Dhanasekaran, R. Mehra, X.W. Sun, et al., Recurrent fusion of TMPRSS2 and ETS transcription factor genes in prostate cancer. Science, 2005. **310**(5748): p. 644-8.
29. Rubin, M.A., C.A. Maher, and A.M. Chinnaiyan, Common gene rearrangements in prostate cancer. J Clin Oncol, 2011. **29**(27): p. 3659-68.
30. Bastus, N.C., L.K. Boyd, X. Mao, E. Stankiewicz, S.C. Kudahetti, R.T. Oliver, et al., Androgen-induced TMPRSS2:ERG fusion in nonmalignant prostate epithelial cells. Cancer Res, 2010. **70**(23): p. 9544-8.
31. Lin, C., L. Yang, B. Tanasa, K. Hutt, B.G. Ju, K. Ohgi, et al., Nuclear receptor-induced chromosomal proximity and DNA breaks underlie specific translocations in cancer. Cell, 2009. **139**(6): p. 1069-83.
32. Mani, R.S., S.A. Tomlins, K. Callahan, A. Ghosh, M.K. Nyati, S. Varambally, et al., Induced chromosomal proximity and gene fusions in prostate cancer. Science, 2009. **326**(5957): p. 1230.
33. Palanisamy, N., B. Ateeq, S. Kalyana-Sundaram, D. Pflueger, K. Ramnarayanan, S. Shankar, et al., Rearrangements of the RAF kinase pathway in prostate cancer, gastric cancer and melanoma. Nat Med, 2010. **16**(7): p. 793-8.
34. Barbieri, C.E., S.C. Baca, M.S. Lawrence, F. Demichelis, M. Blattner, J.P. Theurillat, et al., Exome sequencing identifies recurrent SPOP, FOXA1 and MED12 mutations in prostate cancer. Nat Genet, 2012. **44**(6): p. 685-9.
35. Reid, A.H., G. Attard, L. Ambroisine, G. Fisher, G. Kovacs, D. Brewer, et al., Molecular characterisation of ERG, ETV1 and PTEN gene loci identifies patients at low and high risk of death from prostate cancer. Br J Cancer, 2010. **102**(4): p. 678-84.

36. Robinson, D., E.M. Van Allen, Y.M. Wu, N. Schultz, R.J. Lonigro, J.M. Mosquera, et al., Integrative Clinical Genomics of Advanced Prostate Cancer. Cell, 2015. **162**(2): p. 454.
37. Grasso, C.S., Y.M. Wu, D.R. Robinson, X. Cao, S.M. Dhanasekaran, A.P. Khan, et al., The mutational landscape of lethal castration-resistant prostate cancer. Nature, 2012. **487**(7406): p. 239-43.
38. Ahearn, T.U., A. Pettersson, E.M. Ebot, T. Gerke, R.E. Graff, C.L. Morais, et al., A Prospective Investigation of PTEN Loss and ERG Expression in Lethal Prostate Cancer. J Natl Cancer Inst, 2016. **108**(2).
39. Ferraldeschi, R., D. Nava Rodrigues, R. Riisnaes, S. Miranda, I. Figueiredo, P. Rescigno, et al., PTEN protein loss and clinical outcome from castration-resistant prostate cancer treated with abiraterone acetate. Eur Urol, 2015. **67**(4): p. 795-802.
40. Lotan, T.L., F.L. Carvalho, S.B. Peskoe, J.L. Hicks, J. Good, H. Fedor, et al., PTEN loss is associated with upgrading of prostate cancer from biopsy to radical prostatectomy. Mod Pathol, 2015. **28**(1): p. 128-137.
41. Shah, R.B., J. Bentley, Z. Jeffery, and A.M. DeMarzo, Heterogeneity of PTEN and ERG expression in prostate cancer on core needle biopsies: implications for cancer risk stratification and biomarker sampling. Hum Pathol, 2015. **46**(5): p. 698-706.
42. Tomlins, S.A., D.R. Rhodes, J. Yu, S. Varambally, R. Mehra, S. Perner, et al., The role of SPINK1 in ETS rearrangement-negative prostate cancers. Cancer Cell, 2008. **13**(6): p. 519-28.
43. Flavin, R., A. Pettersson, W.K. Hendrickson, M. Fiorentino, S. Finn, L. Kunz, et al., SPINK1 protein expression and prostate cancer progression. Clin Cancer Res, 2014. **20**(18): p. 4904-11.
44. Huang, S., Z.G. Gulzar, K. Salari, J. Lapointe, J.D. Brooks, and J.R. Pollack, Recurrent deletion of CHD1 in prostate cancer with relevance to cell invasiveness. Oncogene, 2012. **31**(37): p. 4164-70.
45. Liu, W., J. Lindberg, G. Sui, J. Luo, L. Egevad, T. Li, et al., Identification of novel CHD1-associated collaborative alterations of genomic structure and functional assessment of CHD1 in prostate cancer. Oncogene, 2012. **31**(35): p. 3939-48.
46. Kari, V., W.Y. Mansour, S.K. Raul, S.J. Baumgart, A. Mund, M. Grade, et al., Loss of CHD1 causes DNA repair defects and enhances prostate cancer therapeutic responsiveness. EMBO Rep, 2018. **19**(10).
47. Fischer, M., Census and evaluation of p53 target genes. Oncogene, 2017. **36**(28): p. 3943-3956.
48. Beltran, H., R. Yelensky, G.M. Frampton, K. Park, S.R. Downing, T.Y. MacDonald, et al., Targeted next-generation sequencing of advanced prostate cancer identifies potential therapeutic targets and disease heterogeneity. Eur Urol, 2013. **63**(5): p. 920-6.
49. Bauer, J.J., I.A. Sesterhenn, F.K. Mostofi, D.G. McLeod, S. Srivastava, and J.W. Moul, Elevated levels of apoptosis regulator proteins p53 and bcl-2 are independent prognostic biomarkers in surgically treated clinically localized prostate cancer. J Urol, 1996. **156**(4): p. 1511-6.
50. Kuczyk, M.A., J. Serth, C. Bokemeyer, S. Machtens, A. Minssen, W. Bathke, et al., The prognostic value of p53 for long-term and recurrence-free survival following radical prostatectomy. Eur J Cancer, 1998. **34**(5): p. 679-86.

51. Theodorescu, D., S.R. Broder, J.C. Boyd, S.E. Mills, and H.F. Frierson, Jr., p53, bcl-2 and retinoblastoma proteins as long-term prognostic markers in localized carcinoma of the prostate. J Urol, 1997. **158**(1): p. 131-7.
52. He, W.W., P.J. Sciavolino, J. Wing, M. Augustus, P. Hudson, P.S. Meissner, et al., A novel human prostate-specific, androgen-regulated homeobox gene (NKX3.1) that maps to 8p21, a region frequently deleted in prostate cancer. Genomics, 1997. **43**(1): p. 69-77.
53. Cooperberg, M.R., J.M. Broering, and P.R. Carroll, Time trends and local variation in primary treatment of localized prostate cancer. J Clin Oncol, 2010. **28**(7): p. 1117-23.
54. NCCP, *National clinical guideline. Diagnosis, staging and treatment of patients with prostate cancer*, N.C.C. Programme, Editor. 2015.
55. Huggins, C., Endocrine Control of Prostatic Cancer. Science, 1943. **97**(2529): p. 541-4.
56. Loblaw, D.A., K.S. Virgo, R. Nam, M.R. Somerfield, E. Ben-Josef, D.S. Mendelson, et al., Initial hormonal management of androgen-sensitive metastatic, recurrent, or progressive prostate cancer: 2006 update of an American Society of Clinical Oncology practice guideline. J Clin Oncol, 2007. **25**(12): p. 1596-605.
57. Basch, E., D.A. Loblaw, and R.B. Rumble, Systemic Therapy in Men With Metastatic Castration-Resistant Prostate Cancer: American Society of Clinical Oncology and Cancer Care Ontario Clinical Practice Guideline Summary. J Oncol Pract, 2014. **10**(6): p. e418-e420.
58. James, N.D., M.R. Sydes, N.W. Clarke, M.D. Mason, D.P. Dearnaley, M.R. Spears, et al., Addition of docetaxel, zoledronic acid, or both to first-line long-term hormone therapy in prostate cancer (STAMPEDE): survival results from an adaptive, multiarm, multistage, platform randomised controlled trial. Lancet, 2016. **387**(10024): p. 1163-77.
59. de Bono, J.S., C.J. Logothetis, A. Molina, K. Fizazi, S. North, L. Chu, et al., Abiraterone and increased survival in metastatic prostate cancer. N Engl J Med, 2011. **364**(21): p. 1995-2005.
60. Scher, H.I., K. Fizazi, F. Saad, M.E. Taplin, C.N. Sternberg, K. Miller, et al., Increased survival with enzalutamide in prostate cancer after chemotherapy. N Engl J Med, 2012. **367**(13): p. 1187-97.
61. Locke, J.A., E.S. Guns, A.A. Lubik, H.H. Adomat, S.C. Hendy, C.A. Wood, et al., Androgen levels increase by intratumoral de novo steroidogenesis during progression of castration-resistant prostate cancer. Cancer Res, 2008. **68**(15): p. 6407-15.
62. Montgomery, R.B., E.A. Mostaghel, R. Vessella, D.L. Hess, T.F. Kalhorn, C.S. Higano, et al., Maintenance of intratumoral androgens in metastatic prostate cancer: a mechanism for castration-resistant tumor growth. Cancer Res, 2008. **68**(11): p. 4447-54.
63. Visakorpi, T., E. Hyytinen, P. Koivisto, M. Tanner, R. Keinanen, C. Palmberg, et al., In vivo amplification of the androgen receptor gene and progression of human prostate cancer. Nat Genet, 1995. **9**(4): p. 401-6.
64. Bubendorf, L., J. Kononen, P. Koivisto, P. Schraml, H. Moch, T.C. Gasser, et al., Survey of gene amplifications during prostate cancer progression by high-throughout fluorescence in situ hybridization on tissue microarrays. Cancer Res, 1999. **59**(4): p. 803-6.

65. Korpal, M., J.M. Korn, X. Gao, D.P. Rakiec, D.A. Ruddy, S. Doshi, et al., An F876L mutation in androgen receptor confers genetic and phenotypic resistance to MDV3100 (enzalutamide). Cancer Discov, 2013. **3**(9): p. 1030-43.
66. Taplin, M.E., G.J. Bubley, T.D. Shuster, M.E. Frantz, A.E. Spooner, G.K. Ogata, et al., Mutation of the androgen-receptor gene in metastatic androgen-independent prostate cancer. N Engl J Med, 1995. **332**(21): p. 1393-8.
67. Antonarakis, E.S., C. Lu, H. Wang, B. Luber, M. Nakazawa, J.C. Roeser, et al., AR-V7 and resistance to enzalutamide and abiraterone in prostate cancer. N Engl J Med, 2014. **371**(11): p. 1028-38.
68. Antonarakis, E.S., A.J. Armstrong, S.M. Dehm, and J. Luo, Androgen receptor variant-driven prostate cancer: clinical implications and therapeutic targeting. Prostate Cancer Prostatic Dis, 2016. **19**(3): p. 231-41.
69. Antonarakis, E.S., C. Lu, B. Luber, H. Wang, Y. Chen, Y. Zhu, et al., Clinical Significance of Androgen Receptor Splice Variant-7 mRNA Detection in Circulating Tumor Cells of Men With Metastatic Castration-Resistant Prostate Cancer Treated With First- and Second-Line Abiraterone and Enzalutamide. J Clin Oncol, 2017. **35**(19): p. 2149-2156.
70. Steinestel, J., M. Luedeke, A. Arndt, T.J. Schnoeller, J.K. Lennerz, C. Wurm, et al., Detecting predictive androgen receptor modifications in circulating prostate cancer cells. Oncotarget, 2019. **10**(41): p. 4213-4223.
71. Beltran, H., D. Prandi, J.M. Mosquera, M. Benelli, L. Puca, J. Cyrta, et al., Divergent clonal evolution of castration-resistant neuroendocrine prostate cancer. Nat Med, 2016. **22**(3): p. 298-305.
72. Ruggero, K., S. Farran-Matas, A. Martinez-Tebar, and A. Aytes, Epigenetic Regulation in Prostate Cancer Progression. Curr Mol Biol Rep, 2018. **4**(2): p. 101-115.
73. Rinn, J.L. and H.Y. Chang, Genome regulation by long noncoding RNAs. Annu Rev Biochem, 2012. **81**: p. 145-66.
74. Liu, Z., M. Sun, K. Lu, J. Liu, M. Zhang, W. Wu, et al., The long noncoding RNA HOTAIR contributes to cisplatin resistance of human lung adenocarcinoma cells via downregualtion of p21(WAF1/CIP1) expression. PLoS One, 2013. **8**(10): p. e77293.
75. Pan, J., X. Li, W. Wu, M. Xue, H. Hou, W. Zhai, et al., Long non-coding RNA UCA1 promotes cisplatin/gemcitabine resistance through CREB modulating miR-196a-5p in bladder cancer cells. Cancer Lett, 2016. **382**(1): p. 64-76.
76. Zheng, Z.G., H. Xu, S.S. Suo, X.L. Xu, M.W. Ni, L.H. Gu, et al., The Essential Role of H19 Contributing to Cisplatin Resistance by Regulating Glutathione Metabolism in High-Grade Serous Ovarian Cancer. Sci Rep, 2016. **6**: p. 26093.
77. Kung, J.T., D. Colognori, and J.T. Lee, Long noncoding RNAs: past, present, and future. Genetics, 2013. **193**(3): p. 651-69.
78. Ponting, C.P., P.L. Oliver, and W. Reik, Evolution and functions of long noncoding RNAs. Cell, 2009. **136**(4): p. 629-41.
79. Derrien, T., R. Johnson, G. Bussotti, A. Tanzer, S. Djebali, H. Tilgner, et al., The GENCODE v7 catalog of human long noncoding RNAs: analysis of their gene structure, evolution, and expression. Genome Res, 2012. **22**(9): p. 1775-89.
80. O'Brien, J., H. Hayder, Y. Zayed, and C. Peng, Overview of MicroRNA Biogenesis, Mechanisms of Actions, and Circulation. Front Endocrinol (Lausanne), 2018. **9**: p. 402.

81. Ma, L., A. Li, D. Zou, X. Xu, L. Xia, J. Yu, et al., LncRNAWiki: harnessing community knowledge in collaborative curation of human long non-coding RNAs. Nucleic Acids Res, 2015. **43**(Database issue): p. D187-92.
82. Lin, C. and L. Yang, Long Noncoding RNA in Cancer: Wiring Signaling Circuitry. Trends Cell Biol, 2018. **28**(4): p. 287-301.
83. Lee, J.T., Epigenetic regulation by long noncoding RNAs. Science, 2012. **338**(6113): p. 1435-9.
84. Gibb, E.A., C.J. Brown, and W.L. Lam, The functional role of long non-coding RNA in human carcinomas. Mol Cancer, 2011. **10**: p. 38.
85. Prensner, J.R. and A.M. Chinnaiyan, The emergence of lncRNAs in cancer biology. Cancer Discov, 2011. **1**(5): p. 391-407.
86. Gutschner, T. and S. Diederichs, The hallmarks of cancer: a long non-coding RNA point of view. RNA Biol, 2012. **9**(6): p. 703-19.
87. Aird, J., A.M. Baird, M.C.J. Lim, R. McDermott, S.P. Finn, and S.G. Gray, Carcinogenesis in prostate cancer: The role of long non-coding RNAs. Noncoding RNA Res, 2018. **3**(1): p. 29-38.
88. Zhang, A., J.C. Zhao, J. Kim, K.W. Fong, Y.A. Yang, D. Chakravarti, et al., LncRNA HOTAIR Enhances the Androgen-Receptor-Mediated Transcriptional Program and Drives Castration-Resistant Prostate Cancer. Cell Rep, 2015. **13**(1): p. 209-221.
89. Takayama, K., K. Horie-Inoue, S. Katayama, T. Suzuki, S. Tsutsumi, K. Ikeda, et al., Androgen-responsive long noncoding RNA CTBP1-AS promotes prostate cancer. EMBO J, 2013. **32**(12): p. 1665-80.
90. Fang, Z., C. Xu, Y. Li, X. Cai, S. Ren, H. Liu, et al., A feed-forward regulatory loop between androgen receptor and PlncRNA-1 promotes prostate cancer progression. Cancer Lett, 2016. **374**(1): p. 62-74.
91. Kino, T., D.E. Hurt, T. Ichijo, N. Nader, and G.P. Chrousos, Noncoding RNA gas5 is a growth arrest- and starvation-associated repressor of the glucocorticoid receptor. Sci Signal, 2010. **3**(107): p. ra8.
92. Xue, D., C. Zhou, H. Lu, R. Xu, X. Xu, and X. He, LncRNA GAS5 inhibits proliferation and progression of prostate cancer by targeting miR-103 through AKT/mTOR signaling pathway. Tumour Biol, 2016.
93. Crea, F., A. Watahiki, L. Quagliata, H. Xue, L. Pikor, A. Parolia, et al., Identification of a long non-coding RNA as a novel biomarker and potential therapeutic target for metastatic prostate cancer. Oncotarget, 2014. **5**(3): p. 764-74.
94. Misawa, A., K. Takayama, T. Urano, and S. Inoue, Androgen-induced Long Noncoding RNA (lncRNA) SOCS2-AS1 Promotes Cell Growth and Inhibits Apoptosis in Prostate Cancer Cells. J Biol Chem, 2016. **291**(34): p. 17861-80.
95. Sakurai, K., B.J. Reon, J. Anaya, and A. Dutta, The lncRNA DRAIC/PCAT29 Locus Constitutes a Tumor-Suppressive Nexus. Mol Cancer Res, 2015. **13**(5): p. 828-38.
96. Shukla, S., X. Zhang, Y.S. Niknafs, L. Xiao, R. Mehra, M. Cieslik, et al., Identification and Validation of PCAT14 as Prognostic Biomarker in Prostate Cancer. Neoplasia, 2016. **18**(8): p. 489-99.
97. Yang, Z.T., F. An, J.D. Hu, and W.H. Zhao, Long noncoding RNA AFAP1-AS1 accelerates the proliferation and metastasis of prostate cancer via inhibiting RBM5 expression. Eur Rev Med Pharmacol Sci, 2019. **23**(8): p. 3284-3290.
98. Zhao, B., Y.L. Lu, Y. Yang, L.B. Hu, Y. Bai, R.Q. Li, et al., Overexpression of lncRNA ANRIL promoted the proliferation and migration of prostate cancer cells via

regulating let-7a/TGF-beta1/ Smad signaling pathway. Cancer Biomark, 2018. **21**(3): p. 613-620.

99. Zhang, Y., S. Pitchiaya, M. Cieslik, Y.S. Niknafs, J.C. Tien, Y. Hosono, et al., Analysis of the androgen receptor-regulated lncRNA landscape identifies a role for ARLNC1 in prostate cancer progression. Nat Genet, 2018. **50**(6): p. 814-824.
100. Yang, F., Y. Shen, W. Zhang, J. Jin, D. Huang, H. Fang, et al., An androgen receptor negatively induced long non-coding RNA ARNILA binding to miR-204 promotes the invasion and metastasis of triple-negative breast cancer. Cell Death Differ, 2018. **25**(12): p. 2209-2220.
101. Cai, Z., Y. Wu, Y. Li, J. Ren, and L. Wang, BCAR4 activates GLI2 signaling in prostate cancer to contribute to castration resistance. Aging (Albany NY), 2018. **10**(12): p. 3702-3712.
102. Li, W., Z. Dou, S. We, Z. Zhu, D. Pan, Z. Jia, et al., Long noncoding RNA BDNF-AS is associated with clinical outcomes and has functional role in human prostate cancer. Biomed Pharmacother, 2018. **102**: p. 1105-1110.
103. Chen, Z., M. Zhen, and J. Zhou, LncRNA BRE-AS1 interacts with miR-145-5p to regulate cancer cell proliferation and apoptosis in prostate carcinoma and has early diagnostic values. Biosci Rep, 2019. **39**(3).
104. Zheng, J., S. Zhao, X. He, Z. Zheng, W. Bai, Y. Duan, et al., The up-regulation of long non-coding RNA CCAT2 indicates a poor prognosis for prostate cancer and promotes metastasis by affecting epithelial-mesenchymal transition. Biochem Biophys Res Commun, 2016. **480**(4): p. 508-514.
105. Liu, S., L. Wang, Y. Li, Y. Cui, Y. Wang, and C. Liu, Long non-coding RNA CHRF promotes proliferation and mesenchymal transition (EMT) in prostate cancer cell line PC3 requiring up-regulating microRNA-10b. Biol Chem, 2019.
106. Jia, J., F. Li, X.S. Tang, S. Xu, Y. Gao, Q. Shi, et al., Long noncoding RNA DANCR promotes invasion of prostate cancer through epigenetically silencing expression of TIMP2/3. Oncotarget, 2016. **7**(25): p. 37868-37881.
107. Zhao, R., F. Sun, X. Bei, X. Wang, Y. Zhu, C. Jiang, et al., Upregulation of the long non-coding RNA FALEC promotes proliferation and migration of prostate cancer cell lines and predicts prognosis of PCa patients. Prostate, 2017. **77**(10): p. 1107-1117.
108. Zhang, G., G. Han, X. Zhang, Q. Yu, Z. Li, Z. Li, et al., Long non-coding RNA FENDRR reduces prostate cancer malignancy by competitively binding miR-18a-5p with RUNX1. Biomarkers, 2018. **23**(5): p. 435-445.
109. Zhu, L.F., L.D. Song, Q. Xu, and J.F. Zhan, Highly expressed long non-coding RNA FEZF1-AS1 promotes cells proliferation and metastasis through Notch signaling in prostate cancer. Eur Rev Med Pharmacol Sci, 2019. **23**(12): p. 5122-5132.
110. Chen, Y., M. Gu, C. Liu, X. Wan, Q. Shi, Q. Chen, et al., Long noncoding RNA FOXC2-AS1 facilitates the proliferation and progression of prostate cancer via targeting miR-1253/EZH2. Gene, 2019. **686**: p. 37-42.
111. Wu, X., Y. Xiao, Y. Zhou, Z. Zhou, and W. Yan, LncRNA FOXP4-AS1 is activated by PAX5 and promotes the growth of prostate cancer by sequestering miR-3184-5p to upregulate FOXP4. Cell Death Dis, 2019. **10**(7): p. 472.
112. Pickard, M.R., M. Mourtada-Maarabouni, and G.T. Williams, Long non-coding RNA GAS5 regulates apoptosis in prostate cancer cell lines. Biochim Biophys Acta, 2013. **1832**(10): p. 1613-23.

113. Li, Z., H. Liu, W. Ju, Y. Xing, X. Zhang, and J. Yang, LncRNA GASL1 inhibits growth and promotes expression of apoptosis-associated proteins in prostate carcinoma cells through GLUT-1. Oncol Lett, 2019. **17**(6): p. 5327-5334.
114. Zhu, Y., Y. Tong, J. Wu, Y. Liu, and M. Zhao, Knockdown of LncRNA GHET1 suppresses prostate cancer cell proliferation by inhibiting HIF-1alpha/Notch-1 signaling pathway via KLF2. Biofactors, 2019. **45**(3): p. 364-373.
115. Zhang, Y., P. Zhang, X. Wan, X. Su, Z. Kong, Q. Zhai, et al., Downregulation of long non-coding RNA HCG11 predicts a poor prognosis in prostate cancer. Biomed Pharmacother, 2016. **83**: p. 936-941.
116. Jiang, H., W. Xiong, L. Chen, Z. Lv, C. Yang, and Y. Li, Knockdown of the long noncoding RNA HOTTIP inhibits cell proliferation and enhances cell sensitivity to cisplatin by suppressing the Wnt/beta-catenin pathway in prostate cancer. J Cell Biochem, 2019. **120**(6): p. 8965-8974.
117. Zheng, P., H. Li, P. Xu, X. Wang, Z. Shi, Q. Han, et al., High lncRNA HULC expression is associated with poor prognosis and promotes tumor progression by regulating epithelial-mesenchymal transition in prostate cancer. Arch Med Sci, 2018. **14**(3): p. 679-686.
118. Chen, Q., T. Sun, F. Wang, B. Gong, W. Xie, M. Ma, et al., Long Noncoding RNA IGF2AS is Acting as an Epigenetic Tumor Suppressor in Human Prostate Cancer. Urology, 2019. **124**: p. 310 e1-310 e8.
119. Liu, D.C., L.L. Song, Q. Liang, L. Hao, Z.G. Zhang, and C.H. Han, Long noncoding RNA LEF1-AS1 silencing suppresses the initiation and development of prostate cancer by acting as a molecular sponge of miR-330-5p via LEF1 repression. J Cell Physiol, 2019. **234**(8): p. 12727-12744.
120. Zhang, P., Y. Lu, Z. Kong, Y. Zhang, F. Fu, X. Su, et al., Androgen-responsive lncRNA LINC00304 promotes cell cycle and proliferation via regulating CCNA1. Prostate, 2019. **79**(9): p. 994-1006.
121. He, J., M. Sun, H. Geng, and S. Tian, Long non-coding RNA Linc00518 promotes paclitaxel resistance of the human prostate cancer by sequestering miR-216b-5p. Biol Cell, 2019. **111**(2): p. 39-50.
122. Li, N., L.Y. Zhang, Y.H. Qiao, and R.J. Song, Long noncoding RNA LINC00662 functions as miRNA sponge to promote the prostate cancer tumorigenesis through targeting miR-34a. Eur Rev Med Pharmacol Sci, 2019. **23**(9): p. 3688-3698.
123. Liu, Y., B. Yang, Y. Su, Q. Xiang, and Q. Li, Downregulation of long noncoding RNA LINC00683 associated with unfavorable prognosis in prostate cancer based on TCGA. J Cell Biochem, 2019. **120**(8): p. 14165-14174.
124. Lingadahalli, S., S. Jadhao, Y.Y. Sung, M. Chen, L. Hu, X. Chen, et al., Novel lncRNA LINC00844 Regulates Prostate Cancer Cell Migration and Invasion through AR Signaling. Mol Cancer Res, 2018. **16**(12): p. 1865-1878.
125. Wu, J., G. Cheng, C. Zhang, Y. Zheng, H. Xu, H. Yang, et al., Long noncoding RNA LINC01296 is associated with poor prognosis in prostate cancer and promotes cancer-cell proliferation and metastasis. Onco Targets Ther, 2017. **10**: p. 1843-1852.
126. Wu, Z., W. Huang, Y. Chen, B. Chen, R. Liu, P. Bai, et al., LINC01638 lncRNA promotes the proliferation, migration and invasion of prostate carcinoma cells by interacting with Notch1. Cancer Biomark, 2019. **25**(2): p. 161-168.

127. Wu, H.F., L.G. Ren, J.Q. Xiao, Y. Zhang, X.W. Mao, and L.F. Zhou, Long non-coding RNA LINP1 promotes the malignant progression of prostate cancer by regulating p53. Eur Rev Med Pharmacol Sci, 2018. **22**(14): p. 4467-4476.
128. Wang, X., Y. Xu, X. Wang, C. Jiang, S. Han, K. Dong, et al., LincRNA-p21 suppresses development of human prostate cancer through inhibition of PKM2. Cell Prolif, 2017. **50**(6).
129. Xu, S., X.M. Yi, C.P. Tang, J.P. Ge, Z.Y. Zhang, and W.Q. Zhou, Long non-coding RNA ATB promotes growth and epithelial-mesenchymal transition and predicts poor prognosis in human prostate carcinoma. Oncol Rep, 2016. **36**(1): p. 10-22.
130. Gu, P., X. Chen, R. Xie, W. Xie, L. Huang, W. Dong, et al., A novel AR translational regulator lncRNA LBCS inhibits castration resistance of prostate cancer. Mol Cancer, 2019. **18**(1): p. 109.
131. Wang, L., Y. Lin, H. Meng, C. Liu, J. Xue, Q. Zhang, et al., Long non-coding RNA LOC283070 mediates the transition of LNCaP cells into androgen-independent cells possibly via CAMK1D. Am J Transl Res, 2016. **8**(12): p. 5219-5234.
132. Wang, J., G. Cheng, X. Li, Y. Pan, C. Qin, H. Yang, et al., Overexpression of long non-coding RNA LOC400891 promotes tumor progression and poor prognosis in prostate cancer. Tumour Biol, 2016. **37**(7): p. 9603-13.
133. Zhang, C., C. Liu, J. Wu, Y. Zheng, H. Xu, G. Cheng, et al., Upregulation of long noncoding RNA LOC440040 promotes tumor progression and predicts poor prognosis in patients with prostate cancer. Onco Targets Ther, 2017. **10**: p. 4945-4954.
134. Long, B., N. Li, X.X. Xu, X.X. Li, X.J. Xu, J.Y. Liu, et al., Long noncoding RNA LOXL1-AS1 regulates prostate cancer cell proliferation and cell cycle progression through miR-541-3p and CCND1. Biochem Biophys Res Commun, 2018. **505**(2): p. 561-568.
135. Liu, C., L. Wang, Y.W. Li, Y.S. Cui, Y.Q. Wang, and S. Liu, Long noncoding RNA LUCAT1 promotes migration and invasion of prostate cancer cells by inhibiting KISS1 expression. Eur Rev Med Pharmacol Sci, 2019. **23**(8): p. 3277-3283.
136. Ren, S., Y. Liu, W. Xu, Y. Sun, J. Lu, F. Wang, et al., Long noncoding RNA MALAT-1 is a new potential therapeutic target for castration resistant prostate cancer. J Urol, 2013. **190**(6): p. 2278-87.
137. Luo, G., M. Wang, X. Wu, D. Tao, X. Xiao, L. Wang, et al., Long Non-Coding RNA MEG3 Inhibits Cell Proliferation and Induces Apoptosis in Prostate Cancer. Cell Physiol Biochem, 2015. **37**(6): p. 2209-20.
138. Sun, T., S.Y. Du, J. Armenia, F. Qu, J. Fan, X. Wang, et al., Expression of lncRNA MIR222HG co-transcribed from the miR-221/222 gene promoter facilitates the development of castration-resistant prostate cancer. Oncogenesis, 2018. **7**(3): p. 30.
139. Wang, J., X. Yang, R. Li, L. Wang, Y. Gu, Y. Zhao, et al., Long non-coding RNA MYU promotes prostate cancer proliferation by mediating the miR-184/c-Myc axis. Oncol Rep, 2018. **40**(5): p. 2814-2825.
140. Zheng, Y., Y. Gao, X. Li, S. Si, H. Xu, F. Qi, et al., Long non-coding RNA NAP1L6 promotes tumor progression and predicts poor prognosis in prostate cancer by targeting Inhibin-beta A. Onco Targets Ther, 2018. **11**: p. 4965-4977.
141. Chakravarty, D., A. Sboner, S.S. Nair, E. Giannopoulou, R. Li, S. Hennig, et al., The oestrogen receptor alpha-regulated lncRNA NEAT1 is a critical modulator of prostate cancer. Nat Commun, 2014. **5**: p. 5383.

142. Yang, J., S. Zhao, and B. Li, Long noncoding RNA PANDAR promotes progression and predicts poor prognosis via upregulating ROCK1 in prostate cancer. Eur Rev Med Pharmacol Sci, 2019. **23**(11): p. 4706-4712.
143. Sun, M., D. Geng, S. Li, Z. Chen, and W. Zhao, LncRNA PART1 modulates toll-like receptor pathways to influence cell proliferation and apoptosis in prostate cancer cells. Biol Chem, 2018. **399**(4): p. 387-395.
144. He, J.H., B.X. Li, Z.P. Han, M.X. Zou, L. Wang, Y.B. Lv, et al., Snail-activated long non-coding RNA PCA3 up-regulates PRKD3 expression by miR-1261 sponging, thereby promotes invasion and migration of prostate cancer cells. Tumour Biol, 2016.
145. Prensner, J.R., W. Chen, S. Han, M.K. Iyer, Q. Cao, V. Kothari, et al., The long non-coding RNA PCAT-1 promotes prostate cancer cell proliferation through cMyc. Neoplasia, 2014. **16**(11): p. 900-8.
146. Ylipaa, A., K. Kivinummi, A. Kohvakka, M. Annala, L. Latonen, M. Scaravilli, et al., Transcriptome Sequencing Reveals PCAT5 as a Novel ERG-Regulated Long Noncoding RNA in Prostate Cancer. Cancer Res, 2015. **75**(19): p. 4026-31.
147. White, N.M., S.G. Zhao, J. Zhang, E.B. Rozycki, H.X. Dang, S.D. McFadden, et al., Multi-institutional Analysis Shows that Low PCAT-14 Expression Associates with Poor Outcomes in Prostate Cancer. Eur Urol, 2017. **71**(2): p. 257-266.
148. Hua, J.T., M. Ahmed, H. Guo, Y. Zhang, S. Chen, F. Soares, et al., Risk SNP-Mediated Promoter-Enhancer Switching Drives Prostate Cancer through lncRNA PCAT19. Cell, 2018. **174**(3): p. 564-575 e18.
149. Malik, R., L. Patel, J.R. Prensner, Y. Shi, M.K. Iyer, S. Subramaniyan, et al., The lncRNA PCAT29 inhibits oncogenic phenotypes in prostate cancer. Mol Cancer Res, 2014. **12**(8): p. 1081-7.
150. Bawa, P.S., S. Ravi, S. Paul, B. Chaudhary, and S. Srinivasan, A novel molecular mechanism for a long non-coding RNA PCAT92 implicated in prostate cancer. Oncotarget, 2018. **9**(65): p. 32419-32434.
151. Parolia, A., F. Crea, H. Xue, Y. Wang, F. Mo, V.R. Ramnarine, et al., The long non-coding RNA PCGEM1 is regulated by androgen receptor activity in vivo. Mol Cancer, 2015. **14**: p. 46.
152. Yang, X., L. Wang, R. Li, Y. Zhao, Y. Gu, S. Liu, et al., The long non-coding RNA PCSEAT exhibits an oncogenic property in prostate cancer and functions as a competing endogenous RNA that associates with EZH2. Biochem Biophys Res Commun, 2018. **502**(2): p. 262-268.
153. Misawa, A., K.I. Takayama, T. Fujimura, Y. Homma, Y. Suzuki, and S. Inoue, Androgen-induced lncRNA POTEF-AS1 regulates apoptosis-related pathway to facilitate cell survival in prostate cancer cells. Cancer Sci, 2017. **108**(3): p. 373-379.
154. Chung, S., H. Nakagawa, M. Uemura, L. Piao, K. Ashikawa, N. Hosono, et al., Association of a novel long non-coding RNA in 8q24 with prostate cancer susceptibility. Cancer Sci, 2011. **102**(1): p. 245-52.
155. Wang, D., X. Wan, Y. Zhang, Z. Kong, Y. Lu, X. Sun, et al., A novel androgen-reduced prostate-specific lncRNA, PSLNR, inhibits prostate-cancer progression in part by regulating the p53-dependent pathway. Prostate, 2019. **79**(12): p. 1362-1377.
156. Yang, J., C. Li, A. Mudd, and X. Gu, LncRNA PVT1 predicts prognosis and regulates tumor growth in prostate cancer. Biosci Biotechnol Biochem, 2017: p. 1-6.

157. Tian, C., Y. Deng, Y. Jin, S. Shi, and H. Bi, Long non-coding RNA RNCR3 promotes prostate cancer progression through targeting miR-185-5p. Am J Transl Res, 2018. **10**(5): p. 1562-1570.
158. Qin, X., W. Zhu, A. Lu, G. Wang, X. Ye, and G. Weng, Long non-coding RNA SAP30L-AS1 promotes prostate cancer growth through repressing SAP30L. Gene, 2019. **690**: p. 120-128.
159. Zhai, W., Y. Sun, C. Guo, G. Hu, M. Wang, J. Zheng, et al., LncRNA-SARCC suppresses renal cell carcinoma (RCC) progression via altering the androgen receptor(AR)/miRNA-143-3p signals. Cell Death Differ, 2017. **24**(9): p. 1502-1517.
160. Mehra, R., Y. Shi, A.M. Udager, J.R. Prensner, A. Sahu, M.K. Iyer, et al., A novel RNA in situ hybridization assay for the long noncoding RNA SChLAP1 predicts poor clinical outcome after radical prostatectomy in clinically localized prostate cancer. Neoplasia, 2014. **16**(12): p. 1121-7.
161. Schmidt, K., J.S. Carroll, E. Yee, D.D. Thomas, L. Wert-Lamas, S.C. Neier, et al., The lncRNA SLNCR Recruits the Androgen Receptor to EGR1-Bound Genes in Melanoma and Inhibits Expression of Tumor Suppressor p21. Cell Rep, 2019. **27**(8): p. 2493-2507 e4.
162. Li, J., Z. Zhang, L. Xiong, C. Guo, T. Jiang, L. Zeng, et al., SNHG1 lncRNA negatively regulates miR-199a-3p to enhance CDK7 expression and promote cell proliferation in prostate cancer. Biochem Biophys Res Commun, 2017. **487**(1): p. 146-152.
163. Yan, Y., Z. Chen, Y. Xiao, X. Wang, and K. Qian, Long non-coding RNA SNHG6 is upregulated in prostate cancer and predicts poor prognosis. Mol Biol Rep, 2019. **46**(3): p. 2771-2778.
164. Qi, H., B. Wen, Q. Wu, W. Cheng, J. Lou, J. Wei, et al., Long noncoding RNA SNHG7 accelerates prostate cancer proliferation and cycle progression through cyclin D1 by sponging miR-503. Biomed Pharmacother, 2018. **102**: p. 326-332.
165. Song, J., X. Wu, R. Ma, L. Miao, L. Xiong, and W. Zhao, Long noncoding RNA SNHG12 promotes cell proliferation and activates Wnt/beta-catenin signaling in prostate cancer through sponging microRNA-195. J Cell Biochem, 2019. **120**(8): p. 13066-13075.
166. Zhang, Y., D. Zhang, J. Lv, S. Wang, and Q. Zhang, LncRNA SNHG15 acts as an oncogene in prostate cancer by regulating miR-338-3p/FKBP1A axis. Gene, 2019. **705**: p. 44-50.
167. Lee, B., J. Mazar, M.N. Aftab, F. Qi, J. Shelley, J.L. Li, et al., Long noncoding RNAs as putative biomarkers for prostate cancer detection. J Mol Diagn, 2014. **16**(6): p. 615-26.
168. Dong, L., H. Ding, Y. Li, D. Xue, and Y. Liu, LncRNA TINCR is associated with clinical progression and serves as tumor suppressive role in prostate cancer. Cancer Manag Res, 2018. **10**: p. 2799-2807.
169. Huang, W., X. Su, W. Yan, Z. Kong, D. Wang, Y. Huang, et al., Overexpression of AR-regulated lncRNA TMPO-AS1 correlates with tumor progression and poor prognosis in prostate cancer. Prostate, 2018. **78**(16): p. 1248-1261.
170. Orfanelli, U., E. Jachetti, F. Chiacchiera, M. Grioni, P. Brambilla, A. Briganti, et al., Antisense transcription at the TRPM2 locus as a novel prognostic marker and therapeutic target in prostate cancer. Oncogene, 2015. **34**(16): p. 2094-102.

171. Xiao, G., J. Yao, D. Kong, C. Ye, R. Chen, L. Li, et al., The Long Noncoding RNA TTTY15, Which Is Located on the Y Chromosome, Promotes Prostate Cancer Progression by Sponging let-7. Eur Urol, 2018.
172. Li, G., Y. Zhang, J. Mao, P. Hu, Q. Chen, W. Ding, et al., LncRNA TUC338 is overexpressed in prostate carcinoma and downregulates miR-466. Gene, 2019. **707**: p. 224-230.
173. Yang, B., X. Tang, Z. Wang, D. Sun, X. Wei, and Y. Ding, TUG1 promotes prostate cancer progression by acting as a ceRNA of miR-26a. Biosci Rep, 2018. **38**(5).
174. Zhang, S., X. Dong, T. Ji, G. Chen, and L. Shan, Long non-coding RNA UCA1 promotes cell progression by acting as a competing endogenous RNA of ATF2 in prostate cancer. Am J Transl Res, 2017. **9**(2): p. 366-375.
175. Du, Y., X.D. Weng, L. Wang, X.H. Liu, H.C. Zhu, J. Guo, et al., LncRNA XIST acts as a tumor suppressor in prostate cancer through sponging miR-23a to modulate RKIP expression. Oncotarget, 2017. **8**(55): p. 94358-94370.
176. Su, W., M. Xu, X. Chen, N. Chen, J. Gong, L. Nie, et al., Long noncoding RNA ZEB1-AS1 epigenetically regulates the expressions of ZEB1 and downstream molecules in prostate cancer. Mol Cancer, 2017. **16**(1): p. 142.
177. Horoszewicz, J.S., S.S. Leong, E. Kawinski, J.P. Karr, H. Rosenthal, T.M. Chu, et al., LNCaP model of human prostatic carcinoma. Cancer Res, 1983. **43**(4): p. 1809-18.
178. Balbas, M.D., M.J. Evans, D.J. Hosfield, J. Wongvipat, V.K. Arora, P.A. Watson, et al., Overcoming mutation-based resistance to antiandrogens with rational drug design. Elife, 2013. **2**: p. e00499.
179. Joseph, J.D., N. Lu, J. Qian, J. Sensintaffar, G. Shao, D. Brigham, et al., A clinically relevant androgen receptor mutation confers resistance to second-generation antiandrogens enzalutamide and ARN-509. Cancer Discov, 2013. **3**(9): p. 1020-9.
180. Bello, D., M.M. Webber, H.K. Kleinman, D.D. Wartinger, and J.S. Rhim, Androgen responsive adult human prostatic epithelial cell lines immortalized by human papillomavirus 18. Carcinogenesis, 1997. **18**(6): p. 1215-23.
181. Webber, M.M., D. Bello, H.K. Kleinman, D.D. Wartinger, D.E. Williams, and J.S. Rhim, Prostate specific antigen and androgen receptor induction and characterization of an immortalized adult human prostatic epithelial cell line. Carcinogenesis, 1996. **17**(8): p. 1641-6.
182. Liu, Y.N., Y. Liu, H.J. Lee, Y.H. Hsu, and J.H. Chen, Activated androgen receptor downregulates E-cadherin gene expression and promotes tumor metastasis. Mol Cell Biol, 2008. **28**(23): p. 7096-108.
183. Young, L., J. Sung, G. Stacey, and J.R. Masters, Detection of Mycoplasma in cell cultures. Nat Protoc, 2010. **5**(5): p. 929-34.
184. Cabili, M.N., C. Trapnell, L. Goff, M. Koziol, B. Tazon-Vega, A. Regev, et al., Integrative annotation of human large intergenic noncoding RNAs reveals global properties and specific subclasses. Genes Dev, 2011. **25**(18): p. 1915-27.
185. Clark, M.B., T.R. Mercer, G. Bussotti, T. Leonardi, K.R. Haynes, J. Crawford, et al., Quantitative gene profiling of long noncoding RNAs with targeted RNA sequencing. Nat Methods, 2015. **12**(4): p. 339-42.
186. Iyer, M.K., Y.S. Niknafs, R. Malik, U. Singhal, A. Sahu, Y. Hosono, et al., The landscape of long noncoding RNAs in the human transcriptome. Nat Genet, 2015. **47**(3): p. 199-208.
187. Zhai, W., Y. Sun, M. Jiang, M. Wang, T.A. Gasiewicz, J. Zheng, et al., Differential regulation of LncRNA-SARCC suppresses VHL-mutant RCC cell proliferation yet

promotes VHL-normal RCC cell proliferation via modulating androgen receptor/HIF-2alpha/C-MYC axis under hypoxia. Oncogene, 2016. **35**(37): p. 4866-80.
188. Lin, B., J.T. White, C. Ferguson, R. Bumgarner, C. Friedman, B. Trask, et al., PART-1: a novel human prostate-specific, androgen-regulated gene that maps to chromosome 5q12. Cancer Res, 2000. **60**(4): p. 858-63.
189. Han, Y., H. Hu, and J. Zhou, Knockdown of LncRNA SNHG7 inhibited epithelial-mesenchymal transition in prostate cancer though miR-324-3p/WNT2B axis in vitro. Pathol Res Pract, 2019: p. 152537.
190. Li, Y., L. Wang, M. Zhang, J. Melamed, X. Liu, R. Reiter, et al., LEF1 in androgen-independent prostate cancer: regulation of androgen receptor expression, prostate cancer growth, and invasion. Cancer Res, 2009. **69**(8): p. 3332-8.
191. Cheng, G., Z. Song, Y. Liu, H. Xiao, H. Ruan, Q. Cao, et al., Long noncoding RNA SNHG12 indicates the prognosis of prostate cancer and accelerates tumorigenesis via sponging miR-133b. J Cell Physiol, 2019.
192. Zhao, Y., L. Zhao, J. Li, and L. Zhong, Silencing of long noncoding RNA RP11-476D10.1 enhances apoptosis and autophagy while inhibiting proliferation of papillary thyroid carcinoma cells via microRNA-138-5p-dependent inhibition of LRRK2. J Cell Physiol, 2019. **234**(11): p. 20980-20991.
193. Prensner, J.R., W. Chen, M.K. Iyer, Q. Cao, T. Ma, S. Han, et al., PCAT-1, a long noncoding RNA, regulates BRCA2 and controls homologous recombination in cancer. Cancer Res, 2014. **74**(6): p. 1651-60.
194. Mehra, R., A.M. Udager, T.U. Ahearn, X. Cao, F.Y. Feng, M. Loda, et al., Overexpression of the Long Non-coding RNA SChLAP1 Independently Predicts Lethal Prostate Cancer. Eur Urol, 2016. **70**(4): p. 549-552.
195. Prensner, J.R., M.K. Iyer, A. Sahu, I.A. Asangani, Q. Cao, L. Patel, et al., The long noncoding RNA SChLAP1 promotes aggressive prostate cancer and antagonizes the SWI/SNF complex. Nat Genet, 2013. **45**(11): p. 1392-8.
196. Yang, L., C. Lin, C. Jin, J.C. Yang, B. Tanasa, W. Li, et al., lncRNA-dependent mechanisms of androgen-receptor-regulated gene activation programs. Nature, 2013. **500**(7464): p. 598-602.
197. Lemos, A.E., L.B. Ferreira, N.M. Batoreu, P.P. de Freitas, M.H. Bonamino, and E.R. Gimba, PCA3 long noncoding RNA modulates the expression of key cancer-related genes in LNCaP prostate cancer cells. Tumour Biol, 2016. **37**(8): p. 11339-48.
198. Schalken, J.A., D. Hessels, and G. Verhaegh, New targets for therapy in prostate cancer: differential display code 3 (DD3(PCA3)), a highly prostate cancer-specific gene. Urology, 2003. **62**(5 Suppl 1): p. 34-43.
199. Lerman, I., X. Ma, C. Seger, A. Maolake, M.L. Garcia-Hernandez, J. Rangel-Moreno, et al., Epigenetic Suppression of SERPINB1 Promotes Inflammation-Mediated Prostate Cancer Progression. Mol Cancer Res, 2019. **17**(4): p. 845-859.
200. Rong, Y.P., F. Liu, L.C. Zeng, W.J. Ma, D.Z. Wei, and Z.G. Han, Cloning and characterization of a novel human secretory protein: secretogranin III. Sheng Wu Hua Xue Yu Sheng Wu Wu Li Xue Bao (Shanghai), 2002. **34**(4): p. 411-7.
201. Cao, X., J. Qin, Y. Xie, O. Khan, F. Dowd, M. Scofield, et al., Regulator of G-protein signaling 2 (RGS2) inhibits androgen-independent activation of androgen receptor in prostate cancer cells. Oncogene, 2006. **25**(26): p. 3719-34.

202. Linder, A., M. Hagberg Thulin, J.E. Damber, and K. Welen, Analysis of regulator of G-protein signalling 2 (RGS2) expression and function during prostate cancer progression. Sci Rep, 2018. **8**(1): p. 17259.
203. Liu, L., D. Feng, G. Chen, M. Chen, Q. Zheng, P. Song, et al., Mitochondrial outer-membrane protein FUNDC1 mediates hypoxia-induced mitophagy in mammalian cells. Nat Cell Biol, 2012. **14**(2): p. 177-85.
204. Jhun, B.H., B. Rivnay, D. Price, and H. Avraham, The MATK tyrosine kinase interacts in a specific and SH2-dependent manner with c-Kit. J Biol Chem, 1995. **270**(16): p. 9661-6.
205. Grupp, K., D. Ospina-Klinck, M.C. Tsourlakis, C. Koop, W. Wilczak, M. Adam, et al., NY-ESO-1 expression is tightly linked to TMPRSS2-ERG fusion in prostate cancer. Prostate, 2014. **74**(10): p. 1012-22.
206. de Windt, F.E. and C. van der Drift, Purification and some properties of hydroxypyruvate isomerase of Bacillus fastidiosus. Biochim Biophys Acta, 1980. **613**(2): p. 556-62.
207. Pellon-Maison, M., M.A. Montanaro, E. Lacunza, M.B. Garcia-Fabiani, M.C. Soler-Gerino, E.R. Cattaneo, et al., Glycerol-3-phosphate acyltranferase-2 behaves as a cancer testis gene and promotes growth and tumorigenicity of the breast cancer MDA-MB-231 cell line. PLoS One, 2014. **9**(6): p. e100896.
208. Akamatsu, S., A.W. Wyatt, D. Lin, S. Lysakowski, F. Zhang, S. Kim, et al., The Placental Gene PEG10 Promotes Progression of Neuroendocrine Prostate Cancer. Cell Rep, 2015. **12**(6): p. 922-36.
209. Kim, S., D. Thaper, S. Bidnur, P. Toren, S. Akamatsu, J.L. Bishop, et al., PEG10 is associated with treatment-induced neuroendocrine prostate cancer. J Mol Endocrinol, 2019. **63**(1): p. 39-49.
210. Ribarska, T., K.M. Bastian, A. Koch, and W.A. Schulz, Specific changes in the expression of imprinted genes in prostate cancer--implications for cancer progression and epigenetic regulation. Asian J Androl, 2012. **14**(3): p. 436-50.
211. Contrepois, K., C. Coudereau, B.A. Benayoun, N. Schuler, P.F. Roux, O. Bischof, et al., Histone variant H2A.J accumulates in senescent cells and promotes inflammatory gene expression. Nat Commun, 2017. **8**: p. 14995.
212. Kim, J., W.D. Frey, H. He, H. Kim, M.B. Ekram, A. Bakshi, et al., Peg3 mutational effects on reproduction and placenta-specific gene families. PLoS One, 2013. **8**(12): p. e83359.
213. Jain, P., P.L. Clermont, F. Desmeules, A. Zoubeidi, B. Neveu, and F. Pouliot, Development of a Transcriptional Amplification System Based on the PEG3 Promoter to Target Androgen Receptor-Positive and -Negative Prostate Cancer Cells. Int J Mol Sci, 2019. **20**(1).
214. Ulrix, W., J.V. Swinnen, W. Heyns, and G. Verhoeven, Androgens down-regulate the expression of the human homologue of paternally expressed gene-3 in the prostatic adenocarcinoma cell line LNCaP. Mol Cell Endocrinol, 1999. **155**(1-2): p. 69-76.
215. Grisanzio, C., L. Werner, D. Takeda, B.C. Awoyemi, M.M. Pomerantz, H. Yamada, et al., Genetic and functional analyses implicate the NUDT11, HNF1B, and SLC22A3 genes in prostate cancer pathogenesis. Proc Natl Acad Sci U S A, 2012. **109**(28): p. 11252-7.
216. Karypidis, A.H., M. Olsson, S.O. Andersson, A. Rane, and L. Ekstrom, Deletion polymorphism of the UGT2B17 gene is associated with increased risk for prostate

cancer and correlated to gene expression in the prostate. Pharmacogenomics J, 2008. **8**(2): p. 147-51.
217. Allioli, N., S. Vincent, V. Vlaeminck-Guillem, M. Decaussin-Petrucci, F. Ragage, A. Ruffion, et al., TM4SF1, a novel primary androgen receptor target gene over-expressed in human prostate cancer and involved in cell migration. Prostate, 2011. **71**(11): p. 1239-50.
218. Chouinard, S., G. Pelletier, A. Belanger, and O. Barbier, Isoform-specific regulation of uridine diphosphate-glucuronosyltransferase 2B enzymes in the human prostate: differential consequences for androgen and bioactive lipid inactivation. Endocrinology, 2006. **147**(11): p. 5431-42.
219. Dougan, J., O. Hawsawi, L.J. Burton, G. Edwards, K. Jones, J. Zou, et al., Proteomics-Metabolomics Combined Approach Identifies Peroxidasin as a Protector against Metabolic and Oxidative Stress in Prostate Cancer. Int J Mol Sci, 2019. **20**(12).
220. Fagerberg, L., B.M. Hallstrom, P. Oksvold, C. Kampf, D. Djureinovic, J. Odeberg, et al., Analysis of the human tissue-specific expression by genome-wide integration of transcriptomics and antibody-based proteomics. Mol Cell Proteomics, 2014. **13**(2): p. 397-406.
221. Janssens, B., S. Goossens, K. Staes, B. Gilbert, J. van Hengel, C. Colpaert, et al., alphaT-catenin: a novel tissue-specific beta-catenin-binding protein mediating strong cell-cell adhesion. J Cell Sci, 2001. **114**(Pt 17): p. 3177-88.
222. Yoshikawa, T., N. Seki, T. Azuma, Y. Masuho, M. Muramatsu, N. Miyajima, et al., Isolation of a cDNA for a novel human RING finger protein gene, RNF18, by the virtual transcribed sequence (VTS) approach(1). Biochim Biophys Acta, 2000. **1493**(3): p. 349-55.
223. Bishop, J.L., D. Thaper, S. Vahid, A. Davies, K. Ketola, H. Kuruma, et al., The Master Neural Transcription Factor BRN2 Is an Androgen Receptor-Suppressed Driver of Neuroendocrine Differentiation in Prostate Cancer. Cancer Discov, 2017. **7**(1): p. 54-71.
224. Kidd, M., I.M. Modlin, S.M. Mane, R.L. Camp, and M.D. Shapiro, Q RT-PCR detection of chromogranin A: a new standard in the identification of neuroendocrine tumor disease. Ann Surg, 2006. **243**(2): p. 273-80.
225. Bolha, L., M. Ravnik-Glavac, and D. Glavac, Long Noncoding RNAs as Biomarkers in Cancer. Dis Markers, 2017. **2017**: p. 7243968.
226. Yu, G., W. Yao, J. Wang, X. Ma, W. Xiao, H. Li, et al., LncRNAs expression signatures of renal clear cell carcinoma revealed by microarray. PLoS One, 2012. **7**(8): p. e42377.
227. Gauri Shishodia, P.S.S., Sweaty Koul, and Hari Koul, *Abstract 1079: PCDH7 is overexpressed in advanced prostate cancer and modulates aggressive phenotype in prostate cancer cells*. 2018, American Association for Cancer Research. p. 1079.
228. Heery, R., S.P. Finn, S. Cuffe, and S.G. Gray, Long Non-Coding RNAs: Key Regulators of Epithelial-Mesenchymal Transition, Tumour Drug Resistance and Cancer Stem Cells. Cancers (Basel), 2017. **9**(4).
229. Leach, F.S., A. Velasco, J.T. Hsieh, A.I. Sagalowsky, and J.D. McConnell, The mismatch repair gene hMSH2 is mutated in the prostate cancer cell line LNCaP. J Urol, 2000. **164**(5): p. 1830-3.

230. Abida, W., M.L. Cheng, J. Armenia, S. Middha, K.A. Autio, H.A. Vargas, et al., Analysis of the Prevalence of Microsatellite Instability in Prostate Cancer and Response to Immune Checkpoint Blockade. JAMA Oncol, 2019. **5**(4): p. 471-478.
231. Szczesniak, M.W. and I. Makalowska, lncRNA-RNA Interactions across the Human Transcriptome. PLoS One, 2016. **11**(3): p. e0150353.
232. Ji, Q., L. Zhang, X. Liu, L. Zhou, W. Wang, Z. Han, et al., Long non-coding RNA MALAT1 promotes tumour growth and metastasis in colorectal cancer through binding to SFPQ and releasing oncogene PTBP2 from SFPQ/PTBP2 complex. Br J Cancer, 2014. **111**(4): p. 736-48.
233. Ransohoff, J.D., Y. Wei, and P.A. Khavari, The functions and unique features of long intergenic non-coding RNA. Nat Rev Mol Cell Biol, 2018. **19**(3): p. 143-157.
234. Maxwell, P.H., C.W. Pugh, and P.J. Ratcliffe, Activation of the HIF pathway in cancer. Curr Opin Genet Dev, 2001. **11**(3): p. 293-9.
235. Li, J., Y. Chen, Z. Chen, A. He, H. Xie, Q. Zhang, et al., SPRY4-IT1: A novel oncogenic long non-coding RNA in human cancers. Tumour Biol, 2017. **39**(6): p. 1010428317711406.
236. Mazar, J., W. Zhao, A.M. Khalil, B. Lee, J. Shelley, S.S. Govindarajan, et al., The functional characterization of long noncoding RNA SPRY4-IT1 in human melanoma cells. Oncotarget, 2014. **5**(19): p. 8959-69.
237. Yang, F., S. Lyu, S. Dong, Y. Liu, X. Zhang, and O. Wang, Expression profile analysis of long noncoding RNA in HER-2-enriched subtype breast cancer by next-generation sequencing and bioinformatics. Onco Targets Ther, 2016. **9**: p. 761-72.
238. Hu, B., C. Shi, H.X. Jiang, and S.Y. Qin, Identification of novel therapeutic target genes and pathway in pancreatic cancer by integrative analysis. Medicine (Baltimore), 2017. **96**(42): p. e8261.
239. Feng, Y., Y. Shen, H. Chen, X. Wang, R. Zhang, Y. Peng, et al., Expression profile analysis of long non-coding RNA in acute myeloid leukemia by microarray and bioinformatics. Cancer Sci, 2018. **109**(2): p. 340-353.
240. Englund, C., A. Fink, C. Lau, D. Pham, R.A. Daza, A. Bulfone, et al., Pax6, Tbr2, and Tbr1 are expressed sequentially by radial glia, intermediate progenitor cells, and postmitotic neurons in developing neocortex. J Neurosci, 2005. **25**(1): p. 247-51.
241. Lou, Y., H. Jiang, Z. Cui, X. Wang, L. Wang, and Y. Han, Gene microarray analysis of lncRNA and mRNA expression profiles in patients with highgrade ovarian serous cancer. Int J Mol Med, 2018. **42**(1): p. 91-104.
242. Lan, H., J. Zeng, G. Chen, and H. Huang, Survival prediction of kidney renal papillary cell carcinoma by comprehensive LncRNA characterization. Oncotarget, 2017. **8**(67): p. 110811-110829.
243. Thomas, R., G. Al-Khadairi, J. Roelands, W. Hendrickx, S. Dermime, D. Bedognetti, et al., NY-ESO-1 Based Immunotherapy of Cancer: Current Perspectives. Front Immunol, 2018. **9**: p. 947.
244. Gjerstorff, M.F., M.H. Andersen, and H.J. Ditzel, Oncogenic cancer/testis antigens: prime candidates for immunotherapy. Oncotarget, 2015. **6**(18): p. 15772-87.
245. Wilson, E.M., Androgen receptor molecular biology and potential targets in prostate cancer. Ther Adv Urol, 2010. **2**(3): p. 105-17.
246. Paju, A., K. Hotakainen, Y. Cao, T. Laurila, V. Gadaleanu, A. Hemminki, et al., Increased expression of tumor-associated trypsin inhibitor, TATI, in prostate cancer and in androgen-independent 22Rv1 cells. Eur Urol, 2007. **52**(6): p. 1670-9.

247. Ritika Tiwari, N.M., Vipul Bhatia, Anjali Yadav, Shannon Carskadon, Nilesh Gupta, Amina Zoubeidi, Nallasivam Palanisamy and Bushra Ateeq, *Abstract 5225: Androgen deprivation upregulates SPINK1 expression and potentiates cellular plasticity in prostate cancer*, in *AACR Annual Meeting 2019*. 2019, Cancer Research: Atlanta. p. 5225.
248. Nimmrich, I., A.M. Sieuwerts, M.E. Meijer-van Gelder, I. Schwope, J. Bolt-de Vries, N. Harbeck, et al., DNA hypermethylation of PITX2 is a marker of poor prognosis in untreated lymph node-negative hormone receptor-positive breast cancer patients. Breast Cancer Res Treat, 2008. **111**(3): p. 429-37.
249. Sailer, V., H. Gevensleben, J. Dietrich, D. Goltz, G. Kristiansen, F. Bootz, et al., Clinical performance validation of PITX2 DNA methylation as prognostic biomarker in patients with head and neck squamous cell carcinoma. PLoS One, 2017. **12**(6): p. e0179412.
250. Weiss, G., S. Cottrell, J. Distler, P. Schatz, G. Kristiansen, M. Ittmann, et al., DNA methylation of the PITX2 gene promoter region is a strong independent prognostic marker of biochemical recurrence in patients with prostate cancer after radical prostatectomy. J Urol, 2009. **181**(4): p. 1678-85.
251. Nawaz, I., X. Qiu, H. Wu, Y. Li, Y. Fan, L.F. Hu, et al., Development of a multiplex methylation specific PCR suitable for (early) detection of non-small cell lung cancer. Epigenetics, 2014. **9**(8): p. 1138-48.
252. Uhl, B., H. Gevensleben, Y. Tolkach, V. Sailer, M. Majores, M. Jung, et al., PITX2 DNA Methylation as Biomarker for Individualized Risk Assessment of Prostate Cancer in Core Biopsies. J Mol Diagn, 2017. **19**(1): p. 107-114.
253. Vela, I., C. Morrissey, X. Zhang, S. Chen, E. Corey, G.M. Strutton, et al., PITX2 and non-canonical Wnt pathway interaction in metastatic prostate cancer. Clin Exp Metastasis, 2014. **31**(2): p. 199-211.
254. Schayek, H., I. Bentov, J. Jacob-Hirsch, C. Yeung, C. Khanna, L.J. Helman, et al., Global methylation analysis identifies PITX2 as an upstream regulator of the androgen receptor and IGF-I receptor genes in prostate cancer. Horm Metab Res, 2012. **44**(7): p. 511-9.
255. Pillai, S.G., N. Dasgupta, C.M. Siddappa, M.A. Watson, T. Fleming, K. Trinkaus, et al., Paired-like Homeodomain Transcription factor 2 expression by breast cancer bone marrow disseminated tumor cells is associated with early recurrent disease development. Breast Cancer Res Treat, 2015. **153**(3): p. 507-17.
256. Fung, F.K., D.W. Chan, V.W. Liu, T.H. Leung, A.N. Cheung, and H.Y. Ngan, Increased expression of PITX2 transcription factor contributes to ovarian cancer progression. PLoS One, 2012. **7**(5): p. e37076.
257. Ozlu, N., M.H. Qureshi, Y. Toyoda, B.Y. Renard, G. Mollaoglu, N.E. Ozkan, et al., Quantitative comparison of a human cancer cell surface proteome between interphase and mitosis. EMBO J, 2015. **34**(2): p. 251-65.
258. Singh, A.P., S. Bafna, K. Chaudhary, G. Venkatraman, L. Smith, J.D. Eudy, et al., Genome-wide expression profiling reveals transcriptomic variation and perturbed gene networks in androgen-dependent and androgen-independent prostate cancer cells. Cancer Lett, 2008. **259**(1): p. 28-38.
259. Fan, W., T. Yanase, H. Morinaga, T. Okabe, M. Nomura, H. Daitoku, et al., Insulin-like growth factor 1/insulin signaling activates androgen signaling through direct interactions of Foxo1 with androgen receptor. J Biol Chem, 2007. **282**(10): p. 7329-38.

260. Li, Y., S.C. Chan, L.J. Brand, T.H. Hwang, K.A. Silverstein, and S.M. Dehm, Androgen receptor splice variants mediate enzalutamide resistance in castration-resistant prostate cancer cell lines. Cancer Res, 2013. **73**(2): p. 483-9.
261. Greene, J.P., *Novel Molecular Targets in Advanced Prostate Cancer (published doctoral dissertation)*. 2019, University of Dublin, Trinity College, Ireland.

Appendices

Appendix I: Cloning strategy for overexpression of *SARCC* gene

Step 1: Amplify *SARCC* gene by PCR using cDNA from Clone 1 cells

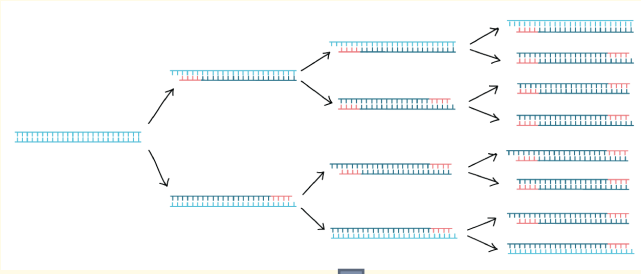

Step 2: Insert *SARCC* into pCR2.1 TOPO plasmid by TOPO cloning

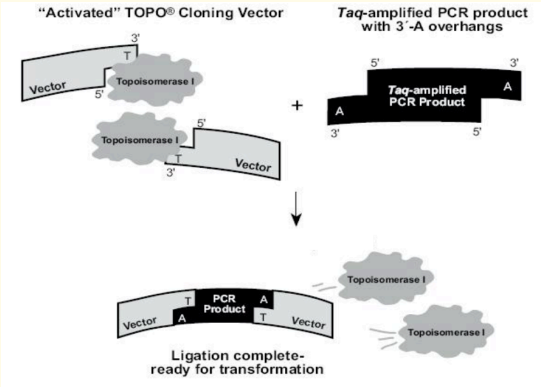

Step 3: Transform *SARCC* into E.coli bacteria and select by blue / white selection

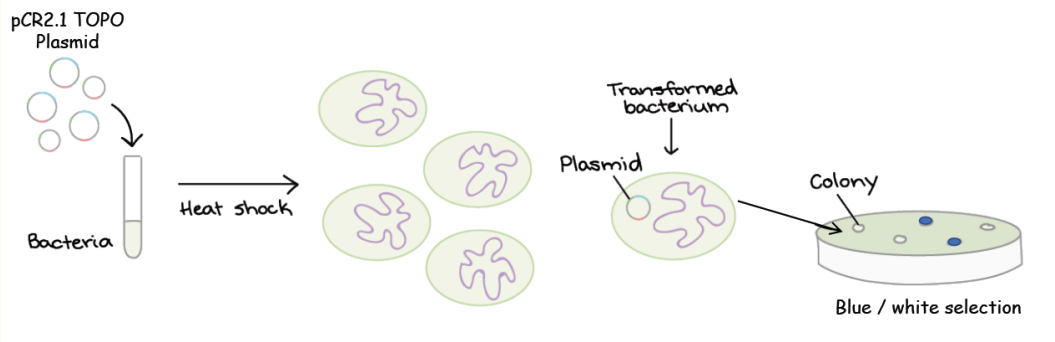

Step 4: Grow bacteria and isolate plasmid DNA. Isolate *SARCC* insert by restriction enzyme digest and band isolation

Step 5: Insert and ligate *SARCC* into plasmid pcDNA3.1(+) with restriction enzymes

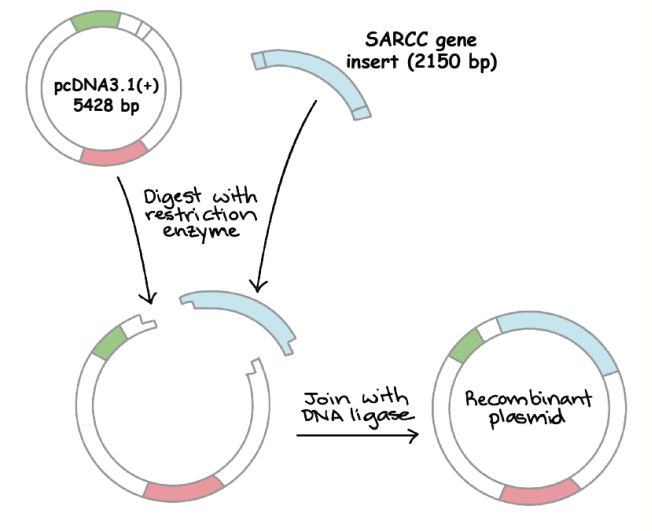

Step 6: Transform into E. coli bacteria

Step 7: Purify plasmid DNA after selection by growth on ampicillin containing media

Step 8: Check for presence of *SARCC* insert by PCR and for correct orientation of insert by restriction enzyme digest

Step 9: Transfect correctly orientated DNA into enzalutamide sensitive cells

Step 10: Select cells containing *SARCC* insert using G418 disulfate

Appendix II: Overview of *SARCC* recombinant plasmid DNA

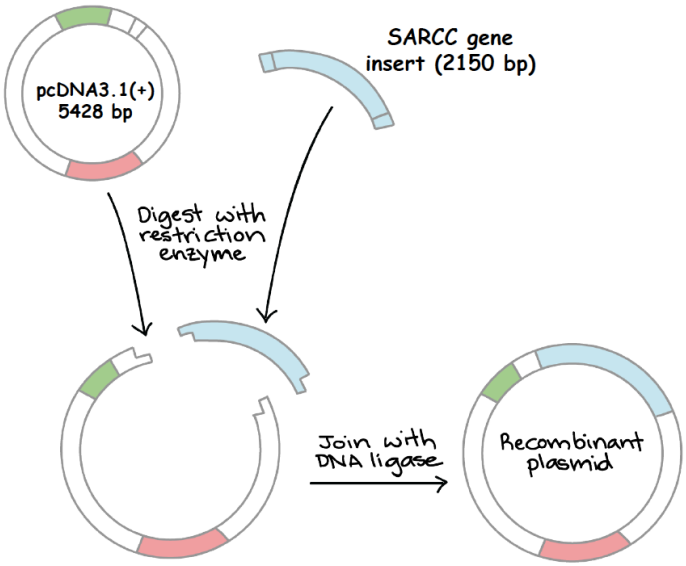

Overview of insertion of SARCC gene into pcDNA3.1(+).
The *SARCC* insert is 2150 bp and the vector is 5428 bp in length. BamH I and Xho I sites are present at each end of the insert.

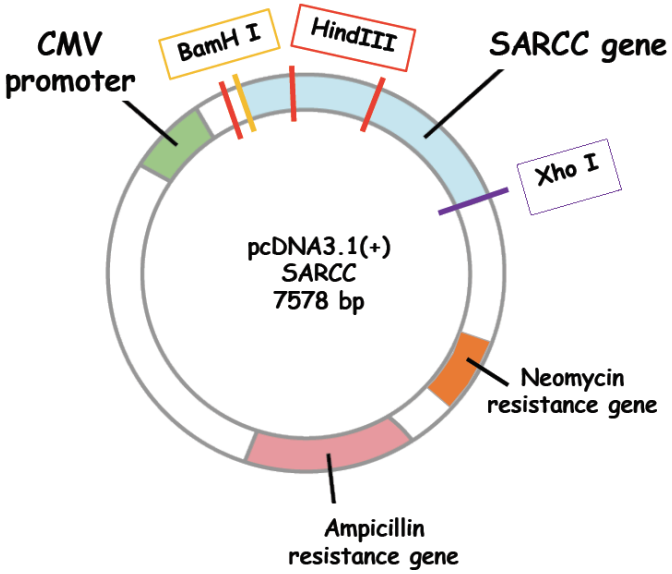

pcDNA3.1(+) containing the SARCC insert in the correct orientation.

There is a CMV promoter upstream from the insert and resistance genes for ampicillin and neomycin. Restriction enzyme sites for BamH I and Xho I are present at each end of the insert and there are three separate sites for Hind III.